50th Anniversary Invited Review

Layered intrusions in the Precambrian: Observations and perspectives

William D. Smith [a,b,*], M. Christopher Jenkins [c], Claudia T. Augustin [b], Ville J. Virtanen [d,e], Zoja Vukmanovic [f], Brian O'Driscoll [g]

[a] *CSIRO Mineral Resources, 26 Dick Perry Avenue, Kensington, Perth, WA 6151, Australia*
[b] *Mineral Deposits Group, Herzberg Laboratories, Department of Earth Sciences, Carleton University, 1125 Colonel By Drive, Ottawa, ON K1S 5B6, Canada*
[c] *U.S. Geological Survey, Geology, Minerals, Energy, and Geophysics Science Center, 904 W. Riverside Ave Rm. 202, Spokane, WA 99201, USA*
[d] *Institut des Sciences de la Terre d'Orléans, UMR 7327, Université d'Orléans, CNRS, BRGM, Orléans, F-45071, OSUC, France*
[e] *Department of Geosciences and Geography, University of Helsinki, Gustaf Hällströminkatu 2, 00014 Helsinki, Finland*
[f] *School of Environmental Sciences, University of East Anglia, Norwich Research Park, Norwich NR4 7TJ, United Kingdom*
[g] *Department of Earth and Environmental Sciences, University of Ottawa, Ottawa K1N 6N5, Canada*

ARTICLE INFO

ABSTRACT

Layered intrusions are plutonic bodies of cumulates that form by the crystallization of mantle-derived melts. These intrusions are characterized by igneous layering distinguishable by shifts in mineralogy, texture, or composition. Layered intrusions have been fundamental to our understanding of igneous petrology; however, it is their status as important repositories of critical metals – such as platinum-group elements, chromium, and vanadium – that has predominantly driven associated research in recent decades. Many layered intrusions were emplaced during the Precambrian, predominantly at the margins of ancient cratons during intervals of supercontinent accretion and destruction. It appears that large, layered intrusions require rigid crust to ensure their preservation, and their geometry and layering is primarily controlled by the nature of melt emplacement.

Layered intrusions are best investigated by integrating observations from various length-scales. At the macroscale, intrusion geometries can be discerned, and their presence understood in the context of the regional geology. At the mesoscale, the layering of an intrusion may be characterized, intrusion-host rock contact relationships studied, and the nature of stratiform mineral occurrences described. At the microscale, the mineralogy and texture of cumulate rocks and any mineralization are elucidated, particularly when novel microtextural and mineral chemical datasets are integrated. For example, here we demonstrate how mesoscale observations and microscale datasets can be combined to understand the petrogenesis of the perplexing *snowball oiks* outcrop located in the Upper Banded Series of the Stillwater Complex. Our data suggest that the orthopyroxene oikocrysts did not form in their present location, but rather formed in a dynamic magma chamber where crystals were transported either by convective currents or within crystal-rich slurries.

Critical metals may be transported to the level of a nascent intrusion as dissolved components in the melt. Alternatively, ore minerals are entrained from elsewhere in a plumbing system, potentially facilitated by volatile-rich phases. There are many ore-forming processes propounded by researchers to occur at the level of emplacement; however, each must address the arrival of the ore mineral, its concentration of metals, and its accumulation into orebodies. In this contribution, several of these processes are described as well as our perspectives on the future of layered intrusion research.

1. Layered intrusions and igneous layering

Layered intrusions are important geological features that record Earth's subsurface processes, particularly with respect to differentiation and solidification of mafic and ultramafic magmas. Over the past half century, many books and special volumes have been published that summarize the body of scientific work dedicated to layered intrusions (*e. g.,* Latypov et al. 2024a and references therein). This article builds on recent reviews by elaborating on construction mechanisms, parent melts, and exploration tools, while also showcasing multiscale and multidisciplinary research through a novel study of the enigmatic *snowball oiks* outcrop of the Stillwater Complex in Montana, USA.


Layered intrusions are found in a variety of tectonic settings and manifest in many different shapes and sizes throughout geologic time. Layered intrusions are particularly well represented in the Precambrian; more than 70 % of known and dated intrusions that exhibit some form of igneous layering were emplaced in the Precambrian (Smith and Maier 2021). In this contribution, we focus on Precambrian layered intrusions, but refer in places to igneous processes best preserved in younger intrusions. In general, igneous layering in layered intrusions can be broadly categorized into mineralogically controlled layering and cryptic layering. Mineralogically controlled layering is defined by conspicuous variations in the modal proportions (uniform or gradational), grain size, and (or) texture of the rock-forming minerals. Some form of mineralogically-controlled layering is characteristic of all layered intrusions. For example, Fig. 1 shows mineralogically controlled layering in outcrop at a variety of length scales from the decimeter scale down to the millimeter scale, exhibited by rocks from the Archean Stillwater Complex (USA), Proterozoic Etoile Suite (Canada), and Proterozoic Lake Owen Complex (USA). Mineralogically controlled layering is often used to subdivide the stratigraphy of layered intrusions into series, zones, and subzones (*e.g.,* Cameron 1978; McCallum 1987). This informal stratigraphic nomenclature is important to correlate the geology of layered intrusions over tens to hundreds of kilometers along strike. Mineralogically controlled layering appears as sharp or gradational changes in rock modal mineralogy or as well-developed rhythmic patterns or sequences (*e.g.,* Wager and Deer 1939; Hess, 1960; Wager and Brown 1968; Irvine 1974). A special kind of rhythmic layering that presents as 10 s to 100 s of meters thick repeated successions of lithologies, termed cyclic layering, is observed in so-called open system layered intrusions and is generally believed to represent the repeated influx of magmas into the nascent intrusion (*e.g.,* Jackson 1961; 1970; Irvine 1976). Mineralogically controlled layering may be 100 s of meters in stratigraphic thickness down to the thickness of a single crystal, and can be laterally continuous for 100 s of km along strike or wispy and discontinuous over 10 s of cm.

In contrast, cryptic layering refers to variations in geochemical compositions that are unidentifiable in the field. This type of layering is seen in places like the Archean ultramafic rocks in Fiskenæsset, Greenland (Polat et al. 2012) and Windimurra, Australia (Parks and Hill 1986). It can manifest as mineralogically homogeneous layers with varying bulk rock major, minor, or trace element geochemistry. Cryptic layering can also be present in more subtle forms, such as variations in mineral major or trace element chemistry (*e.g.,* Boudreau and McCallum 1989; Wilson et al. 1996) or variations in mineral or bulk rock isotopic composition (*e.g.,* Kruger et al. 1987; Kruger 1994).

Various models have been proposed over the years to explain the different types of igneous layering. At the turn of the twentieth century, it was commonly thought that the accumulation of minerals near intrusive body contacts was caused by convection (Becker 1897) or diffusion (Harker 1909). Following the 1831–1836 voyage of the HMS Beagle, Darwin (1844) was among the first to attribute the diversity of igneous rocks to crystal settling, an idea that was later popularized by Bowen (1915) who performed experiments showing olivine sinking in a melt. In an influential paper by Wager and Deer (1939), the sedimentation of crystals precipitating from convective currents of basaltic melt was invoked as the layering forming mechanism for the Skaergaard intrusion in Greenland. This settling mechanism fundamentally changed how researchers considered the formation of layered mafic and ultramafic intrusive rocks and led to several transformative publications (*e.g.,* Hess 1960; Jackson 1961; Wager and Brown 1968). Since then, a variety of dynamic and non-dynamic processes (Boudreau and McBirney 1997; Namur et al. 2015) have been developed and proposed, alone or in combination. These processes include crystal settling, *in situ* crystallization, infiltration metasomatism and competitive particle growth (Fig. 2). Although the relative importance of these and other processes remains heavily debated, it is likely that many of them operate during the formation of layered intrusions and, as such, the interpretation of cumulus rocks should be approached with an open mind and some degree of caution.

Crystal settling (*i.e.,* cumulus theory) refers to the process where crystals homogeneously nucleate within a silicate melt and are deposited at the base of a magma chamber either by gravity-driven settling or convective currents. This process gave rise to the rock name *cumulate* because it was believed the primocrysts crystallized from the melt and *accumulated* on the intrusion floor (Wager and Deer 1939; Wager and Brown 1968; Irvine 1982). Crystal settling first garnered attention because of the noticeable textural similarities between some cumulates
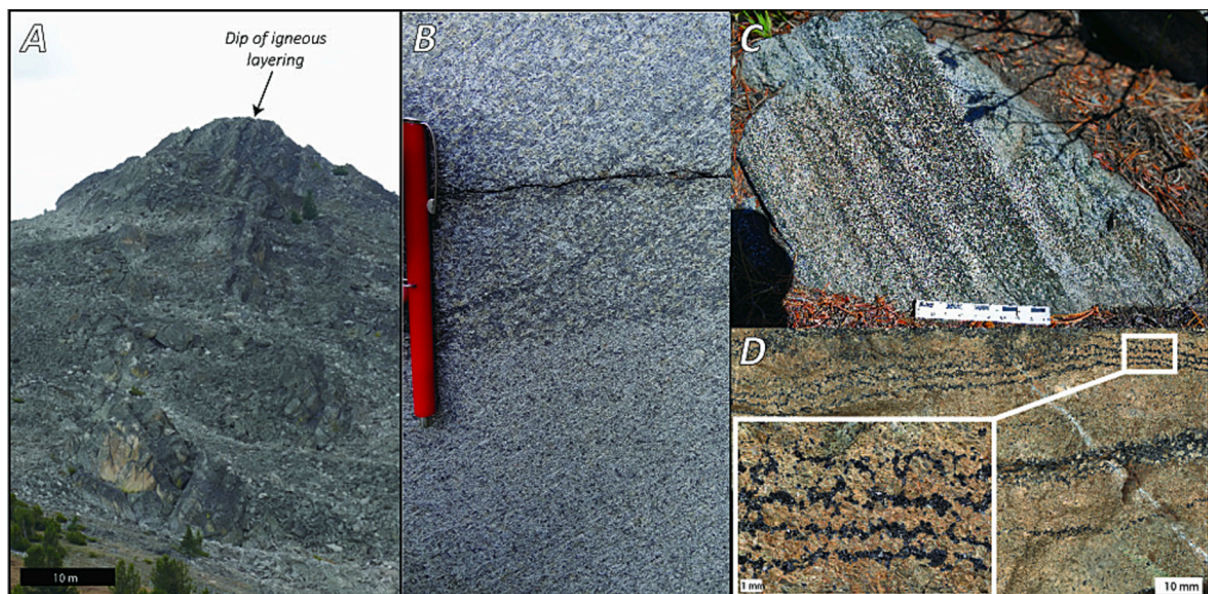
Fig. 1. Photographs of layering at various length scales. **A.** Decimeter-scale igneous layering exposed in the Contact Mountain area of the Neoarchean Stillwater Complex, Montana, USA. Photograph by Chris Jenkins, U.S. Geological Survey, 2023. **B.** A sharp mineralogically-controlled layer contact from the Proterozoic Etoile Suite in Canada (R. Maier et al. 2024). **C.** Fine-scale mineralogically controlled layering in gabbronorites from the Proterozoic Lake Owen Complex, Wyoming, USA. Photograph by Chris Jenkins, U.S. Geological Survey, 2023. Scale bar shows 1 cm tick marks. **D.** Microscopic-scale igneous layering in peridotites from the B chromitite zone of the Neoarchean Stillwater Complex, Montana, USA. Photograph by Chris Jenkins, U.S. Geological Survey, 2024.
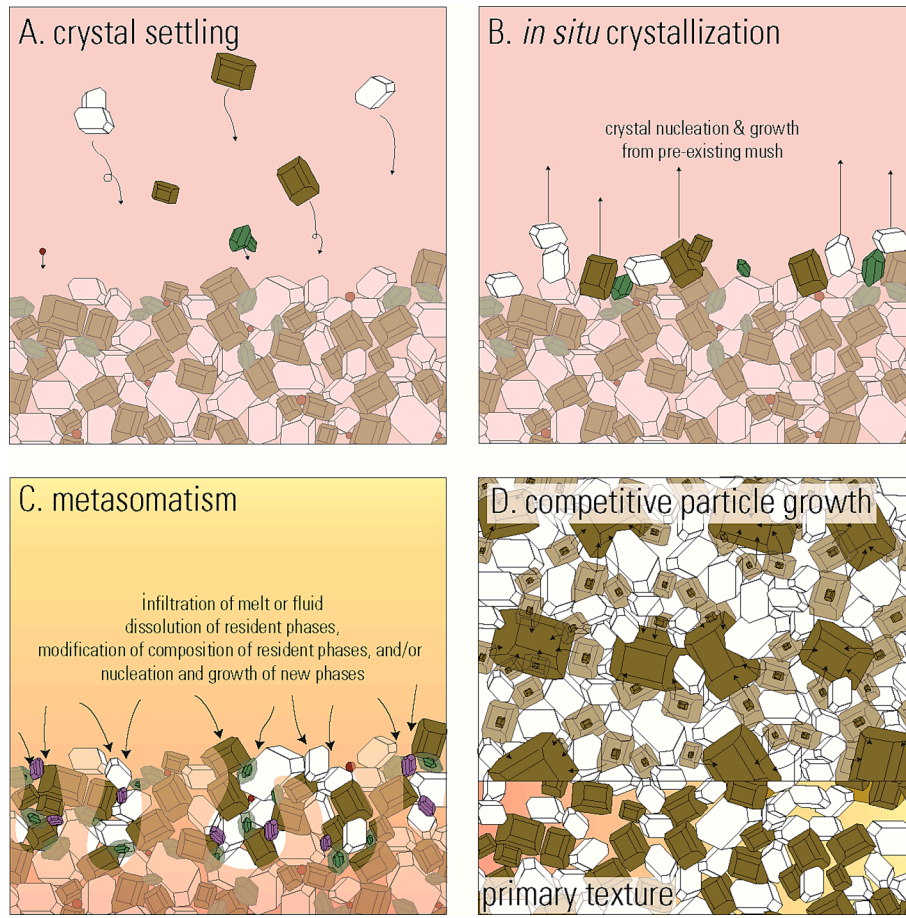
Fig. 2. Cartoon showing various layer forming mechanisms that operate in mafic and ultramafic intrusions as discussed in the text. Hypothetical phases are symbolized as plagioclase (white), orthopyroxene (brown), clinopyroxene (green), olivine (purple), and sulfide liquid (red).

and clastic sedimentary rocks. Indeed, sedimentary structures including cross bedding, graded bedding and slump structures have been documented in layered intrusions including the Precambrian Kiglapait intrusion (*e.g.,* Morse 1969). In addition to the evidence of sedimentary structures preserved in some cumulate rocks, non-cotectic mixtures of cumulus minerals (*e.g.,* Stillwater Complex, Jenkins and Mungall 2018) and monomineralic layering (*e.g.,* Bushveld Complex, Maier et al. 2013; Forien et al. 2015) have been cited as evidence of syn- or post-depositional mechanical sorting of crystals before the crystal mush cools and becomes rigid.

In contrast, layer formation by *in situ* crystallization shares similarities with chemical sedimentary rocks. In the late 1970 s, two seminal papers by Campbell (1978) and McBirney and Noyes (1979) identified several features of layered intrusions that were not compatible with cumulus theory. For example, cumulus theory could not predict how near vertical primary layered sequences containing steeply dipping sequences with apparent sedimentary structures (*e.g.,* cross bedding), observed in the Cretaceous Skaergaard intrusion (Greenland) or the Proterozoic Jimberlana intrusion (Australia), could form. They also pointed out that cumulus theory could not explain how plagioclase crystals—with densities less than the basaltic magmas they are proposed to crystallize from—could settle rather than float (Bottinga and Weill 1970). Further, Campbell (1978) argued that classic nucleation theory posits that the activation energy required for the heterogeneous nucleation of crystals is far less than for homogeneous nucleation. Because of this, heterogeneous nucleation is the much more likely nucleation mechanism operating in layered intrusions. *In situ* crystallization theory suggests that primocrysts heterogeneously nucleate and grow on the outer edges of the intrusion or on pre-existing cumulates (or on a

chamber floor) and grow from the margins of the intrusion inward. In this scenario, nucleation and growth of crystals occur at the interface between the cumulates and the remaining melt (Campbell 1978; McBirney and Noyes 1979). Since that time, overhanging layered sequences in the Merensky Reef (Latypov et al. 2017) and UG1 chromitites (Mukherjee et al. 2017), unidirectional crystal growth patterns (*i.e.,* crescumulate or comb layering; *e.g.,* the Proterozoic Rognsund gabbros from the Seiland Igneous Province in Norway, Robins 1972) and the unidirectional growth of chains of crystals (*e.g.,* UG-2 chromitite of the Bushveld Complex, Latypov et al. 2022) have been cited as evidence in support of this kind of layer-forming mechanism. While crystal settling or *in situ* crystallization may form primary igneous layering during crystal fractionation, metasomatism or competitive particle growth may modify or overprint the original cumulate textures and generate entirely new or different layered successions.

Metasomatism or reactive porous flow refers to the movement of magmatic vapors or fluids through the porous crystal mush layer (*e.g.* McBirney 1987; McBirney and Sonnenthal 1990). Metasomatism occurs when melts or magmatic fluids interact with crystals in the permeable mush layer. This process may change primary mineral chemistry or even the rock type entirely. As crystals accumulate and compact under their own weight or as melts convect in a semi-solid mush zone, the interstitial liquid is forced upwards through the crystal mush (Boudreau and McCallum 1992; Irvine 1980; Latypov et al. 2008; Maier et al. 2021). Tegner et al. (2009) suggest that differential compaction results in variations in trapped liquid content contributing to the modal layering. Others have suggested that the density contrast between overlying dense melts and lower-density melts in the mush may drive infiltration and metasomatic processes in layered intrusions (Kerr and Tait 1985;

McBirney 1995; Jenkins et al. 2021). Yao and Mungall (2022) modelled the formation of the Cr concentration diffusion patterns in the Bushveld's Main Magnetite Layer as the result of metasomatism of a mushy layer of magnetite by an upward percolating melt. These results are of particular interest because they demonstrated how diffusion patterns in an outcrop could be modelled by two distinctly different processes—metasomatism and *in situ* crystal growth. Holness (2024) suggested that fine scale igneous layering in the Stillwater Complex was produced by the percolation and crystallization of silicate melt in a slowly cooled cumulate pile aided by competitive particle growth. These examples demonstrate that different layer forming mechanisms may operate in conjunction.

Competitive particle growth (*i.e.,* Ostwald ripening, textural coarsening, crystal aging) theory suggests that small crystals will dissolve at the expense of large crystals to minimize interfacial energies and achieve textural equilibrium. It has been suggested that such a process can lead to fine-scale layering over long cooling times in layered intrusions because crystal aging occurs at different rates for different phases (Boudreau 1995). Such postcumulus textural equilibration mechanisms have been evoked to explain highly regular fine-scale layering features in layered intrusions including the so-called inch-scale doublet layering in the Stillwater Complex (*e.g.,* Boudreau 1995; Holness 2024). To some extent, this process likely occurs in very slowly cooled layered igneous rocks as demonstrated by their propensity to have equilibrated textures (*e.g.,* 120-degree dihedral angles at monomineralic triple junctions). The effects of the textural maturation process may make it difficult to discern between layer-forming processes because primary igneous textures can be overprinted or even obliterated.

Still, other layer forming processes may operate to create primary or secondary layering. Physical processes operating in magma chambers like magma density currents (*e.g.,* Higgins 1991) or viscous particle segregation in response to slumping of the cumulate mush (Forein et al. 2015) have been invoked to modify primary igneous fabrics or generate sequences of modally layered cumulates, respectively.

2. Debates and controversies

Debates, controversies, and advancements in layered intrusion research have recently been detailed by Latypov et al. (2024a) and as such, we only briefly outline a few issues of contention here. Construction mechanisms remain a controversial topic, with researchers debating whether layered intrusions are the product of large molten magma chambers or mushy systems constructed episodically through repeated sill injection. Key observations driving this debate include the lack of geophysical evidence for magma chambers in the upper crust (Cashman et al. 2017) and the fact that high-precision U-Pb zircon geochronology has revealed that some layers of the Bushveld, West-Pana, and Stillwater complexes are younger than overlying layers (Mungall et al. 2016; Groshev and Karykowski 2019; Scoates et al. 2021). Although there are several studies that infer the non-sequential construction of sill complexes (Marsh et al. 2003; Wilson et al. 2016; Smith et al. 2021) and layered intrusions (Harker 1909; Mitchell and Scoon 2012; Hepworth et al. 2018; 2020; Yao et al. 2021) on other grounds, it remains uncertain as to whether ages derived from geochronology of zircon and baddeleyite hosted in long-lived and (possibly) once mushy layers are truly representative of their host rock crystallization ages (Latypov and Chistyakova 2022). Researchers are continuing to address these debates by thoroughly examining field relationships (Latypov et al. 2022), applying geophysical mapping approaches to the plumbing systems beneath layered intrusions (Cole et al. 2024) and by examining (post-)cumulus processes from the perspective of expansive geochemical datasets (Barnes and Wiliams 2024).

Since the seminal study of Wager et al. (1960), textures of igneous cumulates have been used to infer a variety of magmatic processes in layered intrusions that are expounded in Latypov et al. (2024a; 2024b). One longstanding debate concerns the mechanisms by which planar alignments of cumulus crystals, that were initially interpreted as strong evidence for crystal settling, develop. This phenomenon has since been attributed to *in situ* crystallization (McBirney and Noyes 1979), post-cumulus processes such as compaction (*e.g.,* Meurer and Boudreau 1998), and remobilization or deformation of poorly consolidated crystal mush (Higgins 1991; Irvine et al. 1998; O'Driscoll et al. 2008). Another ongoing debate regards the nucleation and growth of chromite in chromitites, where Holness et al. (2023) showed that the long-accepted mechanism of 'self-nucleation' of chromite crystals (Campbell 1978; Godel et al. 2013; Prichard et al. 2015) was energetically unreasonable. It seems likely instead that the common observation of chromite crystals forming interconnected networks in such rocks is a result of physical aggregation (*i.e.,* synneusis) or an alternative mechanisms of nucleation (*i.e.,* secondary nucleation; Latypov et al. 2024b).

Several debates surround the origin of chromitite-anorthosite relationships and reef-style platinum-group element (PGE) mineralization in layered intrusions. Some researchers argue that coupled chromitite-anorthosite units result from the flux melting of partially molten gabbroic cumulates, whereby chromite becomes supersaturated as Cr_2O_3 and Al_2O_3 are liberated (Nicholson and Mathez 1991; Marsh et al. 2021). Alternatively, these units may form through partial melting of gabbroic cumulates by replenishing melts (O'Driscoll et al. 2009; Scoon and Costin 2018; Jenkins et al. 2021), consistent with the lack of accessory olivine and late-stage volatile-bearing phases in these horizons. So-called *boulders* in the Boulder Bed of the Bushveld Complex could be an exception because several exhibit features consistent with volatile involvement, such as amphibole rinds (Smith et al. 2023). Reef-style PGE mineralization derived from upwelling magmatic volatiles requires that the PGE and base-metals are liberated from an underlying cumulate pile and reconcentrated in laterally extensive stratiform horizons (Boudreau 2019 and references therein). Proponents of this model report a relative increase in the abundance of Cl-rich halogen-bearing phases (Boudreau et al. 1986), melt inclusions hosting late-stage silicates (Ballhaus and Stumpfl 1986), and bulk Cl/Br values (Parker et al. 2022) at the level of mineralization. On the other hand, relative Cl enrichments could reflect devolatilization of fractionating sulfide melts (Mungall and Brenan 2003; Liu et al. 2021) and melt inclusions may sample compositional boundary layers that are not representative of the original melt (Faure and Schiano 2005). Recent experimental work has shown that Cl-rich magmatic brines and (or) carbonic fluids are capable of transporting ore-forming concentrations of Pt, Pd and Au (Simakin et al., 2021; Sullivan et al., 2022a, 2022b). However, there is presently no compelling evidence that Ni and the iridium-group PGE can be effectively transported in these media, which is at odds with Ni/Cu and Pd/Ir values recorded in reef-style occurrences. In the Merensky Reef, chromitite-hosted orthopyroxene crystals have relatively low H_2O concentrations compared to orthopyroxene from the bracketing lithologies (Tang et al. 2023). More experimental studies are required to better constrain the solubility of noble metals in magmatic phases, which should be coupled with bulk and *in situ* (*e.g.,* primocrysts, accessory phases) measurements of volatiles species.

3. Drivers and biases inferred from scientometrics

In layered intrusion research, the number of scientific articles available online has been increasing since the 1950 s and rapidly increased over the 2010 s, possibly influenced by invention of *Google Scholar* (Fig. 3A). Recent articles and their supplementary materials are generally more accessible, which caters to a recency bias in which one overemphasizes the relevance of recent information over older information (Mayo and Crockett 1964). This can ultimately lead to misinformation by transmission chaining, and as such, one should always revisit the earliest works. Other inherent biases in scientific research include apophenia (*i.e.,* the tendency of identifying meaningful patterns where none truly exist; Jones and Martin 2021) and confirmation bias (*i.e.,* the tendency to interpret data in a way that is supportive of existing
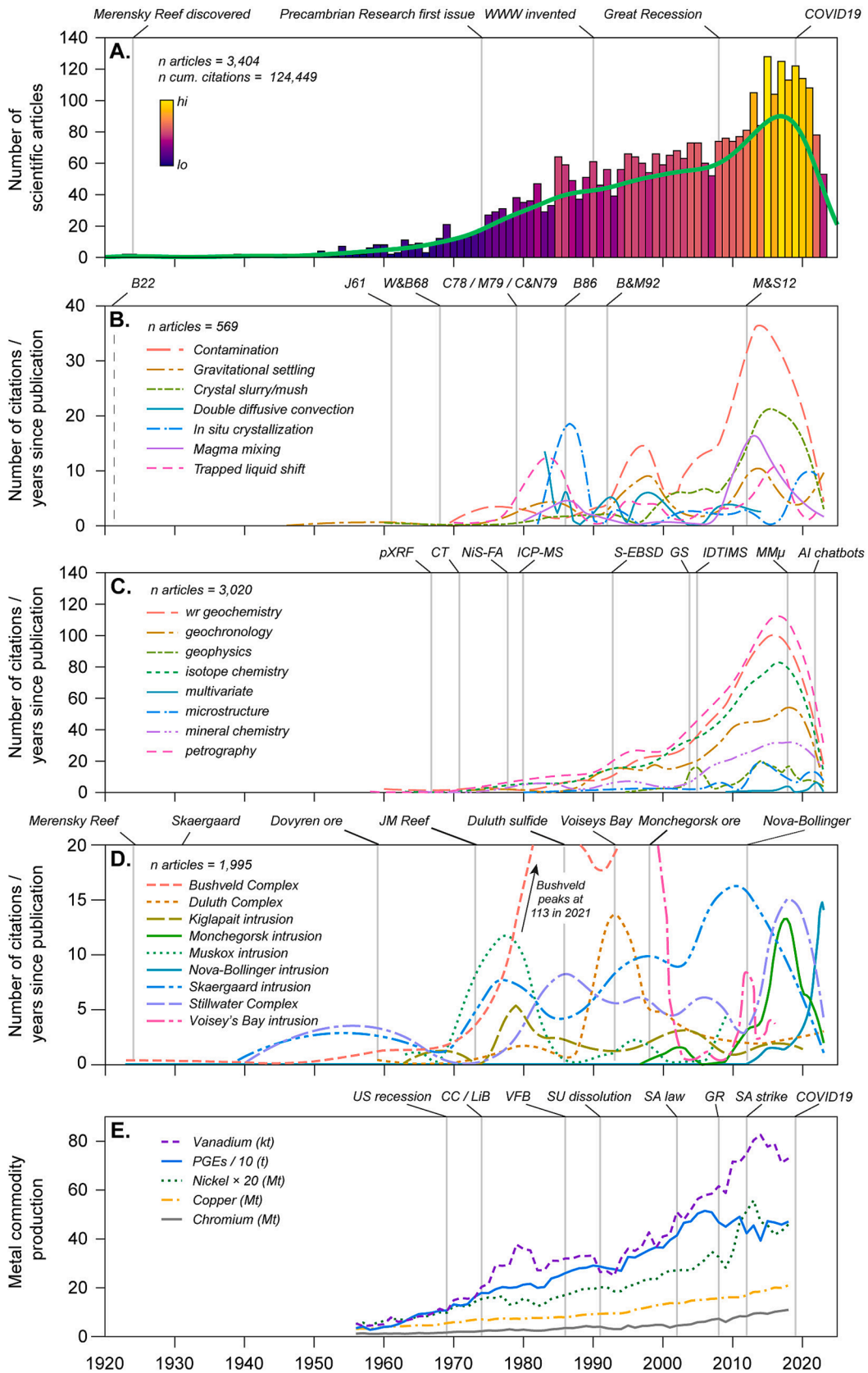
(caption on next page)

Fig. 3. Layered intrusion research over the last century. A. Number of scientific articles (n = 3,404) published for the selected intrusions (ESM 1). B. Number of citations for year 'x' by years since year 'x' for articles pertaining to seven important processes. Note the rise in reference to 'crystal mush' and the coeval fall in reference to 'gravitational settling' and 'magma mixing'. Vertical lines correspond to the publication of influential articles, including: Bowen (1922), Jackson (1961), Wager & Brown (1968), Campbell (1978), McBirney and Noyes (1979), Campbell and Naldrett (1979), Barnes (1986), Boudreau and McCallum (1992), and Mitchell and Scoon (2012). C. Number of citations for year 'x' by years since year 'x' for articles that utilize important methods in layered intrusion research. Note the co-occurrence of petrography and whole-rock geochemistry, as well as the recent rise in microstructural and multivariate analyses. Vertical lines correspond to the advent of important technologies and online resources. D. Number of citations for year 'x' by years since year 'x' for articles pertaining to ten notable intrusions. Note the dominance of the Bushveld Complex as well as post-discovery research peaks for the Stillwater, Duluth, Voisey's Bay, and Nova-Bollinger. Vertical lines represent important discoveries in the field. E. Global production of metals known to occur in layered intrusions. Note that for scaling reasons, PGE tonnages have been divided by 10 and Ni tonnages have been multiplied by 20. Vertical lines correspond to events that may have influenced metal price and production [modified from Zientek et al. (2014) and Jowitt et al. (2020)]. The data and a detailed explanation for constructing the diagram also provided in ESM 1. Abbreviations/acronyms, WWW = world wide web, GS = Google Scholar, AI = artificial intelligence, VW = Vietnam War, CC = catalytic converters, LiB = Li-ion battery, VFB = Vanadium flow battery, SU = Soviet Union, SA = South Africa, GR = Great Recession.

beliefs; Klayman 1995). In general, these biases stem from the human tendency to find immediate reward in confirming one's own hypothesis – consistency is often conflated with correctness. The influence of such biases may be muted through interdisciplinary collaborations and thorough peer-review processes as well as greater data transparency and reproducibility (Jones and Martin 2021).

The popularity of important petrogenetic processes has changed over time, likely influenced by seminal publications, technological advancements and new discoveries (Fig. 3B). Oftentimes, popularized concepts become amplified in subsequent literature, which is partly a consequence of anchoring and availability biases (Yasseri and Reher 2022). For example: (i) mentions of *crystal settling* decrease at the turn of the century, coinciding with a rise in the mentions of *crystal mush*; (ii) mentions of *crystal settling* and *in situ crystallization* have somewhat antithetical trends over time; (iii) *double diffusive convection* was only mentioned to a large extent in the 1980 s; (iv) mentions of *trapped liquid shift* and *in situ crystallization* spike shortly after the publication of Barnes (1986) and Campbell (1978), respectively. These biases could generally be easily mitigated through collaborative research, peer-review and robust statistical examination of interdisciplinary datasets.

Unlike concepts, research methodologies employed to better understand layered intrusions have remained broadly unchanged (Fig. 3C). Fundamental methods such as petrography, geochemistry, and isotope geochemistry have been a staple of layered intrusion research, bolstered by geochronology and mineral chemistry. Studies utilizing *mineral chemistry* increased rapidly during the 2000 s, perhaps due to accessibility and/or technical advancements. Geophysics, microstructural data and multivariate analysis are becoming increasingly utilized in layered intrusion research, suggesting that these analytical methods will play an important role in the future of layered intrusion research. Technological advancement and software development have meant that data are becoming increasingly accessible and, as such, interdisciplinary studies are becoming increasingly common in layered intrusion research. Many studies on layered intrusion research are published in *Journal of Petrology* and *Contributions to Mineralogy and Petrology* consistent with the fact that most studies focus heavily on petrology. *Economic Geology* and *Mineralium Deposita* are also commonly utilized journals, highlighting that many studies focus on ore-forming processes that operate during layered intrusion formation (ESM 1).

Large and/or strongly mineralized layered intrusions receive greater attention than smaller and/or apparently barren intrusions (ESM 1). This is unsurprising given that the mineral potential of layered intrusions is an important reason many institutions are able to study them. Commercial interest generates extensive geophysical and geochemical data on a subject intrusion, whilst driving the drilling programs necessary for sampling campaigns. This is exemplified in what we refer to as post-discovery peaks (Fig. 3D), including: (i) studies on the J-M Reef of the Stillwater Complex increase shortly after discovery, broadly coinciding with the invention of catalytic converters and Ni-sulfide fire assay; (ii) studies on Voisey's Bay peak shortly after its discovery in the 1990 s; (iii) studies on the Skaergaard intrusion increase after the discovery of the Platinova Reef; (iv) research on the Duluth Complex spikes

shortly after PGE-rich sulfides were discovered in the South Kawishiwi intrusion; (v) research on Nova-Bollinger spikes a few years after its discovery in 2014. Notwithstanding their size and economic significance, other reasons why certain layered intrusions are more widely reported than others include accessibility, as well as their degree of alteration, deformation and exposure. The tendency to study specific intrusions unavoidably leads to reporting and sampling biases; observations from a few intrusions dominate the literature and are somewhat indiscriminately extrapolated to intrusions from other eras and geological settings (*i.e.,* generalizability; Simundic 2013; Andringa and Godfroid 2020). Such biases can be partially mitigated by considering multiple analogous subjects (*e.g.,* intrusions, mineral occurrences) in scientific contributions as opposed to centering on a single subject.

4. Layered intrusions in the framework of the Precambrian

The emplacement of layered intrusions in the Precambrian broadly correlates with supercontinent assembly and disassembly, which, in turn, correlates with enhanced periods of juvenile crust production and crustal reworking (Fig. 4A-E; Maier and Groves 2011; Dhuime et al. 2012; Smith and Maier 2021). Moreover, their occurrence generally correlates with episodes of large igneous province (LIP) magmatism (Ernst et al. 2021), and as such, periods of crustal thickening and enhanced magmatic activity appear most favorable for layered intrusion formation. The earliest period of enhanced layered intrusion emplacement occurs from 3.0 to 2.7 Ga, and primarily corresponds to the West Pilbara (Australia; *e.g.,* Munni Munni, Andover, Radio Hill) and Murchison Domain (Australia; *e.g.,* Windimurra, Narndee) intrusions, as well as other notable intrusions such as Stella (South Africa), Monts de Cristal (Gabon), and Fiskenæsset (Greenland). This interval is significant in Earth history as it follows the broadly accepted interval of global-scale subduction initiation (Palin et al. 2020), precedes the assembly of the Superia-Sclavia (or Kenorland) supercontinents (Nance et al. 2014), and correlates with a ramp-up in large igneous province magmatism (Ernst et al. 2021) as well as crustal production and differentiation (Hawkesworth et al. 2010; Dhuime et al. 2015). This newly evolving crust would have interacted with upwelling komatiitic melts generated during relatively voluminous melting (>25 %) in a hotter Archean mantle, leading to the production of siliceous high-Mg basalts that are believed to be parental to many Archean layered intrusions (West Pilbara intrusions, Hoatson and Sun 2002; Stillwater Complex, Jenkins et al. 2021).

The second period of enhanced layered intrusion emplacement occurs from approximately 2.5 to 2.4 Ga, and includes intrusions associated with the Baltic (*e.g.,* Monchegorsk, Kemi, Penikat) and Matachewan (*e.g.,* East Bull Lake, Agnew, River Valley) LIPs. This interval spans the earliest stages of the Great Oxidation Event (GOE), where it correlates with increasing crustal production and differentiation. It has been proposed that this period also coincides with a sharp increase in mineral species resulting from oxidation and biological mediation (Hazen et al. 2008), as well as the cooling of ambient mantle (*i.e.,* Great Thermal Divergence; Condie et al. 2016). Contaminated komatiitic melts are still
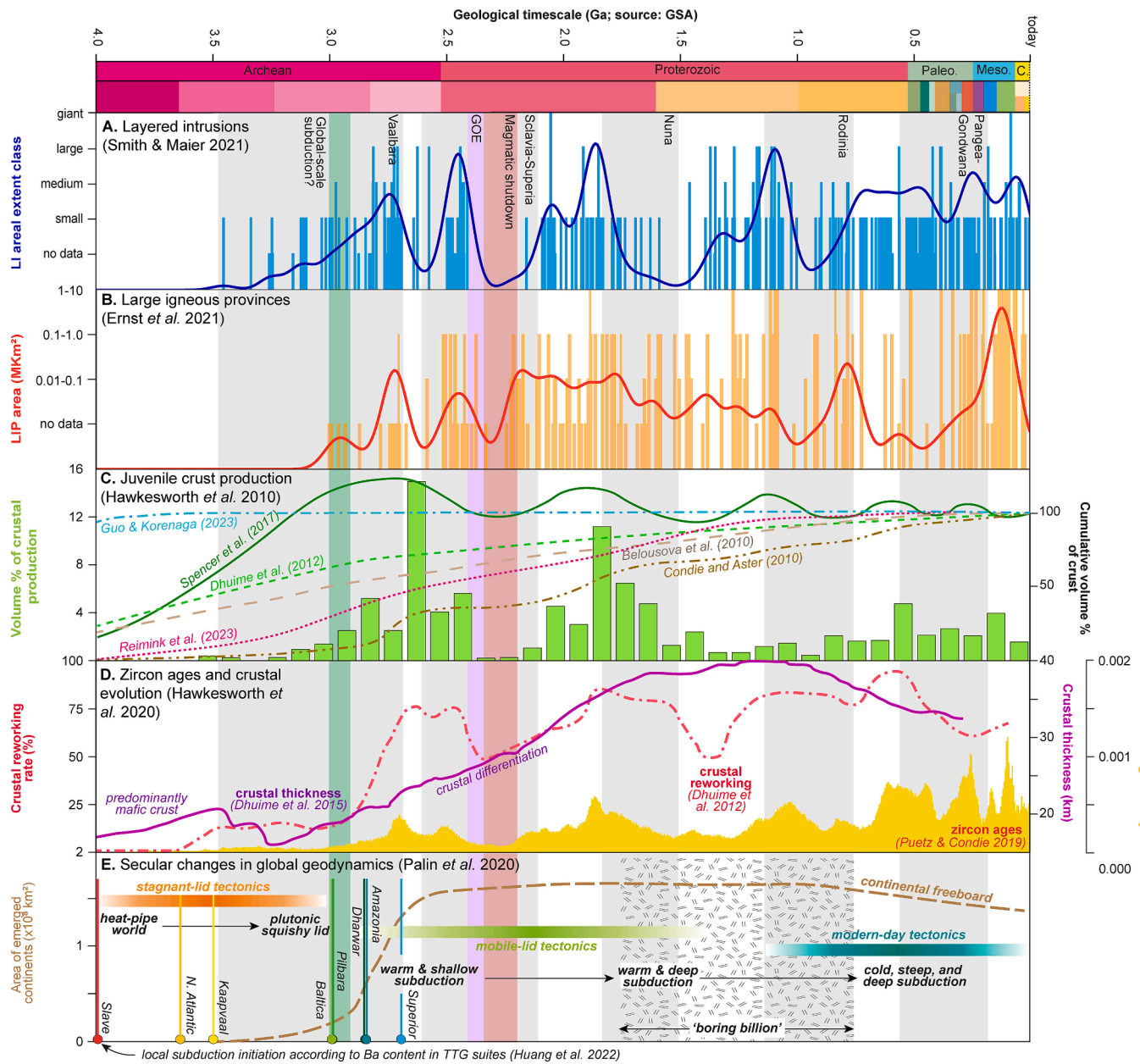
Fig. 4. Summary of magmatism, crustal evolution, and tectonic regimes throughout geological history. A. Emplacement ages of layered intrusions categorized by size class (Smith and Maier 2021). B. Emplacement ages of large igneous provinces (LIPs) categorized by size class (Ernst et al. 2021). C Juvenile crust production (Hawkesworth et al. 2010) overlain by several crustal production models. D. Zircon ages (Puetz and Condie 2019) together with rates of crustal reworking and evolving crustal thickness (Dhuime et al. 2012; 2015). E. Global geodynamics with the continental freeboard (Bada and Korenaga 2018) and ages of local subduction initiation according to Ba contents of TTG suites (Huang et al. 2022). Plots are underlain by supercontinent ages (Bradley 2008; 2011; Nance et al. 2014), global subduction initiation (Palin et al. 2020), and the Great Oxygenation Event (GOE).

interpreted as being parental to many of these intrusions (Agnew, Vogel et al. 1999; Karelian intrusions, Guo et al. 2023), and relatively high degrees of crustal assimilation may have been facilitated by thicker and more fusible siliceous crust (Dhuime et al. 2015). With the exception of the 2.1–2.2 Ga Sandikounda Layered Complex (Senegal; Dia et al. 1997), there are no known layered intrusions emplaced shortly after the GOE (2.4 to 2.2 Ga), particularly now that the emplacement age of the Bacuri Layered Complex (Brazil) was recently revised from ~ 2.2 to ~ 3.3 Ga (Ferreira Filho and Araujo 2009; Spier et al. 2024). The global-scale episode of magmatic quiescence that followed the GOE is known as the 'magmatic shutdown' and has recently been reinterpreted as the result of a ~ 2.7 Ga mantle overturn event (Condie et al. 2022a). The lull in magmatic activity is strongly evidenced in the known layered

intrusion record, yet less apparent in the LIP record which only stalls between 2340 to 2260 Ma (Condie et al. 2022a).

Magmatic activity apparently resumed sometime between 2.1 and 2.0 Ga, with the emplacement of the world's largest known igneous intrusion, the Bushveld Complex, and its associated intrusions (*e.g.,* Uitkomst, Molopo Farms Complex, Losberg) at ~ 2.05 Ga. This is followed by a peak in layered intrusion emplacement at ~ 1.8 Ga during the assembly of the supercontinent Nuna (or Columbia), primarily corresponding to intrusions in the Scandinavian Kotalahti and Vammala Nickel Belts (*e.g.,* Rytky, Ylivieska, Kaipola) as well as those in east Kimberley (*e.g.,* Panton, Savannah, Springvale). There are relative increases in the rate of juvenile crust production at ~ 2.05 Ga and ~ 1.8 Ga (Hawkesworth et al. 2010; Spencer et al. 2018), and crustal

reworking rates also relatively increase at ~ 1.8 Ga (Dhuime et al. 2012). Global spikes in the production of mafic–ultramafic intrusions (layered or not) that host some degree of magmatic Ni-Cu-PGE sulfide mineralization also occur at ~ 2.05 and ~ 1.8 Ga, which seemingly manifest in areas of localized extension within overall contractional tectonic systems (Begg et al. 2010; Pehrsson et al. 2016; Smith and Maier 2021). This metalliferous period is followed by a relative paucity in magmatic Ni-Cu-PGE sulfide occurrences and layered intrusion emplacement despite no apparent lull in large igneous province magmatism (Pehrsson et al. 2016; Ernst et al. 2021). There are, however, relative decreases in crustal production and reworking rates indicative of cratonic stability, which may result in the absence of localized extensional environments favorable for layered intrusion emplacement.

The period of 1800 to 800 Ma is colloquially referred to as the "boring billion" due to prolonged tectonic stability, climatic stasis and a slowing of biological evolution (Santosh and Groves 2023). Also, during this period there is a relative reduction in the number of passive margins (Bradley 2008) and arc magmatism (Liu et al. 2019) which, in turn, led to an apparent reduction in ore deposits related to subduction-related convergent margins (Santosh and Groves 2023). There is a peak in layered intrusion emplacement during the assembly of Rodinia (1.2–1.1 Ga), which includes intrusions of the Giles Complex (*e.g.,* Jameson Range, Gosse Pile, Kalka), the Midcontinent Rift System (*e.g.,* Duluth, Sonju Lake, Coldwell), and the alkaline Greenlandic intrusions (*e.g.,* Ilímaussaq, Klokken). Interestingly, each of these magmatic provinces are associated with failed rift systems (*e.g.,* Ngaanyatjarra Rift, Midcontinent Rift, Gardar Rift), which manifest at the time the crust was particularly thick and buoyant (Dhuime et al. 2015; Santosh and Groves 2023). The 1.2–1.1 Ga emplacement peak is followed by a sharp reduction in LIP magmatism and layered intrusion emplacement, as well as a shallow reduction in crust thickness and production (*i.e.,* erosion rates exceed crust production rates for the first time; Dhuime et al. 2015). There is a relative increase in layered intrusion emplacement towards the end of the Proterozoic, correlating with the break-up of Rodinia and assembly of Gondwana (Smith and Maier 2021). Several of these intrusions were emplaced during the course of the Brasiliano (*e.g.,* Mangabal, Americano do Brasil, Canindé) and Pan African (*e.g.,* Laouni, Motaghairat, Korab Kansi) orogenies, coinciding with a relative peak in crustal reworking rates characteristic of supercontinent construction (Dhuime et al. 2012).

5. Mantles, melts and magmas

Magmas parental to layered intrusions originate in the mantle and evolve *en route* through the crust; *primary melts* refer to melts extracted from the mantle source and *parental melts* refer to the melt from which the layered intrusion forms. Henceforth, the nature of the mantle (*e.g.,* composition) and the conditions under which it melts (*e.g.,* pressure, temperature, volatile content) are first order controls on the nature of primary melt that may eventually form a layered intrusion. The diversity of parent melt compositions proposed for layered intrusions suggests that these conditions vary; putative parent melt compositions include contaminated komatiitic melts (Maier et al. 2016; Solovova et al. 2021; Jenkins et al. 2021), picritic melts (Emeleus et al. 1996; Duchesne et al. 2004), basaltic melts (Namur et al. 2010; Bai et al. 2019), and alkali basaltic melts (Upton et al. 1996). It is widely accepted that high-degree partial melts are required to produce a layered intrusion with magmatic sulfide mineralization, as these conditions are required to ensure total liberation of chalcophile metals as well as a significant amount of Ni from the mantle source (Naldrett 2004). However, relatively low-degree fertile melts may be produced in the subarc mantle where Ni may be concentrated in relatively fusible phases (phlogopite, amphibole, apatite) as opposed to refractory olivine (Straub et al. 2011; Ezad et al. 2024). That said, the convecting mantle and the subcontinental lithospheric mantle (SCLM) are the two more commonly invoked mantle sources for the melts parental to layered intrusions (Maier and Groves 2011) yet distinguishing between these sources has remained a matter of contention.

The convecting (asthenospheric) mantle must be anomalously hot relative to ambient mantle to undergo extensive near-adiabatic melting beneath thick continental lithosphere (*i.e.,* a position with limited decompression). The anomalous heat required is oftentimes explained by the involvement of a mantle plume originating at the core-mantle boundary (Koppers et al. 2021 and references therein). The core-mantle boundary is thought to be a mixture of primordial mantle material, depleted mantle material, subducted lithospheric plates and perhaps even material entrained from the core, with the relative proportions of these materials at this interface not necessarily having remained constant through geological time (Koppers et al. 2021; Condie et al. 2022b). This lithological heterogeneity is interpreted as being represented in the diverse trace element and isotopic signatures of upwelling plumes (Hastie et al. 2016, Koppers et al. 2021). Partial melting of plumes initiates in the upper mantle, where the composition of the melt is largely controlled by stabilities of simple mineral assemblages. The bulk of the convecting mantle has a major element composition that, under upper mantle conditions, is characterized by a peridotitic mineral assemblage of olivine + orthopyroxene ± clinopyroxene and an aluminous phase (plagioclase < 0.9 GPa, spinel at 0.9–3 GPa, and garnet at > 3 GPa; Arndt et al. 2005). A relatively minor proportion of the convecting mantle is pyroxenitic, and is relatively fusible compared with peridotite, as it is mainly composed of clinopyroxene + garnet ± minor olivine and spinel (Hirschmann et al. 2003, Lambart et al. 2013). Plumes derived from the convecting mantle have sourced several LIPs (Brown et al. 2022; Pierru et al. 2022) and layered intrusions (Hoatson and Sun 2002; Arndt 2013; Guo et al. 2023). Identifying a plume source is not a trivial task as the heterogeneities in the core-mantle boundary and possible subsequent assimilation of crustal materials can affect primary melt isotopic and trace element compositions so that they become largely indistinguishable from other mantle-derived melts (Campbell 2001; Arndt 2013). For this reason, multiple chemical proxies are required to conclusively constrain the mantle source of a layered intrusion. As an example, calculated parental melts together with Sr, Nd, and Os isotopic as well as trace element and PGE systematics were used to conclude a mantle plume source for most of the 2.5–2.4 Ga Baltic layered intrusions in the Finnish Lapland (Yang et al. 2016; Guo et al. 2023). In a similar manner, various isotope systems were used in tandem by Day et al. (2008) to infer a mantle source unaffected by long term depletion or recycled crustal components for the ~ 1.27 Ga Muskox layered intrusion, Canada.

The SCLM represents subcratonic buoyant residue that formed as a result of ancient melting events in the convecting mantle, generally agreed to have occurred in the Archean (3.5 to 3.0 Ga; Arndt et al. 2009; Griffin et al. 2013). Following melt extraction, the convecting mantle protolith became depleted (*i.e.,* removal of incompatible elements) lherzolite, harzburgite and possibly dunite. The residual SCLM is refractory and unlikely to experience high degrees of partial melting itself. However, it is theorized that the composition of the SCLM has evolved as the ambient mantle has cooled through time, becoming decreasingly refractory from the Archean to the present day (Griffin et al. 2009). In addition, SCLM xenoliths have shown evidence for infiltration by melts or supercritical fluids from various sources, which introduce relatively fusible components (*e.g.,* alkalis, volatiles; Griffin et al. 2009). The SCLM may be infiltrated by kimberlite or carbonatite melts from the underlying mantle, a cocktail of devolatilized supercritical fluids, and/or partial melts from subducting lithospheric slabs, low-degree partial melts from less refractory mantle, or a combination of all of these (Griffin et al. 2009; Howarth et al. 2014). The aforementioned processes act to form SCLM variants that contain higher abundances of relatively fusible phases; *e.g.,* containing assemblages such as "MARID" (mica, amphibole, rutile, ilmenite and diopside) and "PIC" (phlogopite, ilmenite, and clinopyroxene) have been recorded in mantle xenoliths (Fitzpayne et al. 2018). The melting of metasomatized SCLM would

produce compositionally diverse primary melts that may ultimately form layered intrusions; however, the fertility of such melts is a matter of debate (refer to Arndt 2013). A SCLM mantle source for the Bushveld Complex has been invoked by several researchers to explain the relatively Pt-rich nature of associated fine-grained rocks (Sharpe 1981; Maier and Barnes 2004) as well as the radiogenic Re-Os isotopic signature of Merensky platinum-group minerals (PGM) (Hart and Kinloch 1989; Schoenberg et al. 1999). However, it is broadly accepted that these observations can be explained by primary melts interacting with SCLM and/or continental crust (Arndt, 2013; Barnes et al., 2010; Günther et al., 2018; Yudovskaya et al., 2017).

To identify the mantle source and melting conditions that formed a layered intrusion, it is important to constrain its parental melt composition. Igneous petrologists utilize the cumulates comprising layered intrusions as well as associated fine-grained units (*i.e.,* chilled margins, hypabyssal intrusions, associated volcanic rocks) to constrain the nature of the parent melt and, thus, infer the physicochemical state of the mantle from which it derived. It should be noted, however, that primary melts may experience variable degrees of differentiation, magma mixing and/or contamination as they traverse the crust, which should be considered in detail, and possibly amended, before making the parental to primary melt connection. Parental melt compositions have been approximated using several methods, including: (1) weighted average summation of the layers of the intrusion (*i.e.,* bulk composition; Morse 1981; Naslund 1989); (2) considering the compositions of associated fine-grained rocks as parent melt analogues (Miller and Ripley 1996; Barnes et al. 2010; Virtanen et al. 2022); (3) using the compositions of cumulus minerals, with or without corresponding bulk-rock chemistry, together with parameterized Nernst partition coefficients (Bédard 1994; Godel et al. 2011a); (4) measuring the compositions of cumulus mineral-hosted melt inclusions (Spandler et al. 2000; 2005).

Method (1) utilizes the rocks of the layered intrusion itself; however, it requires an extensive whole-rock and mineral chemistry dataset to sufficiently constrain the relative proportions and compositions of the different rock types. This method further requires that the intrusion has a well constrained geometry, hosts 'wholesale' the crystallized products of the parental melt (*i.e.,* residual melt was not expelled), and that different magma pulses are properly identified and accounted for. For these reasons, this method is most effective for intrusions that formed in a closed system, such as the Kiglapait intrusion (Morse 1981). Morse (1981) reports the summed bulk composition of the Kiglapait intrusion; a S-undersaturated, high-Al and −Fe basaltic composition that was similar to the composition of the chilled margins from the associated Hettasch (Berg 1980), Barth Island (de Waard 1976), and Jonathon (Berg et al. 1994) intrusions. Fine-grained rocks later discovered at the southern margin of Kiglapait were also found to be comparable to the summed bulk composition and led to a refinement of the putative Kiglapait parent melt composition (Morse and Nolan 1985; Nolan and Morse 1986). Based on subsequent trace element and isotopic work, Fourny et al. (2019) proposed that the Kiglapait parent melt represented 25–30 % partial melting of mantle harzburgite that assimilated small proportions (~5%) of lower crustal material. Utilizing Method (4), Fourny et al. (2019) showed that the parent melt had a slight enrichment in incompatible elements, with negative Th-U anomalies and positive Ba-Pb-Sr anomalies. The approximated trace element composition is similar to that of marginal rocks from the Kiglapait (Morse and Nolan 1985; Nolan and Morse 1986) yet is less evolved than marginal rocks of the Hettasch intrusion (Berg et al. 1994). This is in line with the conclusions of Morse (1981), who argued that the Hettasch and Kiglapait primary melts were distinct, as opposed to sharing a genetic lineage, on the basis of incompatible element concentrations inconsistent with fractionation or contamination.

Method (2) assumes that some fine-grained mafic–ultramafic rocks associated with a layered intrusion are relatively rapidly cooled fractions of cogenetic melt that have experienced negligible differentiation upon cooling. As such the rock composition is representative of the parental melt or of a more evolved composition on the liquid line of descent, which can potentially be computationally back-fractionated to infer its original composition. It is important that researchers account for the presence of entrained minerals (primocrysts or xenocrysts; *e.g.,* Marsh et al. 2003) and/or the influence of *in situ* crustal contamination (*i.e.,* by adjacent country rocks; *e.g.,* Mungall et al. 2010), that may lead to erroneous approximations of parental melt composition. It should also be noted that especially adjacent to marginal reversals (*i.e.,* where the rocks towards the margin are more evolved) of layered intrusions, original chilled margins are often disturbed or even replaced by more evolved secondary pseudo chilled margins (*e.g.* Latypov et al. 2007).

Chills within, and fine-grained sills associated with, the Bushveld Complex range from komatiitic to high-Mg basaltic-andesitic to basaltic (Sharpe 1981; Irvine and Sharpe 1982; Barnes et al. 2010; Wilson 2012; Maier et al. 2016). Hamlyn and Keays (1986) highlighted similarities between these fine-grained rocks and boninites; however, it is presently broadly accepted that these rocks derived from contaminated komatiitic melts (*i.e.,* siliceous high-Mg basalts or SHMB), based on independent lines of evidence (Barnes 1989; Eales and Costin 2012; Maier et al. 2016; Mansur and Barnes 2020; Solovova et al. 2021). Comparable parent magmas are proposed for many layered intrusions worldwide, but the uniquely low Pd/Pt values of the Bushveld marginal rocks require that the primary melt assimilated a fusible SCLM component (Barnes et al. 2010). Several studies have suggested that the Midcontinent Rift flood basalts are cogenetic with the Duluth Complex layered intrusions based on their spatiotemporal connection and geochemical evidence (*e.g.,* Miller and Weiblen 1990; Miller and Ripley 1996; Swanson-Hysell et al. 2021). These rapidly cooled volcanic rocks suggest a common lineage from high-Al olivine tholeiitic melts with the lavas and intrusive rocks experiencing variable amounts of fractionation *en route* to emplacement level (*e.g.,* Miller and Weiblen 1990; Miller and Ripley 1996; Swanson-Hysell et al. 2021; Virtanen et al. 2022). Based on major and trace element modelling, it has been suggested that the earliest flood basalts formed from a high-T mantle plume (mantle potential temperature ca. 1480–1630 °C) but that the temperature had cooled nearly to the ambient mantle conditions (ca. 1400–1450 °C) during the formation of the Duluth Complex (Brown et al. 2022). The same models reveal continuous thinning of the lithosphere from about 60–100 km to 45–65 km during the magmatic event and rapid movement of the lithosphere, leading to the spatial disconnection between the rift and the plume (Brown et al. 2022).

Method (3) postulates that the Mg# value of a parent melt can be approximated from olivine-only (or orthopyroxene-only) cumulates using the method of Chai and Naldrett (1992), which may be extrapolated to other cumulates so long as the other cumulus phase can be subtracted from the corresponding whole-rock composition (Li et al. 2000; Smith et al. 2024). Since this approach determines the most evolved melt capable of crystallizing the most forsteritic olivine measured, it is recommended to use the approach in conjunction with Method 2. Trace element concentrations of the parental melt may be approximated by assuming chemical equilibrium between a cumulus mineral and the melt from which it crystallized together with parameterized Nernst partition coefficients (Bédard 1994; Godel et al. 2011a). For such a method to be effective, one must determine the relative phase proportions and appropriate partition coefficients as well as assume negligible migration of interstitial liquid (*i.e.,* closed system; *ibid.*). It should be noted that in long-lived magmatic systems such as layered intrusions, reactive flow of interstitial liquid may disturb the primary mineral compositions (Sparks et al. 2019). This approach has been applied to the Bushveld Complex (Yang et al. 2019), Mirabela intrusion (Barnes and Williams 2024), and the Savannah intrusion (Le Vaillant et al. 2020), amongst many others.

Method (4) uses melt inclusions hosted by early cumulus phases to constrain the nature of the parent melt from which the host mineral crystallized (Veksler 2006; Solovova et al. 2021). This method is analytically challenging as well as prone to sampling compositional

boundary layers and/or affected by subsolidus diffusion (Faure and Schiano 2005; Baker 2008); thus, it is seldom utilized in layered intrusion research. Despite these difficulties, melt inclusions have proven effective in constraining parent melt compositions as well as for detecting liquid immiscibility for several Phanerozoic intrusions (Spandler et al. 2000; Jakobsen et al. 2011; Dong et al. 2013). Spandler et al. (2005) documented two types of chromite-hosted melt inclusions in the G Chromitite of the Stillwater Complex; Type I inclusions represent a relatively volatile-rich high-Mg basaltic magma that were interpreted as an analogue for the magma parental to the ultramafic series and Type II inclusions formed from Si-rich silicate melts interpreted as country rock xenomelts. However, subsequent work on melt inclusions from the same horizon argued that these are not reliable proxies for the parent melt composition, instead representing trapped interstitial melts (Bai et al. 2024), which should be reverse-fractionated to the more primitive parental melt composition. A similar bimodal occurrence of melt inclusion compositions, this time hosted in olivine, were documented in feldspathic peridotite in the lower portion of the Dovyren intrusion (Konnikov et al. 2005). These were interpreted as lower crustal microxenoliths or xenomelt droplets, indicating that the Dovyren parent melt(s) experienced pre-emplacement crustal contamination. A siliceous komatiitic parent melt was proposed for the Bushveld Complex based on olivine-hosted melt inclusions from the comagmatic Uitkomst Complex (Solovova et al. 2021), consistent with the komatiitic chilled margins documented in the Lower Zone of the Bushveld Complex (Maier et al. 2016). The most primitive melt inclusion (~ 22.5 wt% MgO) was thought to represent the primary melt composition (*i.e.,* devoid of significant contamination), and that its relatively high SiO_2 content (~

51.9 wt%) is a characteristic unique to Bushveld-associated melts (*ibid.*).

The above examples highlight that constraining mantle melting conditions, source compositions, and parental melts of layered intrusion is a challenging task. Several innovative methods, however, have already made it possible to make reasonably reliable estimates of the parental melt compositions and their connections to the primary mantle melts. As comprehensive geochemical and isotopic databases are becoming increasingly available for many layered intrusions and as computational models become physiochemically more realistic, we postulate that future research will fine tune our understanding of the evolution of the mantle – currently largely based on studies of lavas – through the lens of layered intrusions.

6. Emplacement conditions and growth mechanisms

Layered intrusions are important components of the Precambrian crust, with giants like the Bushveld Complex, Windimurra and Sept Îles among the largest known igneous bodies in the world. Although there is considerable uncertainty in determining and comparing the physical extents of layered intrusions, their dimensions overlap with those of granite plutons and, rarely, batholiths, which are constructed sequentially over many millions of years (Fig. 5). These plutonic igneous bodies are laterally extensive and able to achieve thicknesses in excess of 10 km (Ivanic et al. 2018), equal to approximately a quarter of the thickness of typical continental crust (Cruden et al. 2018). Although doming and assimilation create space, plutonic intrusions are mainly accommodated by the structural removal of floor rock, driven by mass exchange between host chambers and underlying melt reservoirs (Cruden 2006;
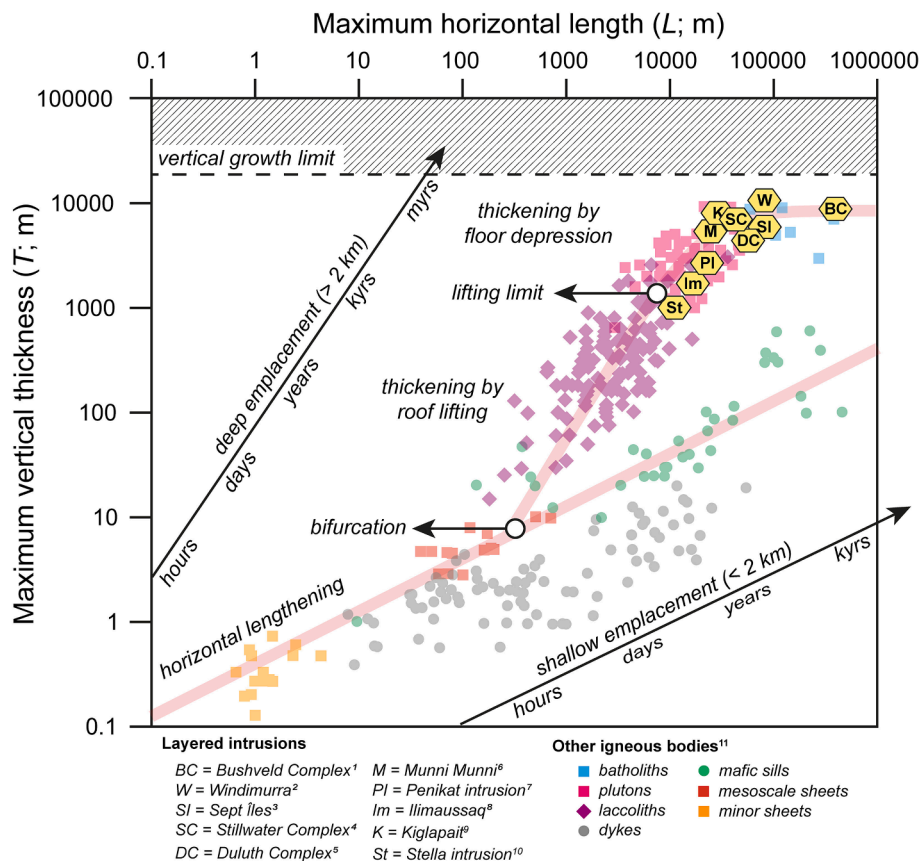

Fig. 5. Horizontal length versus vertical thickness of igneous bodies superimposed on the regime diagram for tabular intrusion scaling and growth mechanisms (Cruden et al. 2018). Note that the considered layered intrusions plot together with felsic plutons and batholiths that appear to grow primarily via floor rock depression over millions of years. 1 = Scoates et al. (2021), 2 = Ivanic et al. (2018), 3 = Namur et al. (2010), 4 = Campbell and Murck (1993), 5 = Miller and Severson (2009), 6 = Hoatson and Keays (1989), 7 = Alapieti and Lahtinen (1986), 8 = Marks and Markl (2015), 9 = Morse (1969), 10 = Maier et al. (2003), 11 = Cruden et al. (2018) and references therein.

Cruden et al. 2018). Depression of the floor rocks is further aided by the accumulation of dense ultramafic cumulates that can induce chamber subsidence as they accumulate and attempt to delaminate (Roman and Jaupart 2016). In the case of the Bushveld, chamber subsidence has been posited as a layer-forming mechanism via slumping of the cumulate pile (Maier et al. 2013) and delamination of cumulates from the intrusion base may be responsible for a thick mafic layer that occurs at a diffuse Moho discontinuity beneath the complex (Kgaswane et al. 2012; Roman and Jaupart 2016). Moreover, several intrusions have cumulate layers that thicken towards their centers as a result of subsidence (*e.g.,* Kemi, Alapieti et al. 1989; Bjerkreim-Sokndal, Bolle et al. 2002).

The bifurcation of growth mechanisms between sheet-like intrusions and laccoliths (Fig. 5) appears to be largely unrelated to emplacement depth and intensive parameters of the parent magma, but rather arises as a result of magma supply rate and tectonic setting (Cruden et al. 2018). However, processes facilitating the thickening of plutonic igneous

bodies vary with depth, primarily as a function of crustal rheology (Condie 2021). The relative importance of roof uplift and floor depression as growth mechanisms has an antithetical relationship with crustal depth, whereas the relative importance of brittle (*e.g.,* fracturing, stoping) and ductile (*e.g.,* viscous flow) processes shifts at the brittle-ductile transition zone (average heat flow of 50 mW/m^2; Condie 2021; Acocella 2021). Crustal aging and thickening throughout the Precambrian is likely to have led to secular changes in the relative importance of the construction mechanism of plutons. Many notable layered intrusions were emplaced in relatively brittle upper crust (< 12 km; Fig. 6); into metamorphosed country rocks that collectively define a relatively high geothermal gradient (*i.e.,* similar to the average thermal gradient of LIPs; Jennings et al. 2021). Their apparent preservation in the upper crust may reflect discovery bias (*i.e.,* exposure) and/or that relatively rigid crust is required to prevent the foundering of dense ultramafic cumulates (Menand 2011; Roman and Jaupart 2016). Rare examples of
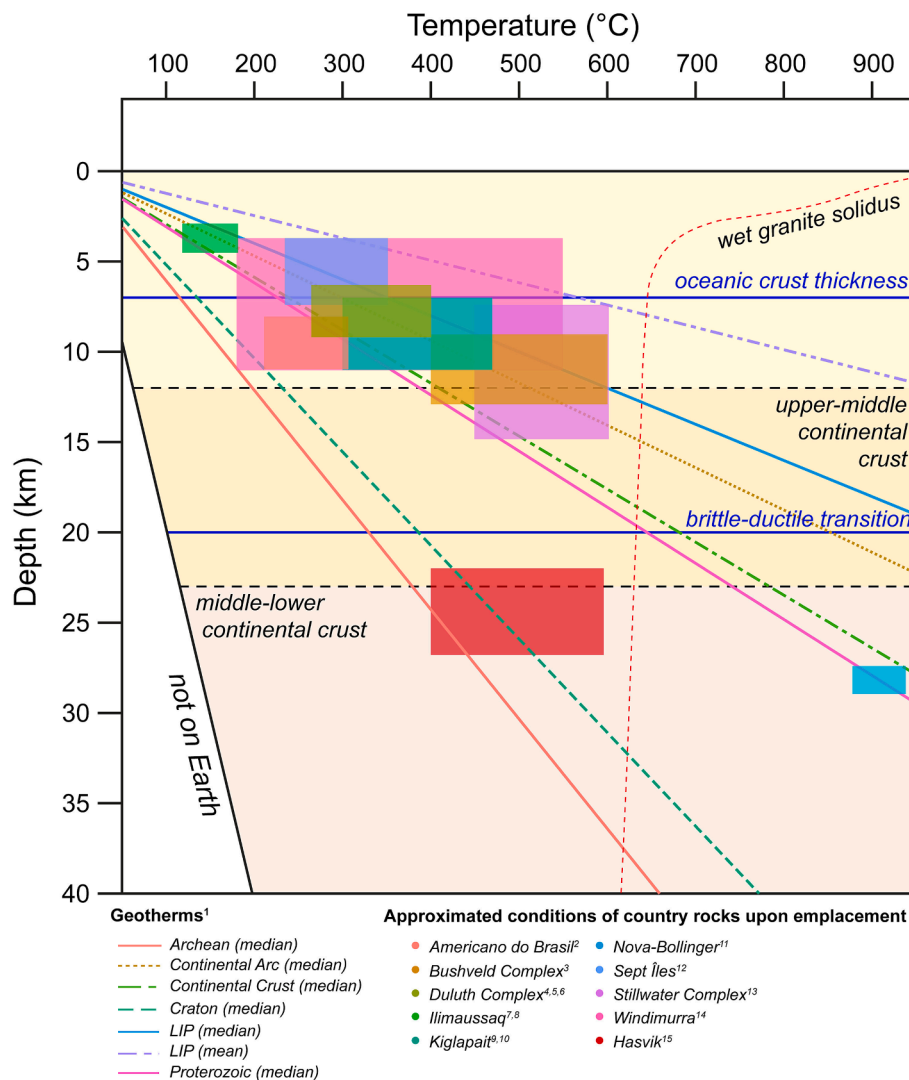
Fig. 6. Temperature versus depth (km) diagram showing approximated emplacement conditions of several intrusions underlain by geotherms (Hasterok and Chapman 2011), the brittle-ductile transition (Condie 2021), and divisions in the crust (Gao et al. 1998). Ranges for the Bushveld Complex, Stillwater Complex, and Kiglapait intrusion were derived from their contact aureole and as such, temperature ranges represent the maximum temperature of the country rocks upon emplacement. Temperature ranges for the Sept Îles, Ilimaussaq, and Americano do Brasil intrusions are estimated by applying the average Proterozoic geotherm (Jennings et al. 2021) to their emplacement depths reported in the literature. Temperature range for the Windimurra intrusion is approximated by apply the median LIP geotherm (Jennings et al. 2021) to the approximated emplacement depth. Emplacement conditions of the Hasvik intrusion, Duluth Complex and Nova-Bollinger intrusion are as reported in the literature. Note that most considered layered intrusions were emplaced into relatively cool brittle upper crust. 1 = Jennings et al. (2021), 2 = Augustin et al. (2023), 3 = Waters and Lovegrove (2002), 4 = Gál et al. (2013), 5 = Sawyer (2014), 6 = Virtanen et al. (2024), 7 = Larsen and Sørensen (1987), 8 = Markl et al. (2001), 9 = Berg and Docka (1983), 10 = Morse (2015), 11 = Chong et al. (2024), 12 = Namur et al. (2011), 13 = Labotka and Kath (2001), 14 = Ahmat (1986), 15 = Tegner et al. (1999).

deep-seated intrusions ($\geq$ 6 kbar) include Nova-Bollinger (Australia; Taranovic et al. 2022) and Hasvik (Norway; Tegner et al. 1999), which although relatively volumetrically small, show evidence for enhanced interaction with their host country rocks in the form of extensive thermal aureoles and incorporation of abundant crustal xenoliths.

With rare exceptions, layered intrusions are products of open-system processes. This means that their physical dimensions and the nature of their layering are primarily controlled by influx and efflux of magma, which may be episodic or progressive (Cruden et al. 2018; Latypov et al. 2024a). Many intrusions develop initially from tabular intrusions (*i.e.,* sills), which may then thicken by: (i) inflation (or ballooning) if magma supply rate exceeds the rate of crystallization and horizontal lengthening; or (ii) under- and over-accretion of distinct sheet-like intrusions if the rate of crystallization far exceeds the magma supply rate (*ibid.*). The Kiglapait intrusion is widely accepted to have formed in a closed system following the progressive emplacement of a single pulse of magma (Morse 2015 and references therein). Cumulate rocks displaying predominantly normally graded layering comprise the lower half of the intrusion and are consistent with having formed in response to gravitational settling of cumulus phases in a convecting melt body (Higgins 2002; Morse 2015). The Muskox intrusion is widely accepted to have formed in an open system, whereby *replenishing* melts were successively emplaced into a *resident* melt that had already fractionated cumulates (Irvine 1976). The cumulates display modally graded, reversely modally graded, and macrorhythmic layering, as well as cross-bedding (Irvine 1976; Scoates and Scoates 2024), indicative of dynamic, open-system processes. Researchers have proposed that the Bushveld and Stillwater complexes were, at least in part, constructed by the non-sequential emplacement of distinct sheet-like intrusions (Mungall et al. 2016; Wall et al. 2018; Scoon and Mitchell 2023). Although it is broadly accepted that silicic plutonic bodies grow by the under-accretion of successive magma pulses (Glazner et al., 2004; Menand et al. 2011), this remains a matter of serious debate for layered intrusions (Latypov et al. 2024a). Out-of-sequence U-Pb zircon ages in layered intrusions that appear contradictory to field observations pose a challenge to the understanding of mush zones and melt percolation in layered intrusions. However, Holness et al. (2017a, 2017b) and Latypov et al. (2024c) suggest that most mush zones are relatively thin (m-scale), and Barnes and Williams (2024) argue that trapped melt (from which zircon crystals crystallize) does not percolate significantly within the mush. Both lines of evidence suggest that zircon crystallizes from trapped liquid complementary to cumulates representing the emplacement sequence of layering.

7. Multiscale and multidisciplinary observations from layered intrusions

Research on layered intrusions intensified following the discovery that these geological formations may contain economically valuable metals (Fig. 3). Their critical metal repositories have meant that, over time, research efforts have employed an impressive array of techniques, including field-based studies, petrography, geophysics, geochemistry, geochronology, fluid dynamics, and thermodynamic modelling (Fig. 3; O'Driscoll and VanTongeren 2017). The study of layered intrusions exemplifies the necessity of multidisciplinary and multiscale approaches in deciphering the petrogenesis of geological formations. By combining insights from various scientific fields and examining structures at different scales—from the microscopic details of minerals to the macroscopic outline of entire intrusions and their associated magmatic systems—we can begin to disentangle the complex array of processes responsible for their formation.

Layered intrusions are components of *trans*-crustal plumbing systems that may only be contextualized at the macroscale (km to 10 s of km). At this scale, one can infer the extent of the magmatic event, the geometry of the subject intrusion(s), and the relationships between magma(s), crustal rocks, and tectonic structures. Macroscale investigations require

comprehensive geological mapping, which enabled the discoveries of the Muskox Intrusion in Canada (Smith and Kapp 1963) and the Giles Complex intrusions in Australia (Maier et al. 2015). Such observations also elucidate regional structural context, illustrating how intrusions interact with surrounding rock formations (Hutton 2009; Schofield et al. 2014). Analyses at the macroscale are important in highlighting relationships between cogenetic intrusions on a regional scale, such as the Americano do Brasil Suite (Augustin et al. 2022) and the Giles Intrusions (Maier et al. 2015), as well as emplacement mechanisms (refer to *Section 6*). Importantly, geophysical methods have significantly contributed to the identification of poorly or unexposed parts of intrusions, sometimes linking seemingly spatially disconnected intrusions. For example, in northern Finland, magnetic and gravimetric measurements have revealed an unexposed ca. 100 km long elongated magma body linking the Näränkävaara dike to the Koillismaa intrusion indicating the existence of a much larger magma system (Alapieti 1982; Järvinen et al. 2022). Geophysical measurements can also reveal staging magma reservoirs or underplating below the exposed levels of intrusions, as for the Bushveld using gravimetric and seismic data (Cole et al. 2024). Airborne and ground-based geophysical surveys are essential for a comprehensive understanding of these complex structures and are frequently used to constrain how the intrusions extend and behave at depth (*e.g.*, Koivisto et al. 2012). Entities with coherent physical properties detected in geophysical data often correlate with specific rock types within the intrusion, underscoring variations in composition and density (Sun et al., 2020; Ferré et al., 2009).

On the mesoscale, which we consider ranging from hand-sample to outcrop size (cm to 10 s of m), studies focus on features visible with minimal magnification. This level of examination connects microscopic mineral analyses with broader geological surveys, offering detailed insights into the internal structure of magmatic intrusions. To ensure unbiased sampling, detailed descriptions of mesoscopic features are crucial, as they significantly influence the representativeness of sample sets for layered intrusions. Some key mesoscopic observations include magma-wall rock contact relationships that provide evidence of chilled margins, for example, are important in the study of parental melts for layered intrusions (Huppert and Sparks 1989; refer to *Section 5*). Styles of *in situ* magma-wall rock interaction processes (*i.e.,* bulk vs. selective assimilation) are often visible on the mesoscale (Barnes et al. 2001; Queffurus and Barnes 2015; Barnes et al. 2023). Identifying how these processes may have affected the composition of the magma is useful for the interpretation of the whole-rock and mineral chemical data. In the case of Pechenga and the Duluth Complex, mesoscopic observations of magma-black shale interaction were important in the interpretation of how sulfur was transported from the shale to the magma to instigate the formation of Cu-Ni(−PGE) deposits (*e.g.,* Barnes et al. 2001; Queffurus and Barnes 2015). Apart from contact relationships, this length-scale often uncovers the mechanical and chemical stratification processes within intrusions, whether through gravitational crystal settling (Irvine, 1980a; Wager and Brown, 1968) or *in situ* crystallization (Campbell, 1978; Latypov et al., 2017). Textures and structures found on this scale offer insights into magma chamber dynamics, including convection currents, crystal settling and magma mingling or mixing. Additionally, variations in magnetic susceptibility observed in mesoscopic scale geophysical studies not only reflect changes in mineral abundance but also, particularly with ferrimagnetic minerals, differences in grain sizes. This helps in identifying stratification, cryptic layering, and postmagmatic alteration (Ferré et al., 2009). The traditional whole-rock geochemical methods are nonetheless still of greater importance to understanding the origins of the rocks.

The mineralogy and texture of cumulates comprising layered intrusions are revealed at the microscale. Although recent years have seen the development of sophisticated micro- to nano-scale techniques for characterizing cumulates, traditional optical microscopy remains the principal method and the first tool to identify mineralogy and textures. Jackson (1961) described the rocks and textures of the ultramafic

cumulates in the Peridotite zone of the Stillwater Complex in remarkable detail and several studies has been based on these initial descriptions. Despite advances in micro- to nano-scale techniques, optical petrography remains essential for identifying microtextures that cannot be discerned through chemical analysis or automated mineralogy. For example, recognizing the distinction between poikilitic and intercumulus textures is crucial for understanding cumulate formation mechanisms, and traditional optical petrography is thus indispensable. The recognition of poikilitic textures has challenged the origins of their formation, with the classical hypothesis suggesting they form as interstitial postcumulus phases crystallizing from intercumulus liquid within a segregated crystal mush (Wager et al., 1960). However, this hypothesis has been contested, with alternative suggestions that oikocrysts may form *in situ* as cumulus phases from supersaturated liquids (Campbell, 1968; Mathison, 1987). Petrography can also be used to detail microtextures and infer processes, as shown by a recent study on the Sept Îles intrusion, Canada, identifying symplectites to infer redistribution and concentration of hydrous fluids in incompletely solidified rock or an increase in water activity of the interstitial melt (Keevil et al. 2020).

Recently developed methods related to microstructure characterization such as high-resolution X-ray computed tomography (HRXCT), electron backscattered diffraction (EBSD) and X-ray fluorescence element mapping analysis enhance our understanding of magmatic processes (Godel et al. 2013; Barnes et al. 2021; Chen et al. 2024). Nondestructive imaging of microscale or sometimes even nanoscale 3-D structures (*e.g.,* crystal shapes, sizes, distribution, and aggregation) has become possible with the development of the HRXCT, revolutionizing our observational capabilities on microstructures (Cnudde and Boone 2013). Recent research used HRXCT to reveal a continuous 3-D framework of interconnected chromite grains in the UG1 chromitite in the Bushveld Complex, with the grains predominantly in face-to-face contact and randomly oriented; supporting the hypothesis that the chromitites form through *in situ* crystallization directly at the magma chamber floor rather than gravity settling (Latypov et al., 2022). Investigations into dihedral angles by Holness et al. (2022) and Fowler and Holness (2022) provide critical insights into mineral formation and growth rates. Crystal nucleation, growth and settling processes can also be studied using EBSD, which provides information on the crystallographic orientation of individual grains within a sample (Wieser et al., 2019). As an example, EBSD analysis revealed that chromite grains in the UG2 chromitite of the Bushveld Complex show no systematic relative orientation. These data indicate the random juxtaposition of individual grains. Chromite-chromite-plagioclase dihedral angle measurements from the UG2 chromitite suggest high degrees of textural equilibration in these rocks. Together these data support the hypothesis that massive chromitite seams formed by chromite grains nucleating heterogeneously on the silicate grains, with subsequent accumulation and sintering of individual grains or clusters (Holness et al., 2023). Similarly, EBSD analyses showed that the presence of plagioclase magmatic foliation in anorthosites and massive magnetitites in the Bushveld Upper Zone is a result of crystal settling from moving, crystal–laden magmas (Vukmanovic et al. 2019).

Microscopic analysis of major and trace elements in minerals and melt inclusions also provides important hints into the process occurring in magma chambers. The study by Xing et al. (2022) investigates the crystallization and cooling history of the Sept Îles layered intrusion by analyzing complex phosphorus zoning in olivine grains using high-resolution EPMA imaging, EPMA for elemental analysis, EBSD for crystallographic orientation, and thermal and diffusion modelling. This study revealed that rapid growth of dendritic and hopper olivine patterns resulted from significant undercooling in the magma chamber. Barnes et al. (2016) used microbeam XRF mapping, LA-ICP-MS, and EPMA to investigate the crystallization mechanisms and zoning patterns in orthopyroxene oikocrysts from the Neoproterozoic Ntaka Ultramafic Complex, revealing that Cr-rich cores, oscillatory zoning and reverse zoning support dynamic magma conditions with primary cumulus

growth and secondary infiltration metasomatism. Schoneveld et al. (2024) investigated Cr zoning patterns in pyroxenes at Nova-Bollinger and Kevitsa, finding that these zoning patterns indicate favorable conditions for upgrading metal content in active and open magmatic systems. Further, they demonstrated that relict pyroxene zoning remains detectable under moderate degrees of alteration (amphibolization), making the indicator robust to moderate and hydrous alteration. Furthermore, melt inclusions within cumulate minerals reveal a wealth of information, including the initial melt composition (Solovova et al., 2021), evidence of rock assimilation (Spandler et al., 2005), and the onset of immiscibility, when the melt separates into distinct liquid phases (*e.g.,* Jakobsen et al. 2011; Fischer et al., 2016; Wang et al., 2018).

8. Investigating the origin of *rolled oikocrysts* in the Stillwater Complex

8.1. Introduction

Multidisciplinary studies that integrate quantitative rock textural analysis, bulk rock geochemistry, mineral chemistry, and/or numerical modelling form an increasingly large part of the layered intrusion published literature. Such integrated approaches can elucidate rock forming processes that are proposed based on field observation and conjecture. To demonstrate the utility of such a multidisciplinary approach, a well-known, but poorly documented outcrop from the Stillwater Complex was sampled and imaged using several microbeam techniques, including Maia Mapper microXRF and scanning electron microscope-electron backscatter diffraction (SEM-EBSD). The purpose of this exercise is to show the utility of a modern multidisciplinary analytical approach to constrain petrogenetic processes in layered intrusions.

8.2. Geological summary of the Stillwater "snowball oiks"

The sampled outcrop is located on the northern side of Picket Pin Mountain in a part of Gabbronorite III zone within the Upper Banded series of the Stillwater Complex (McCallum, 1996). Few studies have focused on rocks from the Upper Banded series, partly due to their inaccessibility and partly because they lack known economic mineral potential. The sampled outcrop is a popular stop on geologic field trips because it is exposed near the Picket Pin sulfide PGE prospect located on the south side of Picket Pin Mountain—another popular field trip stop. The outcrop has been referred to in Stillwater Complex field guides as the "snowball oiks outcrop" and is comprised of complexly interlayered gabbronorite, leucogabbronorite, norite and anorthosite (*e.g.,* Carlson and Zientek 1985; McCallum and Meurer 2002). A distinct feature in this outcrop is the presence of spheroidal orthopyroxene oikocrysts ranging from about 2 to 12 cm in diameter (Fig. 7A-C). These oikocrysts have been informally referred to as "snowball oiks" given their size and superficial resemblance to snowballs. Other features shown in the outcrop include structures interpreted as scour and fill structures, rip up clasts and lenticular autoliths of anorthosite (Fig. 7B; Carlson and Zientek, 1985). The snowball oikocrysts contain chadacrysts of euhedral plagioclase and intercumulus augite (Fig. 7D). The oikocrysts are wrapped by a planar lamination carried by preferentially oriented plagioclase, orthopyroxene and clinopyroxene primocrysts in gabbronorite with subordinate, wispy layers of anorthosite and norite. By contrast, plagioclase chadacrysts hosted within the orthopyroxene oikocrysts appear to have a random orientation. Some of the snowball oikocrysts are characterized by having anorthosite rinds (Fig. 7D). Plagioclase shows very little crystal bending and/or undulose extinction. No deformation twins are present. Field descriptions of this unit have relied on the observations of sedimentary-like structures and the foliation wrapping the poikilitic orthopyroxene to invoke crystallization in a dynamic environment.
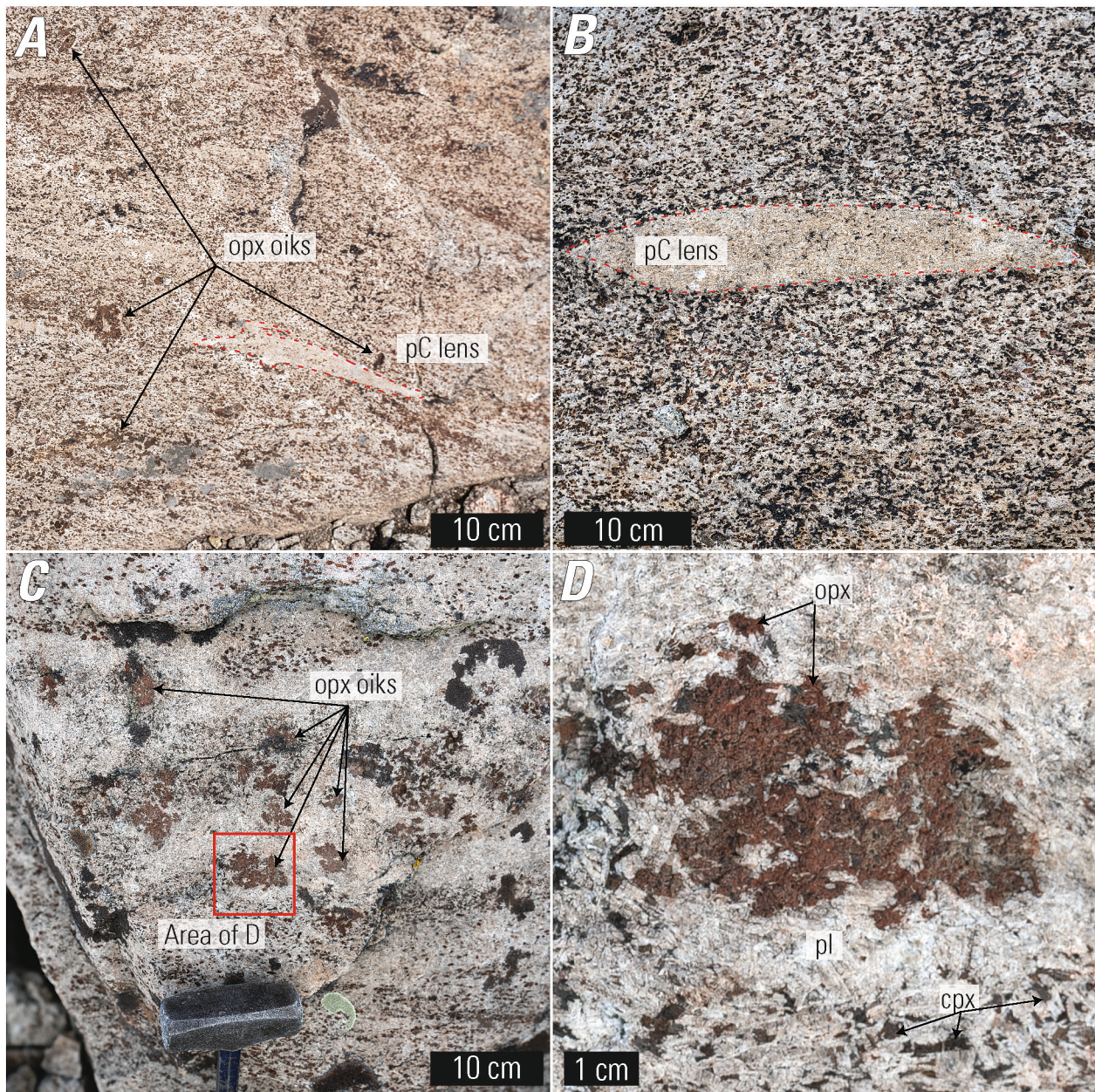
Fig. 7. Photographs taken of the snowball oikocryst outcrop near Picket Pin Mountain in the Upper Banded series of the Stillwater Complex. **A.** Poikilitic orthopyroxenes (opx oiks) and anorthosite lenses (pC lens) distributed throughout modally layered gabbronorite exposed on a glacially polished outcrop. **B.** Lens-shaped anorthosite autolith in gabbronorite. **C.** A dense cluster of poikilitic orthopyroxenes rimmed by anorthosite-leuconorite. **D.** Snowball orthopyroxene oikocryst rimmed by anorthosite. Photographs by Chris Jenkins, U.S. Geological Survey, 2023. Mineral abbreviations are plagioclase (pl) clinopyroxene (cpx), and orthopyroxene (opx).

8.3. New insights into the petrogenesis of the "snowball oiks" outcrop

We describe the detail of the analytical methods used to quantify rock texture and the distribution of elements in the sample studied in ESM 2. This includes short descriptions of the types of maps produced by EBSD analysis that we present here.

Maia Mapper microXRF: The microXRF data are shown as a false-color three element (Ca-Cr-Fe) composite image in Fig. 8 (Ryan et al., 2018).

EBSD: The area mapped by EBSD covers two textural domains in the sample, the area of the orthopyroxene oikocryst (Fig. 9A, shaded area) and the outside of the oikocryst (Fig. 9A). The orthopyroxene oikocryst encloses mostly euhedral plagioclase laths with minor anhedral interstitial clinopyroxene (Fig. 9A-C). Within the oikocryst, plagioclase apparent aspect ratio varies from 1 to 8 (refer to ESM 2). Plagioclase pole

figure data, within the oikocryst, show very weak fabric with point maxima at the (010) and (001) poles (Fig. 9D). The [100] axes do not form a girdle but show disperse point maxima instead. Although the number of plagioclase crystals is lower than outside the oikocryst, this still implies a weak lineated fabric. The clinopyroxene crystals within the oikocryst are mostly randomly orientated, however, a small proportion of the clinopyroxene show an almost identical crystallographic orientation (black arrow; Fig. 9B, D). Orientation data of the large orthopyroxene oikocryst confirms that the oikocryst is mainly a single crystal, but the spread of the data points suggests minor crystal plasticity (black arrow; Fig. 9D), *i.e.,* intra-crystal strain.

Plagioclase outside the oikocryst has a similar apparent aspect ratio to plagioclase within the oikocryst (refer to ESM 2). Plagioclase orientation data outside of the oikocryst show strong preferred orientation of
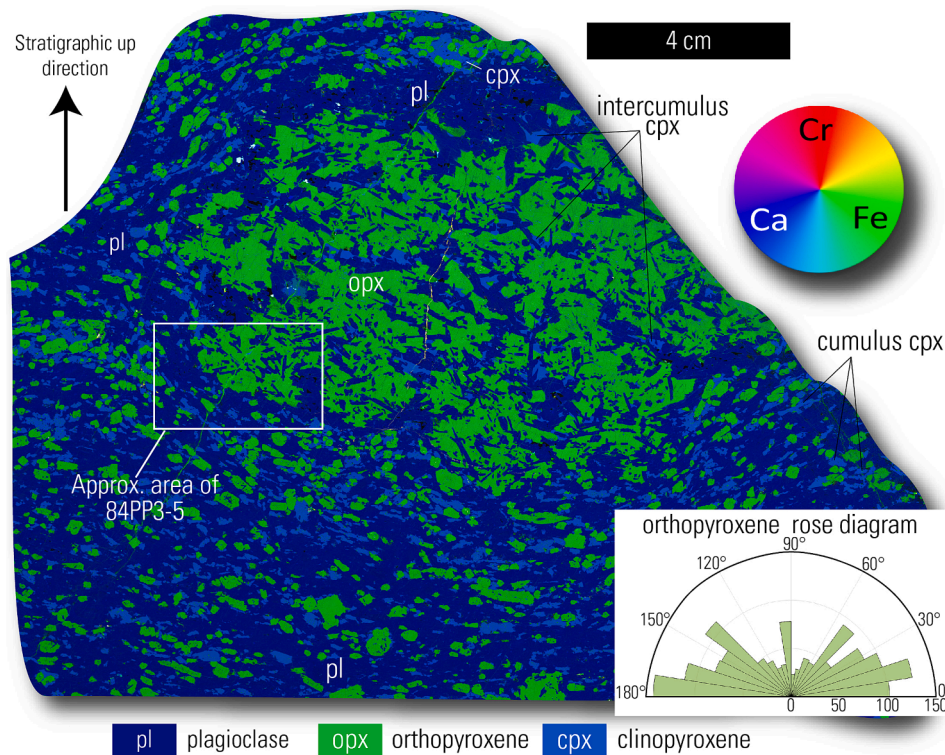
Fig. 8. False color microXRF map of sample 84PP3. The map is a composite made by stacking Ca (blue), Cr (red), and Fe (green) element maps. The approximate area of polished thin section 84PP3-5 imaged by EBSD is shown by the white box. The rose diagram shows the orientation of orthopyroxene crystals. Mineral abbreviations are plagioclase (pl), clinopyroxene (cpx), and orthopyroxene (opx).

both [100] axes and the poles to (010) and (001) planes (Fig. 9E). The [100] axes develop a girdle distribution, parallel to the rock's fabric (Fig. 9E). Within the center of the girdle, a population of plagioclase crystals develops strong point maxima of [100] (Fig. 9D). Poles to clinopyroxene (100) planes develop point maxima parallel to the rock's foliation, whereas [001] axes reveal a weak girdle (Fig. 9E). Poles to the (010) plane show weak multiple point maxima (Fig. 9E). The small number of orthopyroxene grains prevents proper textural analysis, but as seen from the rose diagram (Fig. 9), the major axes of the cumulus orthopyroxene imply the presence of a fabric parallel to the foliation seen in plagioclase (Fig. 9E). The (100) pole data form point maxima orthogonal to rock's foliation, whereas poles to the plane (001) develop a girdle parallel to the foliation (Fig. 9E). Poles to the (010) plane show the least developed texture (Fig. 9E).

8.4. Interpretation of results

The microXRF data show that poikilitic and cumulus crystals in the snowball oikocryst outcrop are not chemically zoned. This contrasts with the markedly zoned poikilitic pyroxene found near the J-M Reef PGE deposit in the Stillwater Complex (Jenkins et al. 2022) and in mineralized mafic magmatic conduit-type Ni-Cu-PGE deposits worldwide (Schoneveld et al. 2020). The absence of chemical zoning indicates that the orthopyroxene oikocryst grew and/or equilibrated with melts with a near constant composition for the duration of its crystallization history. Alternatively, the system may have cooled slowly enough that any primary zoning pattern was overprinted during chemical equilibration; however, this seems unlikely given the large size of the poikilitic crystals and the slow rate of chemical diffusion in orthopyroxene (Cherniak and Dimanov 2010). While the texture of the sample studied points to the formation of the rock in a dynamic environment, there is no indication that the composition of the parental melt was heterogeneous (*i.e.,* by recharge of a melt with a significantly different composition) as the poikilitic crystals grew.

Similar aspect ratios of plagioclase crystals within and outside the oikocryst suggest that all plagioclase crystallized early (refer to ESM 2). The mild evidence of lineated plagioclase crystals within the oikocryst represents early evidence of magma flow before the growth of the oikocryst (Fig. 9D). Outside of the oikocryst, the strong fabric in both plagioclase (*i.e.,* foliation and lineation) and orthopyroxene (*i.e.,* foliation) suggest that the environment of formation was relatively dynamic (Fig. 9E). Due to the absence of significant deformation microstructure (*i.e.,* crystal plasticity) the role of strain as fabric forming process can be disregarded (*e.g.,* viscous compaction). Both plagioclase and orthopyroxene outside the oikocryst are cumulus crystals, their fabric is a result of crystal rearrangement during magma flow of crystal-rich slurry (Vukmanovic et al. 2018). However, the intercumulus clinopyroxene also records a mild fabric. We suggest that intercumulus melt pockets in the pore spaces between plagioclase (and orthopyroxene) acted as lubricants during the flow. They later crystallized parallel to the flow direction. All phases record a mild degree of intracrystalline plasticity (ESM 2), suggesting that this small amount of strain was recorded in the subsolidus. A working hypothesis would be that this strain was a result either of a late viscous compaction or post-emplacement sagging of the intrusion. To come to a more certain scenario, further microstructural characterization of samples above and below the sample shown here is needed.

Chemical mapping and EBSD fabric analysis indicate that the snowball oikocrysts formed early when the melt was co-saturated in orthopyroxene and plagioclase and near clinopyroxene saturation. The oikocrysts interacted with and trapped plagioclase chadacrysts and continued to grow as the entire assemblage was being transported in a flowing slurry. The snowball oikocrysts have been transported within the aligned plagioclase (*i.e.* within the place of foliation). This is notable because it runs contrary to conventional cumulus theory that posits poikilitic crystals grow within intercumulus pore spaces due to compositional convection in the cumulate pile (Kerr and Tait 1985). Further, these textures could not have been developed by or formed by peritectic
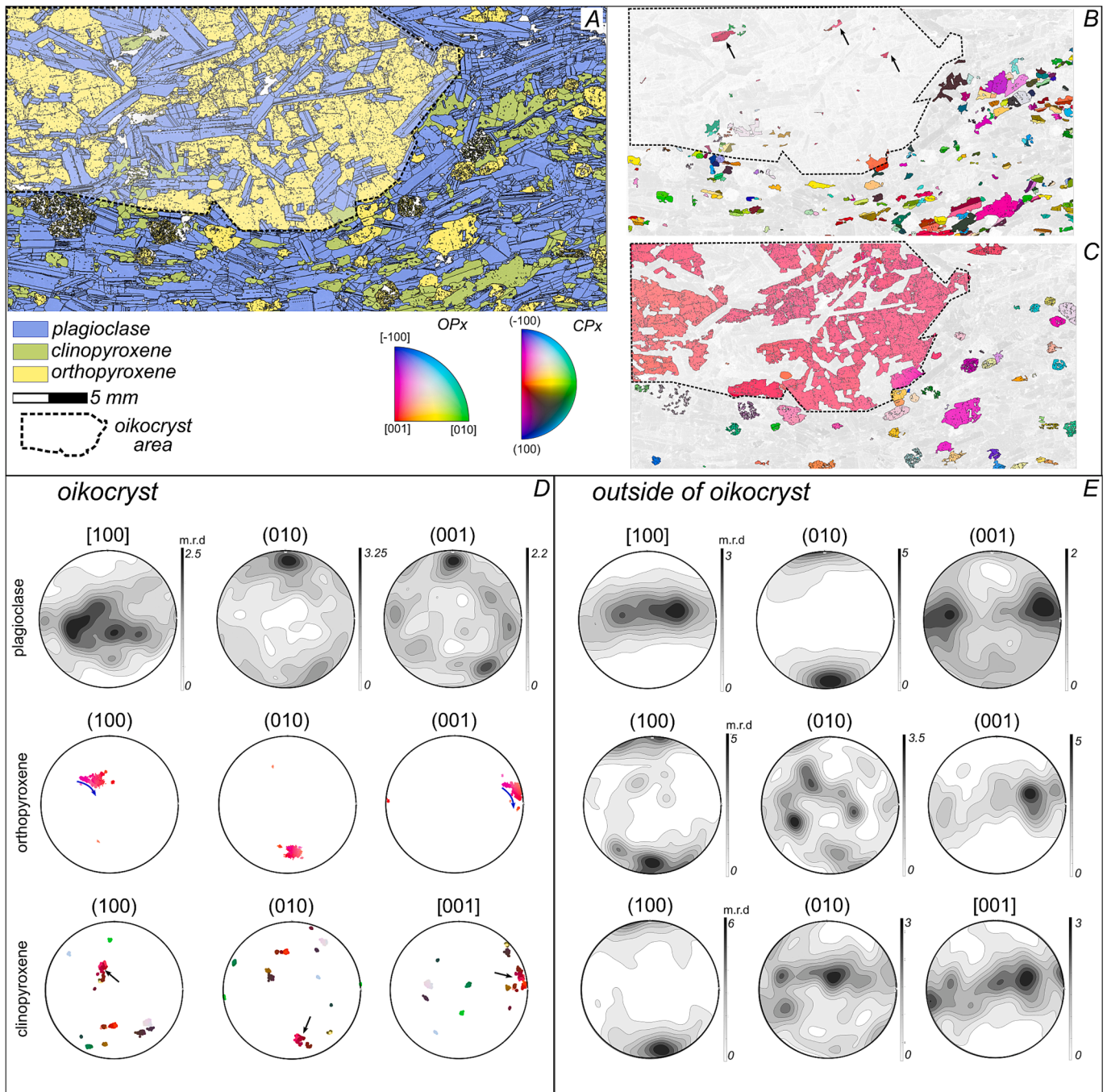
Fig. 9. EBSD analysis of the *snowball oikocrysts*. **A.** Phase map of the sample 84PP3-5. **B.** Clinopyroxene orientation map. **C.** Orthopyroxene orientation map. The orientation maps are colored using the inverse pole figure (IPF) key referenced to X direction of the sample. The dotted area on A-B-C indicates the area of an orthopyroxene oikocryst. **D.** Pole figure data of plagioclase, clinopyroxene and orthopyroxene within the oikocryst. Due to a small number of grains, clinopyroxene and orthopyroxene data are not contoured. **E.** Pole figure data of plagioclase, clinopyroxene and orthopyroxene outside of the oikocryst. Number of data points for D and E are reported in supplementary material. m.r.d: multiples of a random distribution. Squared brackets [] indicate crystallographic axis, and parentheses () indicate pole to the crystallographic planes.

reaction between primocrysts and percolating melts as has been suggested elsewhere for orthopyroxene oikocrysts in olivine crystal mushes (Jackson 1961; Kaufmann et al. 2018). After deposition, as the melt proceeded to crystallize the snowball oikocrysts were deformed by the mass of the overlying mush. An aspect that requires further investigation is how these large oikocrysts were transported during the magma flow.

8.5. Conclusions

Layered intrusions host many labyrinthine features that can be constrained using a multidisciplinary approach. By combining microstructural (EBSD) data with geochemical data we can correlate how the same process affects a rock from different perspectives, without disregarding evidence. Our combined data show that these poikilitic crystals are formed in a dynamic magma chamber where crystals have been transported either by convective currents (Barnes et al., 2016c;

Holness et al., 2017b) or in crystal-rich slurries (Maier et al. 2013; Vukmanovic et al. 2019). The data do not indicate that the poikilitic orthopyroxene crystals grew at their present location either by compositional convection or peritectic reaction.

## 9. Layered intrusions as critical metal repositories

Many Precambrian layered intrusions host repositories of critical metals, including PGE, chromium (Cr), nickel (Ni), copper (Cu), cobalt (Co), vanadium (V), and others (Cawthorn 1996). Mineralization is often stratiform and, between intrusions, varies in stratigraphic occurrence, nature of the host rocks, and tenor (Smith and Maier 2021). For example, reef-style PGE occurrences can occur at almost any stratigraphic level and are sometimes associated with chromitites (Prevec 2018). Nonetheless, most manifest near to the transition from ultramafic to mafic cumulates, derived from a primary melt that itself was generated from a partial melting degree sufficient to liberate all the PGEs (Barnes et al. 1985; Keays 1995; Maier 2005). Moreover, Ti-V rich magnetitites typically occur at higher levels in stratigraphy associated with anorthosites and leuconorites, such as in the Bushveld and Windimurra complexes (Cawthorn 2015; Ivanic et al, 2018); however, the Sept Îles Ti-V rich magnetite layers and pods occur in the middle of the stratigraphy intercalated with olivine gabbro and troctolites (Namur et al. 2010). While the metal content of the primary melt influences the potential for an intrusion to host an ore deposit, it is not the only requirement (Arndt et al. 2005); a combination of melt fertility, fertile melt migration, ore mineral segregation, and accumulation is vital (Mungall 2005).

9.1. Mantle source and crustal transport controls on the metallogeny of layered intrusions

Layered intrusions inherit most of their metallogenic potential from their mantle source(s). Here we consider the Cr, Ti, V, PGE, Cu and Ni

contents of primary mantle magmas, which depend on the composition of the mantle source, the degree of melting, and the P-T conditions they evolve under as well as on certain buoyancy-related processes that may aid in the transport of the main metal-bearing phases from the mantle source.

Chromium is compatible in most of the main phases in the convecting mantle (*i.e.*, clino- and orthopyroxene, garnet, and spinel; McDonough and Sun 1995) and in the metasomatized SCLM (*e.g.,* clinopyroxene, phlogopite, ilmenite, and amphiboles; Foley et al. 2022, Ezad et al. 2024). As such, the Cr content of primary mantle melts increases with higher degrees of partial melting. Mantle melting experiments conducted with pyrolite compositions show that Cr content increases approximately linearly up to the maximum of ca. 0.4–0.6 wt%, when the degree of melting reaches 30–50 % (Hirose and Kushiro 1993; Baker and Stolper 1994; Walter 1998), which is a typical range for komatiitic primary melts. Due to the highly heterogeneous nature of the metasomatized SCLM (refer to *Section 5*), estimating the Cr contents of its partial melting products is more complicated, although Cr is compatible in most of the residual solid phases of PIC and MARID assemblages (Foley et al. 2022). Consequently, those layered intrusions that form by the highest degree of mantle melting should have the highest Cr concentrations and hence are more likely to form chromitite deposits (*e.g.*, Bushveld, Stillwater, Great Dyke). Campbell and Murck (1993) demonstrated through mass balance the difficulty in explaining the occurrence of large stratiform chromite in layered intrusions by showing that Cr_2O_3 is only soluble to about 600 ppm in a basaltic melt. This limitation then requires between 2 and 12 km of complementary melt for every 1 m of massive chromitite produced depending on how efficient Cr extraction is from the melt (Fig. 10). Jenkins and Mungall (2018) suggested that contaminated komatiites were more likely the parental melts to the chromitites in the Peridotite zone of the Stillwater Complex on the basis that the Cr solubility in high temperature, high-Mg melts is considerably higher than a basalt and therefore a still large (700 m to 2 km), but more reasonable complementary melt column was
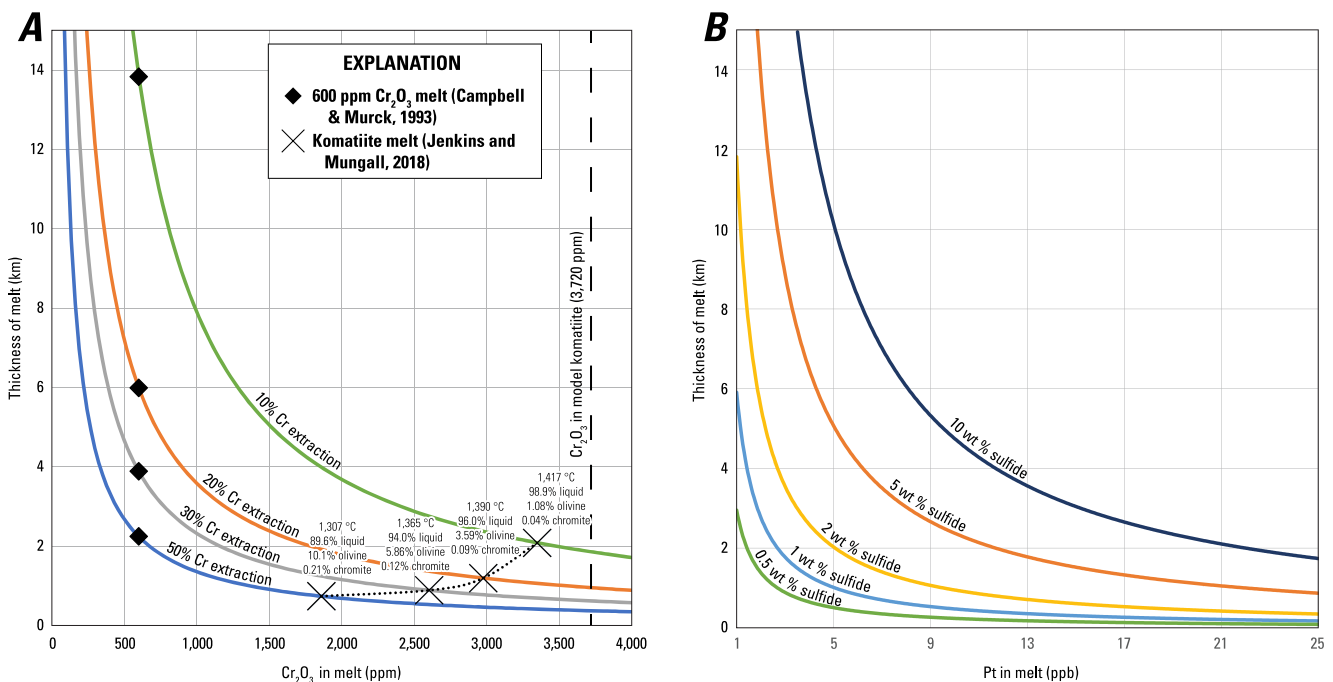
Fig. 10. A. Mass balance calculation showing the thickness of melt needed to form a 1-m-thick chromitite versus Cr_2O_3 dissolved in the silicate melt. Curves represent variable efficiency of Cr extraction from the melt from 10 to 50 %. Diamonds indicate the 600 ppm Cr_2O_3 solubility estimated for a basaltic melt by Campbell and Murck (1993). Crosses show melt-solid assemblages and temperatures for the model contaminated komatiite parental melt used to model the Peridotite chromitites from the Stillwater Complex by Jenkins and Mungall (2018). B. Bivariate plot showing the thickness of melt needed versus Pt solubility in silicate melt to form a 1-m thick Pt reef deposit at variable amounts of sulfide (from 0.5 to 10 wt%). The resulting sulfides in the 1-m thick reef have Pt tenors of 300 ppm. The assumption is made that Pt extraction from the silicate melt is 100 % efficient (*i.e.*, Pt is perfectly compatible in sulfide liquid).

required to satisfy the mass balance (Fig. 10).

Contrary to Cr, Ti is incompatible to most of the minerals in the convecting mantle, hence it is enriched in low degree partial melts and becomes progressively diluted as the degree of melting increases (Hirose and Kushiro 1993; Baker and Stolper 1994; Walter 1998). The effect of pressure during melting is of minor importance for the Ti content of the primary melt forming from the convecting mantle. Experiments conducted with the typical pyrolite composition of the convecting mantle, show that the Ti content of the primary melt decreases from ca. 1.0–2.5 wt% at < 10 % melting to ca. 0.5–1.0 wt% at 10–20 % melting, before reaching a fairly steady level of 0.5 wt% at > 20 % melting (Hirose and Kushiro 1993; Baker and Stolper 1994; Walter 1998). The PIC and MARID assemblages of the metasomatized SCLM contain several minerals such as ilmenite, rutile, and phlogopite, which can contain high Ti contents. These minerals, especially phlogopite, are present in the residual solid with intermediate degrees of melting (roughly 30 %, although highly dependent on the composition: Foley et al. 2022; Ezad et al. 2024) but once they melt completely, the partial melt should attain high Ti content. However, as mentioned above, due to the heterogeneity of the metasomatized SCLM composition, quantitative assessment is difficult. For a layered intrusion to inherit a high Ti budget from a convecting mantle source, the degree of melting should be relatively low, whereas high Ti melts form from a metasomatized SCLM when the Ti-bearing phases are consumed.

Vanadium is a complex trace component in the mantle as it can be present in multiple valence states, which affect its partitioning between phases (Canil 1997; Mallmann and O'Neill 2009). Depending on the fO_2 in the mantle, the bulk partitioning of V ranges gradually from mildly compatible in reducing conditions (<fayalite-magnetite-quartz (FMQ) to −2 log units) to highly incompatible (>FMQ to + 2 log units) (Mallmann and O'Neill 2009). Considering the common minerals in the convecting mantle, the relative partition coefficients of V increase roughly in the following order: olivine < orthopyroxene < clinopyroxene and garnet < Al-spinel < Cr-spinel (Mallmann and O'Neill 2009). Given that the partitioning is weakest in the more refractory olivine and orthopyroxene, V becomes increasingly incompatible (enriched in the melt) as complete melting of the less refractory phases is approached. Generally, ultramafic magmas generated from the convecting mantle tend to have fO_2 at the FMQ buffer or up to about −3 log units below based on a global comparison of V-in-olivine oxybarometry (Nicklas et al. 2024). Based on the same global dataset, there has been gradual increase in fO_2 from the Archean to modern magmas, which in theory could have caused secular change from mildly compatible to incompatible V partitioning during mantle melting. This, however, is not reflected in the temporal occurrence of Fe-Ti-V deposits in layered intrusions (Fig. 4). As V is sometimes found concentrated together with Cr and PGE and sometimes with Fe and Ti, it seems that its partitioning is either controlled by local changes in the fO_2 or that, instead of the degree of mantle melting, the composition of the mantle source composition is the main factor in forming V-rich melts.

The PGE budget inherited from the accretion of the Earth is thought to have been largely stripped from the silicate mantle and crust during the formation of the metallic core (Holzheid et al. 2000). Hence, most of the PGE now concentrated in layered intrusions were originally introduced to their mantle sources by a late veneer following the core formation (Maier et al. 2009). This extraterrestrial input was spatially erratic and imposed a first-order control on the PGE contents of magmas prior to the mantle-wide homogenization of this newly inherited material, which was possibly complete by 2.9 Ga (Maier et al. 2009). Therefore, it is possible that the oldest layered intrusions in the geological record could have originated from mantle sources that were either strongly depleted or enriched in the PGE compared to the mantle that existed from the Neoarchean onward. As with any other elements, the PGE contents of primary melts are not only dependent on the depletion or enrichment of the mantle source.

The iridium-group PGE (Ir, Os, Ru) and palladium-group PGE (Pd, Pt,

Rh) are partly hosted by different phases in the mantle, hence their behavior during mantle melting is decoupled (Mungall and Brenan 2014; Waterton et al. 2021). The PPGE, together with Cu, are mostly hosted in sulfides in the mantle as they are incompatible in silicates and oxides (Fellows and Canil 2012; Mungall and Brenan 2014), although it should be noted that Rh might be more compatible in silicates and oxides than Pt and Pd under some conditions (refer to Barnes et al. 2015). As a result, primary magmas reach highest PPGE (*e.g.*, for Pt, on the order of 10^2 ppb) and Cu (on the order of 10^2 ppm) contents at the point when the mantle sulfides become fully dissolved in the partial melt, whereas further melting causes dilution of these metals (*e.g.*, Mungall and Brenan 2014; Yao et al. 2018). The point at which sulfide is exhausted from the mantle source is highly dependent on the P-T conditions and melt composition (major elements and Ni + Cu), which control the S dissolution capability of the magma (refer to Smythe et al. 2017; O'Neill 2021) as well as the S content of the mantle source. Typically, it is thought that roughly 10–20 % melting is required to fully dissolve sulfide in the mantle (Mungall and Brenan 2014; Yao et al. 2018; Waterton et al. 2021; Virtanen et al. 2024).

Compared to the palladium-group PGE, the iridium-group PGE are significantly more refractory, hence their concentrations are not as strongly controlled by the presence of residual sulfide in the mantle source (Pearson et al. 2004, Barnes et al. 2015). Additionally, iridium-group PGE-bearing metal alloys with very low solubility to silicate melt are generally stable in the mantle (Fonseca et al. 2012; Barnes et al. 2015). Due to the many potential IPGE-hosting phases in the residual mantle assemblage, IPGE concentrations rarely reach as high a primary enrichment as palladium-group PGE in mantle-derived melts. Like the stratiform Cr deposits, reef-type PGE deposits hosted in layered intrusions require very large volumes of mantle-derived melt to satisfy mass balance considerations. To demonstrate this, we show that 370 to 13,000 m of a mantle-derived partial melt is required to form a 1-m thick reef with 1 mass % sulfide with tenors of 300 ppm Pt (Fig. 10) This calculation requires the unrealistic assumption that Pt extraction from the silicate melt is 100 % efficient.

Due to its abundance, olivine dominates the Ni inventory of convecting mantle, while Ni-rich but modally minor sulfide phases are of lesser importance (Yao et al. 2018). Nickel is compatible in olivine with the compatibility showing an inverse correlation with forsterite content and temperature (*e.g.,* Matzen et al. 2017). Typically, generic mantle melting models show that Ni content of the primary melt increases with the degree of melting (Naldrett 2004, Mungall 2013); however, more complex models that account for the P-T path of the upwelling mantle and phase equilibrium, and their effects on Ni partitioning suggest contrarily that Ni content decreases with the degree of melting (Yao et al. 2018). The reason for the contradictory behavior is that when the melting initiates deep in the mantle, temperatures are hotter, and the partial melt has relatively high MgO content as controlled by the melting reactions. However, as upwelling continues, the MgO content of the melt decreases (refer to *e.g.,* experiments of Walter 1998). Consequently, Ni is less compatible in residual highly-forsteritic olivine early in the melting process, compared to less forsteritic residual olivine that forms at a later stage of decompression melting and adiabatic temperature reduction (Yao et al. 2018).

The common denominator of the above considerations of metal contents in primary magmas is that the metals are transported in the magma mainly as dissolved components. However, this might not always be the case. Some researchers consider the mobility of precious metals transported as nanonuggets attached to or dissolved in sulfide liquids. These droplets of sulfide liquid may buoyantly rise through silicate melts when they are attached to supercritical fluid bubbles (*i.e.,* compound droplets: Mungall et al. 2015) or perhaps when they are coated by low-density carbonate melt (Cherdantseva et al. 2024). In general, the transport of sulfide liquids by compound droplets has been invoked for short distance transportation of sulfide liquids in low-pressure settings, where volatile solubility in the silicate melts is

relatively low. As an example, this process has been suggested to have facilitated the upgrading of sulfide tenors in the deposits of the Norilsk-Talnakh intrusion (Iacono-Marziano et al. 2022). Similar buoyant two-phase transport of dense metal-rich phases facilitated either by super-critical CO_2 fluids, with low solubility in silicate melts, or by carbonate melt jackets, has been suggested to be possible from as deep as SCLM (*e. g.,* Blanks et al. 2020, Cherdantseva et al. 2024). However, direct evidence for such mantle-to-crust scale two-phase transportation processes is difficult to find due to the poor preservation of the transport agent, and it remains unclear how important this type of metal transport process is.

To summarize, the metallogenic potential of layered intrusions is strongly affected by the mantle source and the degree of partial melting. In general, high degree partial melts (roughly $\geq$ 25 %) inherit high concentrations of Cr and Ni as well as the PGE, as long as the latter are not diluted by too high a degree of partial melting. In addition, inheriting high V contents may require a high degree of melting if fO_2 in the mantle is low. Medium degrees of melting, high enough to completely dissolve mantle sulfide (roughly 10–20 %), produces primary melts with high concentrations of Ni, Cu, and the PPGE. When the degree of mantle melting is low (roughly $\leq$ 10 %), the primary melts formed have the best metallogenic potential for Ti and for V if the mantle source has sufficiently high fO_2 to cause incompatibility of the latter. This general pattern may, however, be violated if the mantle source has exotic metasomatic phases or if the metal transport is facilitated by two-phase transport.

9.2. Deposit-scale ore-forming processes

Deposit-scale ore-forming processes refer to coincident magmatic, magmatic-hydrothermal, and hydrodynamic processes that ensure the saturation of a given phase (*e.g.,* sulfide melt, chromite, conjugates) and its concentration into economically viable orebodies (Naldrett 2004; Namur et al. 2015; Latypov et al. 2024a). Mineral deposits in layered intrusions often occur as stratiform intervals within which ore minerals are concentrated. Without sufficient concentration, potential orebodies are diluted with gangue minerals and can become high tenor, but low grade disseminated mineral occurrences, such as that reported at the Duluth Complex (Minnesota; Naldrett 2004) and the Fazenda-Mirabela intrusion (Brazil; Barnes et al. 2011). With the exception of the Noril'sk-Talnakh intrusions (Russia), virtually all PGEs are sourced from Precambrian intrusions (refer to Table ST6 of Mudd et al. 2018; Fig. 4). Stratiform massive chromitites in layered intrusions account for most of the world's Cr reserves, and most of these reserves are present within the Precambrian Bushveld Complex and Great Dyke of Zimbabwe (Liu et al. 2024). Layered intrusions are critical V resources (Simandl and Paradis 2022), where many important Fe-Ti-V deposits occur in Precambrian layered intrusions, including the ~ 2.8 Ga Murchison intrusions of Western Australia, the ~ 2.4 Ga Koillismaa Complex in Finland, and the ~ 2.6 Ga Lac Doré intrusion in Québec (Smith and Maier 2021). Moreover, most layered intrusions with reported nelsonites (*i.e.,* Fe-Ti oxide- and apatite-rich rocks) were emplaced in the Precambrian (*e.g.,* Sept Îles intrusion, Tollari et al. 2008; Grader intrusion, Charlier et al. 2008).

Early models for the formation of stratiform mineral occurrences were founded on cumulus theory (Wager and Brown 1968), and although many ore-forming processes have since been invoked (refer to review by Smith and Maier 2021), the differentiation of parental melts and gravitational accumulation of their saturated phases remain relevant for stratiform mineral occurrences (Naldrett et al. 2012; Song et al. 2013; Holness et al. 2023). Gravitational settling and/or density-driven stratification are key processes in the formation of Fe-Ti-V oxide-rich occurrences, whether formed by cumulus oxides (Charlier et al. 2008; Zhang et al. 2012; She et al. 2015) or conjugate (immiscible) liquids (Holness et al. 2011; Wang et al. 2018). Prolonged fractionation of silicate minerals may produce an Fe- and Ti-rich residual melt from which

oxides crystallize and segregate from coprecipitating silicates according to density contrast (Charlier et al. 2008; Nebel et al. 2013; Mokchah and Mathieu 2022). It is worth noting that the $D^{mgt/melt}_{V(bulk)}$ value increases with decreasing fO_2, which favors the formation of relatively V-rich magnetite should negligible V partition into prior-forming clinopyroxene and ilmenite (Toplis and Carroll 1995; Toplis and Corgne 2002). The Main Magnetite Layer of the Bushveld Complex is thought to have formed via *in situ* crystallization from such an Fe- and Ti-rich residual melt (Reynolds 1985), whereby the cryptic dome-shaped Cr enrichments in the constituent magnetite are interpreted as nucleation sites (*i.e.,* growth nodes; Cawthorn and McCarthy 1980; Cawthorn 1994; Kruger and Latypov 2020). *In situ* growth in a chemically stratified magma was also invoked to explain the formation of the Mustavaara oxide-rich gabbros in the Koillismaa intrusion (Finland; Karinen et al. 2022). Alternatively, Yao and Mungall (2022) argued that the Main Magnetite Layer formed by homogeneous nucleation and settling of dense magnetite crystals, where the dome-shaped Cr profiles were explained as representing sites of upwelling Cr-bearing melts.

Silicate liquid immiscibility may also be responsible for Fe-Ti-V oxide-rich occurrences and this process has been recently reviewed by Veksler and Charlier (2015). Although magma mixing may influence silicate liquid immiscibility (Von Gruenewaldt 1993; Charlier and Grove 2012), it is broadly accepted to be a product of extensive fractionation, where efficient unmixing of Si-rich and Fe-Ti-rich conjugates is facilitated by the slow cooling rates of plutonic intrusions (Namur et al. 2012; Charlier et al. 2013). Experimental studies continue to explore the triggers (Honour et al. 2019) and relative timing (Hou and Veksler 2015) of silicate liquid immiscibility in basaltic systems, which has been evidenced by the preservation of both conjugate liquids as apatite-hosted melt inclusions (Fischer et al. 2016; Wang et al. 2018; Lino et al. 2023) and inferred from apatite chemistry (Kieffer et al. 2023). The Sept Îles (Charlier et al. 2011; Namur et al. 2012), Bushveld (VanTongeren and Mathez 2012), and Duluth (Ripley et al. 1998) intrusions are all proposed as having experienced large-scale silicate liquid immiscibility that led to the formation of magnetitites, ferrogabbros, and leucocratic gabbros. Immiscibility was also invoked to explain the formation of oxide-rich lenses in ultramafic cumulates of the ~ 3.5 Ga São Tomé intrusion (Brazil; Ruiz et al. 2019), which would argue that liquid–liquid immiscibility can occur relatively early in the differentiation of ferro-basaltic melts. Iron- and Ti-rich conjugate melt is likely to be under-saturated with respect to sulfide melt and will likely partially or completely dissolve any magmatic sulfide it encounters, leading to the upgrading or redistribution of chalcophile metals (Godel et al. 2014; Nielsen et al. 2015; 2019).

Chromitites may occur in the lower ultramafic (*e.g.,* Stillwater Complex), central mafic (*e.g.,* Bushveld Complex), or upper evolved (*e. g.,* Akanvaara) portions of layered intrusions (Smith and Maier 2021 and references therein). It is important to note that many chromitites have radiogenic isotope signatures consistent with crustal contamination (*e. g.,* Schoenberg et al. 1999), a process long considered to be involved in chromitite formation (*cf.* Irvine 1976). Thin chromitite stringers that are associated with anorthosite likely form during the reaction between resident cumulates and replenishing melts (O'Driscoll et al. 2009; Scoon and Costin 2018) or infiltrating supercritical fluids (Mathez and Kinzler 2017; Marsh et al. 2021); however, the origin of massive chromitites is heavily debated. Massive chromitites, even more so than chromitite stringers, necessitate the existence of melts that volumetrically exceed that inferred from the preserved cumulates and their lateral persistence implies chamber-wide phenomena (Campbell and Murck 1993; Cawthorn and Walraven 1998; Latypov et al. 2022; Fig. 10). The dilemma of mass balance for chromitite petrogenesis is mitigated for by many workers by invoking the existence of an underlying staging chamber from which chromite crystals are entrained and deposited, either as monomineralic slurries (Voordouw et al. 2009) or within silicate-chromite slurries that unmix through kinetic sieving (Eales 2000;

Mondal and Mathez 2007; Eales and Costin 2012). Indeed, a dike-like massive chromitite unit associated with the Kemi intrusion, interpreted as a feeder conduit, has been used to implicate either the existence of chromite-charged melts or the backflow of chromite-rich slurries (Alapieti and Lahtinen 2002; Yang et al. 2016). Chamber-wide phenomena, such as magma mixing (Irvine 1977; Campbell and Murck 1993; Spandler 2005), shifts in fO_2 (Ulmer 1969), melt stratification (Naldrett et al. 2012), and pressure shifts [decrease (Cameron 1977; Lipin 1993; Cawthorn 2005); increase (Latypov et al. 2018; Drage and Brenan 2023)] have also been proposed as triggers for chromite saturation; however, any model that implicates gravitational settling and sorting has difficulty addressing the issues of chromitite topography and, in some cases, mass balance and uniformity of their bracketing units (Latypov et al. 2017).

Although PGMs may crystallize directly from mantle-derived melts (Peck et al. 1992; Maier et al. 2014), it is generally accepted that immiscible sulfide melts play a key role in scavenging chalcophile metals from silicate melts (Naldrett 2004; Mungall and Brenan 2014). Recent models show that the S solubility of basaltic melt varies only slightly under crustal pressures (O'Neill 2021). Relatively high S solubilities at lower pressures (< 1 GPa; Mavrogenes and O'Neill 1999; Smythe et al. 2017) indicates that melts pooling in shallow reservoirs must either undergo extensive degrees of differentiation and/or assimilate crustal materials to reach sulfide saturation (Ripley and Li 2013). Crustal contamination may trigger sulfide melt saturation in basaltic magmas by altering the composition of the melt (Irvine 1976; Virtanen et al. 2021), modifying the redox conditions (Jugo and Lesher 2005; Iacono-Marziano et al. 2017), introducing volatile species (Naldrett 2004; Liu et al. 2007), and/or introducing sulfide xenomelts (Lesher 2017). Section 9.1 outlines the importance of pre-emplacement contamination in PGE reef formation; however, the *in situ* assimilation of sulfide xenomelts is relevant to some contact-style magmatic sulfide occurrences. One example is the Partridge River Intrusion of the Duluth Complex, whereby Samalens et al. (2017) showed that semi-metal concentrations in sulfides decrease and PGE concentrations in sulfides increase with increasing distance from country rock xenoliths. Also at the Duluth Complex, Virtanen et al. (2021) have shown that S and chalcophile metals could be liberated from the contact aureole during *in situ* devolatilization, providing a mechanism for increasing melt fertility without wholesale assimilation of wall-rocks.

As detailed in Latypov et al. (2015; 2024a), many models have been proposed for the formation of stratiform PGE reef-style mineralization, which, like chromitites, necessitate chamber-wide phenomena. They may occur at any stratigraphic level within an intrusion and can manifest in several different host rocks (Latypov et al. 2024a); no single petrogenetic model has been able to account for their diversity. Crustal contamination, likely in an underlying staging chamber, is believed to have played a role in the formation of relatively uncommon ultramafic-hosted PGE reefs, such as the Sopcha Reef in the Monchegorsk intrusion (Russia; Karykowski et al. 2018) and Volspruit Zone of the Bushveld Complex (Tanner et al. 2019). Conversely, PGE reefs hosted in upper, more evolved portions of layered intrusions, such as in the Jameson (Musgraves Region, Australia; Polito et al. 2017) and Nuasahi (India; Prichard et al. 2018) intrusions, are thought to have formed from strongly fractionated melts in response to magnetite saturation. Each "reef", however, requires high R-factors (mass ratio of silicate:sulfide melt; Campbell and Naldrett 1979) that are broadly believed to only be attained via open-system processes, such as entrainment of sulfide melts from depth (McDonald and Holwell 2011; Kaavera et al. 2020) or dissolution-upgrading (Kerr and Leitch 2005; Cao et al. 2021). Recognition that the $D^{sul/sil}$ values of the PGE are on the order of 10^6 (Mungall and Brenan 2014) has led to the conclusion that many PGE reefs can be explained by closed-system processes (Mungall et al. 2020), but it has been proposed that these $D^{sul/sil}$ values are overestimated due to the mechanical inclusion of PGE nanonuggets in sulfide liquid (Anenburg and Mavrogenes 2020).

Alternatives to orthomagmatic models are hydromagmatic models that propose PGE concentration in stratiform horizons during the (re-)dissolution of upwelling Cl- and PGE-bearing fluids exsolved from underlying cumulates (Boudreau and McCallum 1992). These models are supported by, amongst other things, the relative increase in the abundance of Cl-bearing accessory phases (Boudreau et al. 1986; Boudreau and McCallum 1989), presence of saline fluid inclusions (Ballhaus and Stumpfl 1986; Ripley 2005; Hanley et al. 2008), and the existence of pegmatitic rocks, discordant pipes, and potholes (Boudreau 2019 and references therein). Reef-style PGE mineralization in the Stillwater and Bushveld complexes are taken as key case studies for hydromagmatic models (Boudreau et al. 1986), yet similar Cl enrichments are not observed in the Main Sulfide Zone of the Great Dike (Boudreau et al. 1995), the Munni Munni intrusion (Boudreau et al. 1993), or Fedorova-Pana Complex (Sushchenko et al. 2023). Although the role of halogens in ore formation is debated, it is broadly accepted that PGEs (Pt and Pd) can be transported as chloride complexes in aqueous brines (Sullivan et al. 2020a; 2020b).

Although not mutually inclusive, many stratiform chromitites and magnetitites host elevated PGE concentrations (Maier 2005; Smith and Maier 2021). Contrary to experimental results (Rose and Brenan 2001), Godel et al. (2006) argued that chromitites trap sulfide liquid as it cannot percolate as effectively through them as they can through silicate cumulates. Any "trapped" sulfide liquid may become further enriched in PGEs if it loses Fe to neighboring chromite crystals and S_2 to the surrounding rocks (Naldrett and Lehmann 1988). Alternatively, the association between chromite and sulfides could reflect sulfide, PGM and/or PGE-nanonuggets preferentially [heterogeneously] nucleating in reduced boundary layers that encompass crystallizing chromite crystals (Finnigan et al. 2008; Anenburg and Mavrogenes 2016; Barnes et al. 2021). Magnetitites with elevated PGE concentrations are almost universally explained as the product of S-saturation triggered by saturation of magnetite (*i.e.,* removal of Fe^{2+} from the melt; Polito et al. 2017), and further stratification of oxides ($\pm$ sulfides) may be achieved by granular flow (*i.e.,* Stella intrusion; Maier et al. 2023). The sulfides may be PGE-poor if the silicate melt had previously experienced sulfide melt saturation (Étoile Suite in Quebec; R. Maier *et al.* in-press).

Several reef-style PGE occurrences exhibit 'offsets' in peak concentrations of chalcophile metals and are, thus, aptly referred to as offset-style reefs. Although the term has been founded on offset-style mineralization observed at the mafic–ultramafic transition in Munni Munni (Barnes et al. 1992) and the Great Dike (Wilson and Tredoux 1990), this pattern has been documented in several other intrusions, where it displays remarkable variability in its relative stratigraphic position [*e.g.,* basal ultramafic cumulates in Kapalagulu (Prendergast 2021) to upper magnetitites in Jameson (Karykowski et al. 2017)] and the nature of the offsets. Although the sequential offsets observed for peak Pd + Pt, Au, and Cu concentrations are consistent with generally accepted partition coefficients (*i.e.,* upwards-decreasing $D^{sul/sil}$ values), some workers have suggested that fractional sulfide segregation and instantaneous equilibration is unable to sufficiently account for the offsets (Barnes 1993; Mungall 2002). This has led to offsets being described as a result of fluctuations in the efficiency of PGE scavenging by sulfide melt (*i.e.,* 'virtual' partition coefficients; Barnes 1993) or differences in the diffusivities of chalcophile and highly siderophile elements (Mungall 2002); the latter process has been applied to a number of offset-type reefs (Holwell et al. 2016; Guice et al. 2017; Prendergast 2021). The latter models describe the offsets as primary features, but in an alternative model for the Stella (Maier et al. 2003) and Skaergaard (Andersen et al. 1998) reefs, researchers proposed that offsets form as accumulated sulfide liquid differentiates whilst being displaced upward during cumulate compaction.

9.3. Detecting mineral occurrences in layered intrusions

The final key components of the layered intrusion mineral systems

are *detectability* and *delineation* – how can one determine whether an ore-forming process was active in a given system and can the preserved rock record be exploited to vector toward mineral deposit occurrences (Maier and Barnes 2005; Barnes et al. 2016). Layered intrusions typically host thick mafic–ultramafic cumulates that may be spatially associated with *trans*-crustal structural networks through which fertile parent melts ascended. Such cumulates often display elevated concentrations of Mg, Fe, Cr, and Ni, low incompatible trace element contents (*e.g.,* Ti, Zr, REE), gravitational anomalies (>2.6 g/cm^3), and anomalous electromagnetic signatures that are enhanced by serpentinization as well as the presence of contact-style sulfides and oxide-rich occurrences (Finn et al. 2015; Blanchard et al. 2017; Kharbish et al. 2022).

Cumulus sulfides and gossanous outcrops are favorable mineralization indicators and translate to anomalous concentrations of S and chalcophile metals in the rocks, overlying soils and flora, and emanating stream sediments. In contrast, mafic–ultramafic rocks that are depleted in chalcophile elements likely experienced upstream sulfide melt segregation, indicating that cumulus sulfides may exist elsewhere in the accessible plumbing system (Maier 2005). The presence of S-bearing country rocks and evidence of their interaction with mantle-derived melts (*e.g.,* thermal aureoles, xenoliths) are also positive indicators, because the assimilation of such rocks can trigger sulfide melt saturation in fertile mantle-derived melts (Ripley and Li 2013) and chalcophile metals may even be liberated during country rock devolatilization (Virtanen et al. 2021). Many of these attributes translate to mappable criteria that can be used for mineral prospectivity exploration (Porwal et al. 2010). This exercise leverages increasingly popular machine learning algorithms to delineate areas of heightened prospectivity, which has proven to be effective in delineating chromitites in the Gawler Craton (Farahbakhsh et al. 2023) and Fe-Ti-V occurrences in southwest China (Cong et al. 2017).

Siliceous high-Mg basalts (SHMBs) are parental to many of the world's notable layered intrusions, such as the Bushveld (Solovova et al. 2021), Stillwater (Jenkins et al. 2021) and Penikat (Maier et al. 2018) complexes. These magmas represent komatiitic melts that assimilated crustal rocks during their ascent (Arndt and Jenner 1986), perhaps in a staging chamber within which sulfide melts may also segregate and become entrained (Eales and Costin 2012; Kaavera et al. 2020). Cumulates derived from contaminated melts often contain cumulus orthopyroxene (Jenkins and Mungall 2018), and these grains may show erratic zoning profiles when associated with dynamic systems conductive to magmatic sulfide ore formation (Schoneveld et al. 2020). However, subsolidus diffusion of cations under prolonged cooling rates will dilute zoning profiles (Barnes et al. 2016), hence further research could determine its suitability for vectoring mineral occurrences in layered intrusions. The degree of interaction between mantle-derived melts and crustal rocks is often evaluated by determining whether trace element ratios and isotopic signatures of host rocks have deviated from that expected of mantle-derived melts (Maier and Barnes 2005; Queffurus and Barnes 2015; Tang et al. 2021).

In studies of magmatic sulfides, $\delta^{34}S$ [$(^{34}S/^{32}S)$ sample/$(^{34}S/^{32}S)$ standard – 1) × 1000] values have been widely used to evaluate the S sources, since the assimilation of exogenous S by mantle-derived melts typically results in $\delta^{34}S$ values that deviate toward relatively heavy or relatively light end members (Lesher and Groves 1986; Ripley and Li 2003). However, because the $\delta^{34}S$ values of Archean mantle and crust are similar, many studies in Archean terranes now also consider $\Delta^{33}S$ values {$\delta^{33}S – 1000 \times (1 + \delta^{34}S/1000)^{0.515} – 1$}, which only deviate from 0 prior to 2.4 Ga as a result of UV-induced photochemical processes in the oxygen-deficient Archean atmosphere (Farquhar and Wing 2003). It must be noted that immiscible sulfide melts (or xenomelts) will continue to equilibrate with coexisting silicate melt, diluting and possibly eradicating non-zero S isotopic signatures (Lesher and Burnham 2001). This was demonstrated at the Duluth Complex, where diluted S isotopic signatures coincided with low semi-metal (As and Sb) and high PGE (Pd and Ir) concentrations of sulfides, consistent with increasing *R*-factors

(Samalens et al. 2017). Nonetheless, the concentrations of semi-metals (or 'TABS'; Te, As, Bi, and Sb; Mansur and Barnes 2020) and the presence of sulfarsenides (Knight et al. 2017) may be used to evaluate the nature of crustal contamination in each system.

Whole-rock Cu/Pd and Cu/Zr values remain among the most widely used indicators of sulfide melt segregation, having been effective in inferring pre-emplacement sulfide melt segregation and in vectoring many of the world's reef-style PGE occurrences regardless of their host rock and stratigraphic position (Fig. 11; Barnes 1990; Li and Naldrett 1999; Maier 2005). The Ni concentration of olivine is another widely used indicator of S-saturation and vector of sulfide mineralization (Bulle and Layne 2016; Taranovic et al. 2022; Smith et al. 2025) and refer to the review of Barnes et al. (2023a). The trace element concentrations of Fe-Ti oxides are sensitive to the wide variety of conditions under which they can crystallize (*e.g.,* silicate melts, sulfide melts, hydrothermal fluids), meaning they can be used to determine provenance and vector towards magmatic sulfide and Fe-Ti-V occurrences (Dupuis and Beaudoin 2011; Dare et al. 2014). Oxides exsolved from immiscible sulfide melts may have characteristically high Cr, V, and Ni concentrations depending on the degree of sulfide melt fractionation (Dare et al. 2012), whereas those associated with Fe-Ti-V occurrences can have elevated Ti and V concentrations (Dupuis and Beaudoin 2011).

Accessory apatite that is spatially associated with reef-style PGE occurrences has been known to be relatively Cl-rich (Boudreau et al. 1986) and its trace element concentrations may be used to discover Fe-Ti-P mineral deposits (Kieffer et al. 2023) or reveal insights into the petrogenesis of layered intrusions (Kieffer et al. 2024). For example, cumulus apatite associated with Fe-Ti-P(−V) oxide mineralization has relatively high Sr concentrations and Eu/Eu* values as well as low ΣREE + Y concentrations (Kieffer et al. 2023). Lastly, the use of sulfide chemistry for exploration targeting has been discussed by Mansur et al. (2020). Pentlandite compositions may be most applicable to layered intrusion mineral occurrences as their Pd, Rh, and TABs concentrations are sensitive to deposit origin (Ni-Cu versus PGE), sulfide melt fractionation, PGM exsolution and metal tenors (Mansur et al. 2020; 2024).

10. Future avenues of layered intrusion research

Layered intrusions occur in a variety of different geodynamic settings throughout Earth's history and are well represented by geologically diverse examples in the Precambrian (Namur et al. 2015). Although much progress has been made in understanding layered intrusion petrology, many aspects of their origin remain heavily debated in the literature. Here we reiterate the next steps of Latypov et al. (2024a) regarding the future of layered intrusion research in the specific context of Precambrian geodynamics.

1. Regional mapping campaigns of surface outcrops and underground mine exposures, as well as logging drill cores, will likely always underpin layered intrusion research. Primary field observations and their correlation on the macroscale facilitate appropriate sampling campaigns, making them essential for contextualizing subsequent data and constraining interpretations. Field observations are always where the maximum uncertainty potentially occurs in a dataset. Field methods may be bolstered by spectral imagery (Barnes 2020; Hill et al. 2021) and/or combined with geophysical data (Finn et al. 2015; 2023) to better understand the morphology and architecture of layered intrusions, particularly in areas with little-to-no exposure (Lima et al. 2008; Balch et al. 2010). For example, Cole et al. (2024) demonstrated that geophysical data can elucidate deep high-density features, which could represent staging chambers or magmatic underplating beneath layered intrusions.

2. Element mapping and microtextural analyses are powerful in testing hypotheses and forming new ones. Combinations of these methods can elucidate the physicochemical conditions under which rocks and their ores were formed and modified. Although element mapping has
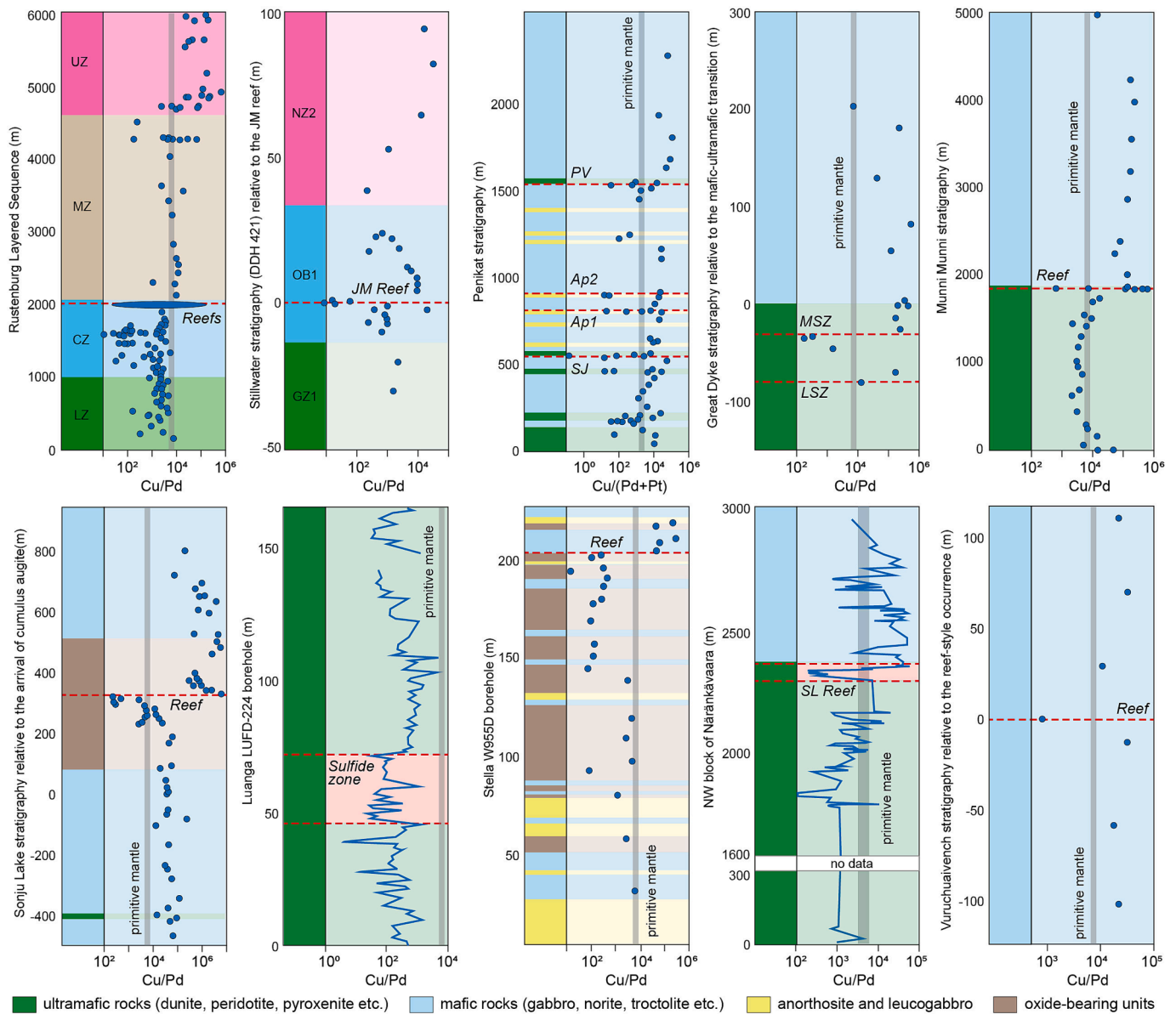
Fig. 11. Identification of reef-style PGE occurrences in layered intrusions using whole-rock Cu/Pd values. Intrusions and references include the Rustenburg Layered Suite of the Bushveld Complex (Barnes et al. 2004), Stillwater Complex (Keays et al. 2012), Penikat intrusion (Maier et al. 2018), Great Dyke (Maier et al. 2015), Munni Munni intrusion (Hoatson and Keays 1989), Sonju Lake intrusion (Miller Jr 1999), Luanga intrusion (Mansur et al. 2020), Stella intrusion (Maier et al. 2023), Näränkävaara intrusion (Järvinen et al. 2020), and the Vuruchuaivench occurrence of the Monchegorsk intrusion (Karykowski et al. 2018).

gained traction for mineralogical characterization (Barnes et al. 2016; 2021; Smith et al. 2021), microtextural analyses remain underutilized despite the valuable petrogenetic insights they offer (Vukmanovic et al. 2019; Jenkins et al. 2022; Holness et al. 2024). As demonstrated in *Section 8*, element mapping and microtextural analysis were used to constrain the petrogenesis of the snowball oikocryst unit of the Stillwater Complex. Our analysis demonstrated deposition of poikilitic crystals in a dynamic environment prior to the formation of a mush.

3. High-resolution X-ray computed tomography and novel laboratory diffraction contrast tomography are non-destructive methods that allow for visualization and quantification of three-dimensional features in polycrystalline rocks (Godel 2013; Chen et al. 2023). These methods can be utilized in conjunction with two-dimensional petrographic observations to document magmatic fabrics, melt percolation, diffusion kinetics, crystal nucleation mechanisms, and likely other as yet unidentified applications.

4. Greater constraints on the parameters under which a given intrusion formed can be achieved through the use and discovery of mineral thermobarometers, oxybarometers, and hygrometers (Lindsley and Andersen 1983; Ballhaus et al. 1991; Godel et al. 2011; Molina et al. 2021). Empirically determined parameters may then be used to inform thermodynamically constrained forward modelling (Ghiorso and Sack 1995; Bohrson et al. 2020; Ariskin et al. 2023) that might, for example, lead to a better understanding of sulfur content at sulfide saturation (O'Neill 2021; Wieser and Gleeson 2022), alloy solubility (Mungall and Brenan 2014), and the effects of degassing (Burgisser and Degruyter 2015; Ding et al. 2023). These mineral indicators may help to identify secular changes in the nature of layered intrusion petrogenesis throughout the Precambrian.

5. The successful implementation of Point (4) could be supported by experimental studies that explore the various conditions under which layered intrusions typically form. Petrological experiments that consider a range of intensive parameters can help to constrain

liquid lines of descent (Leuthold et al. 2015; Drage and Brenan 2023), understand element partitioning (Blundy and Wood 2003; Shephard et al. 2022), and simulate crustal assimilation (Iacono-Marziano et al. 2017; Virtanen et al. 2022; Deegan et al. 2022). Furthermore, analogue experiments may also be used to model processes such as magma mixing (Sato and Sato 2009) or layer formation (Forien et al. 2015), providing insights into emplacement mechanisms and layer-forming processes.

6. Future studies could aim to better understand the role of volatile species in layer- and ore-forming processes. These studies may utilize experimental or computer-based simulations of the interaction between immiscible phases (Mungall 2015; Yao and Mungall 2020; Cherdantseva et al. 2024), as well as directly analyze the volatile budgets of volatile-bearing and nominally volatile-free minerals (Boudreau et al. 1995; Pedersen et al. 2021; Bai et al. 2024). These studies could help to elucidate the volatile budgets of magmas, melts, and fluids associated with layered intrusions, mineralized or not, and provide insight into the cycling of volatile species throughout the Precambrian.

7. Development of workflows for the handling of expansive and interdisciplinary datasets, particularly commercial datasets that may far exceed academic datasets in size (Jenkins et al. 2020; Barnes and Williams 2024). Systematic handling of such datasets will allow for meaningful comparisons between intrusions and their critical metal occurrences, potentially illuminating spatiotemporal changes in their nature. Such workflows will likely consider machine learning algorithms that can be leveraged for chemical domaining (Horrocks et al. 2019) or intensive parameter prediction (Higgins et al. 2022).

8. As layered intrusions are hosts of important critical metal occurrences, many studies will likely center on identifying traits that are characteristic of mineralized examples as well as on developing practical tools to assist in their delineation (Dare et al. 2014; Schoneveld et al. 2020; Barnes et al. 2023). Effective tools are founded on a deep understanding of the processes that govern critical metal deposition, yet commercially viable exploration tools are lacking for mineral occurrences with no systematic haloes. In the absence of deposit-scale footprints, research could utilize the mineral system approach (*e.g.,* McCuaig et al. 2010; Barnes et al. 2016) to infer prospectivity through identifying processes that are favorable for ore deposition.

9. As multifaceted datasets become commonplace for layered intrusions and their genetically associated rocks (*i.e.,* dikes, volcanics), global spatiotemporal comparisons of their petrogeneses become possible. These data can potentially shed light on fundamental planetary scale processes such as the physicochemical evolution of the mantle through time, mantle heterogeneity on local and regional scales, material flux between the mantle and the lithosphere, magmatic fractionation, and stabilization of continents.

The future of layered intrusion research can be enhanced by multidisciplinary collaborations between geoscientists, material scientists, data scientists, mathematicians, and (or) geophysicists, amongst others, that generate and interpret holistic datasets. Integrated studies that are transparent and reproducible could lead to new discoveries in layered intrusion research and support the next generation of researchers.

CRediT authorship contribution statement

William D. Smith: Writing – review & editing, Writing – original draft, Methodology, Investigation, Formal analysis, Data curation, Conceptualization. **M. Christopher Jenkins:** Writing – review & editing, Writing – original draft, Methodology, Investigation, Formal analysis, Data curation, Conceptualization. **Claudia T. Augustin:** Writing – review & editing, Writing – original draft, Methodology, Investigation, Conceptualization. **Ville J. Virtanen:** Writing – review & editing, Writing – original draft, Methodology, Investigation, Conceptualization.

Zoja Vukmanovic: Writing – review & editing, Writing – original draft, Methodology, Investigation, Formal analysis, Data curation, Conceptualization. **Brian O'Driscoll:** Writing – review & editing, Validation, Supervision, Conceptualization.

Declaration of competing interest

The authors declare that they have no known competing financial interests or personal relationships that could have appeared to influence the work reported in this paper.

Appendix A. Supplementary data

Supplementary data to this article can be found online at https://doi.org/10.1016/j.precamres.2024.107615.

Data availability

Data are available in the supplementary materials. Requests for the raw EBSD and element map data can be made to the authors.

References

Acocella, V. (2021). Magma Emplacement and Accumulation: From Sills to Magma Chambers. In *Volcano-Tectonic Processes* (pp. 117–161). Springer.

Ahmat, A. L. (1986). *Petrology, structure, regional geology and age of the gabbroic Windimurra complex, Western Australia: University of Western Australia, Perth, Western Australia.* PhD thesis (unpublished).

Alapieti, T., 1982. *The Koillismaa Layered Igneous Complex, Finland-Its Structure, Mineralogy and Geochemistry with Emphasis on the Distribution Of Chromium.* Geological Survey of Finland. Bulletin 319 (116).

Alapieti, T.T., Kujanpaa, J., Lahtinen, J.J., Papunen, H., 1989. The Kemi stratiform chromitite deposit, northern Finland. Econ. Geol. 84 (5), 1057–1077.

Alapieti, T.T., Lahtinen, J.J., 1986. Stratigraphy, petrology, and platinum-group element mineralization of the early Proterozoic Penikat layered intrusion, northern Finland. Econ. Geol. 81 (5), 1126–1136.

Alapieti, T.T., Lahtinen, J.J., 2002. Platinum-group element mineralization in layered intrusions of northern Finland and the Kola Peninsula, Russia. *The Geology,*

Geochemistry, Mineralogy and Mineral Beneficiation of Platinum-Group Elements. Cana. Inst. Mining, Metallurg. Petroleum, Special 54, 507–546.

Andersen, J.C.Ø., Rasmussen, H., Nielsen, T.F.D., Ronsbo, J.G., 1998. The Triple Group and the Platinova gold and palladium reefs in the Skaergaard Intrusion; stratigraphic and petrographic relations. Econ. Geol. 93 (4), 488–509.

Andringa, S., Godfroid, A., 2020. Sampling bias and the problem of generalizability in applied linguistics. Annual Review of Applied Linguistics 40, 134–142.

Anenburg, M., Mavrogenes, J.A., 2016. Experimental observations on noble metal nanonuggets and Fe-Ti oxides, and the transport of platinum group elements in silicate melts. Geochim. Cosmochim. Acta 192, 258–278.

Anenburg, M., Mavrogenes, J.A., 2020. Noble metal nanonugget insolubility in geological sulfide liquids. Geology 48 (9), 939–943.

Ariskin, A. A., Barmina, G. S., Koptev-Dvornikov, E. v, Bychkov, K. A., & Nikolaev, G. S. (2023). Intrusive COMAGMAT: From simple magma differentiation models to complex algorithms simulating the structure of layered intrusions. In Advances in Geochemistry, Analytical Chemistry, and Planetary Sciences: 75th Anniversary of the Vernadsky Institute of the Russian Academy of Sciences (pp. 101–119). Springer.

Arndt, N., 2013. The lithospheric mantle plays no active role in the formation of orthomagmatic ore deposits. Econ. Geol. 108 (8), 1953–1970.

Arndt, N.T., Jenner, G.A., 1986. Crustally contaminated komatiites and basalts from Kambalda, Western Australia. Chem. Geol. 56 (3–4), 229–255.

Arndt, N.T., Coltice, N., Helmstaedt, H., Gregoire, M., 2009. Origin of Archean subcontinental lithospheric mantle: Some petrological constraints. Lithos 109 (1–2), 61–71.

Arndt, N. T., Lesher, C. M., & Czamanske, G. K. (2005). Mantle-derived magmas and magmatic Ni-Cu-(PGE) deposits. *Economic Geology, 100th Anni*, 5–24.

Augustin, C.T., Mungall, J.E., Schutesky, M.E., Ernst, R., Garcia, V.B., 2022. Petrological and geochemical characteristics of the mafic-ultramafic Americano do Brasil Complex, central Brazil, and the implications for its genesis. Ore Geol. Rev. 105126.

Augustin, C.T., Mungall, J.E., Schutesky, M.E., Chamberlain, K.R., Ernst, R., Garcia, V.B., 2023. U-Pb in-situ SIMS baddeleyite and zircon dates and thermodynamic modeling of the Mangabal Complex: Indications of asthenospheric mantle influence in the formation of layered intrusions of the Brasília orogen. Gondw. Res. 122, 93–111.

Bada, J.L., Korenaga, J., 2018. Exposed areas above sea level on Earth> 3.5 Gyr ago: Implications for prebiotic and primitive biotic chemistry. Life 8 (4), 55.

Bai, Y., Cui, M.-M., Su, B.-X., Liu, X., Xiao, Y., Robinson, P. T., & Gu, X.-Y. (2024). FTIR study of H2O in silicate minerals and mineral inclusions in chromite from the peridotite zone of the Stillwater complex (Montana, USA): Evidence for chromitite formation in an H2O-rich environment. *Bulletin, 136*(3–4), 1661–1674.

Bai, Z.-J., Zhong, H., Hu, R.-Z., Zhu, W.-G., Hu, W.-J., 2019. Composition of the chilled marginal rocks of the Panzhihua layered intrusion, Emeishan Large Igneous Province, SW China: Implications for parental magma compositions, sulfide saturation history and Fe–Ti oxide mineralization. J. Petrol. 60 (3), 619–648.

Baker, D.R., 2008. The fidelity of melt inclusions as records of melt composition. Contrib. Miner. Petrol. 156, 377–395.

Baker, M.B., Stolper, E.M., 1994. Determining the composition of high-pressure mantle melts using diamond aggregates. Geochim. Cosmochim. Acta 58 (13), 2811–2827.

Balch, S. J., Mungall, J. E., & Niemi, J. (2010). Present and future geophysical methods for Ni-Cu-PGE exploration: Lessons from McFaulds Lake, northern Ontario.

Ballhaus, C., Berry, R.F., Green, D.H., 1991. High pressure experimental calibration of the olivine-orthopyroxene-spinel oxygen geobarometer: implications for the oxidation state of the upper mantle. Contrib. Miner. Petrol. 107, 27–40.

Ballhaus, C.G., Stumpfl, E.F., 1986. Sulfide and platinum mineralization in the Merensky Reef: evidence from hydrous silicates and fluid inclusions. Contrib. Miner. Petrol. 94 (2), 193–204.

Barnes, S.J., 1986. The effect of trapped liquid crystallization on cumulus mineral compositions in layered intrusions. Contrib. Miner. Petrol. 93 (4), 524–531.

Barnes, S.J., 1989. Are Bushveld U-type parent magmas boninites or contaminated komatiites? Contrib. Miner. Petrol. 101 (4), 447–457.

Barnes, S.J., 1990. The use of metal ratios in prospecting for platinum-group element deposits in mafic and ultramafic intrusions. J. Geochem. Explor. 37 (1), 91–99.

Barnes, S.J., 1993. Partitioning of the platinum group elements and gold between silicate and sulfide magmas in the Munni Munni Complex. Western Australia. *Geochimica et Cosmochimica Acta* 57 (6), 1277–1290.

Barnes, S.-J., Naldrett, A.J., Gorton, M.P., 1985. The origin of the fractionation of platinum-group elements in terrestrial magmas. Chem. Geol. 53 (3–4), 303–323.

Barnes, S.-J., Melezhik, V. A., & Sokolov, S. v. (2001). The composition and mode of formation of the Pechenga nickel deposits, Kola Peninsula, northwestern Russia. *The Canadian Mineralogist, 39*(2), 447–471.

Barnes, S.J., Keays, R.R., Hoatson, D.M., 1992. Distribution of sulfides and PGE within the porphyritic websterite zone of the Munni Munni Complex, Western Australia. Aust. J. Earth Sci. 39 (3), 289–302.

Barnes, S.-J., Maier, W.D., Ashwal, L.D., 2004. Platinum-group element distribution in the main zone and upper zone of the Bushveld Complex. South Africa. *Chemical Geology* 208 (1–4), 293–317.

Barnes, S.-J., Maier, W.D., Curl, E.A., 2010. Composition of the marginal rocks and sills of the Rustenburg Layered Suite, Bushveld Complex, South Africa: implications for the formation of the platinum-group element deposits. Econ. Geol. 105 (8), 1491–1511.

Barnes, S.J., Osborne, G.A., Cook, D., Barnes, L., Maier, W.D., Godel, B.M., 2011. The Santa Rita nickel sulfide deposit in the Fazenda Mirabela Intrusion, Bahia, Brazil: Geology, sulfide geochemistry, and genesis. Econ. Geol. 106 (7), 1083–1110.

Barnes, S.J., Mungall, J.E., Maier, W.D., 2015. Platinum group elements in mantle melts and mantle samples. Lithos 232, 395–417.

Barnes, S.J., Cruden, A.R., Arndt, N., Saumur, B.M., 2016a. The mineral system approach applied to magmatic Ni–Cu–PGE sulfide deposits. Ore Geol. Rev. 76, 296–316.

Barnes, S.J., Fisher, L.A., Godel, B., Pearce, M.A., Maier, W.D., Paterson, D., Howard, D. L., Ryan, C.G., Laird, J.S., 2016b. Primary cumulus platinum minerals in the Monts de Cristal Complex, Gabon: magmatic microenvironments inferred from high-definition X-ray fluorescence microscopy. Contrib. Miner. Petrol. 171, 1–18.

Barnes, S.J., Mole, D.R., Le Vaillant, M., Campbell, M.J., Verrall, M.R., Roberts, M.P., Evans, N.J., 2016c. Poikilitic Textures, Heteradcumulates and Zoned Orthopyroxenes in the Ntaka Ultramafic Complex, Tanzania : Implications for Crystallization Mechanisms of Oikocrysts. J. Petrol. 57 (6), 1171–1198. https://doi.org/10.1093/petrology/egw036.

Barnes, S.J., Latypov, R., Chistyakova, S., Godel, B., Schoneveld, L.E., 2021a. Idiomorphic oikocrysts of clinopyroxene produced by a peritectic reaction within a solidification front of the Bushveld Complex. Contrib. Miner. Petrol. 176, 1–19.

Barnes, S.J., Ryan, C., Moorhead, G., Latypov, R., Maier, W.D., Yudovskaya, M., Godel, B., Schoneveld, L.E., Le Vaillant, M., Pearce, M.B., 2021b. Spatial association between platinum minerals and magmatic sulfides imaged with the Maia Mapper and implications for the origin of the chromite-sulfide-PGE association. The Canadian Mineralogist 59 (6), 1775–1799.

Barnes, S.J., Williams, M., 2024. Postcumulus processes recorded in whole-rock geochemistry: a case study from the Mirabela layered intrusion. Brazil. *Journal of Petrology* 65 (4), egae019.

Barnes, S.J., Yao, Z.-S., Mao, Y.-J., Jesus, A.P., Yang, S., Taranovic, V., Maier, W.D., 2023a. Nickel in olivine as an exploration indicator for magmatic Ni-Cu sulfide deposits: A data review and re-evaluation. Am. Mineral. 108 (1), 1–17.

Barnes, S.J., Yudovskaya, M.A., Iacono-Marziano, G., le Vaillant, M., Schoneveld, L.E., Cruden, A.R., 2023b. Role of volatiles in intrusion emplacement and sulfide deposition in the supergiant Norilsk-Talnakh Ni-Cu-PGE ore deposits. Geology 51 (11), 1027–1032.

Barnes, E. (2020). *Assessment of Drone-Borne Multispectral Mapping in the Exploration of Magmatic Ni-Cu Sulfides–an Example from Disko Island, West Greenland*. PhD thesis (unpublished).

Becker, G.F., 1897. Fractional crystallization of rocks. Am. J. Sci. s4–4(22), 257–261. https://doi.org/10.2475/ajs.s4-4.22.257.

Bédard, J.H., 1994. A procedure for calculating the equilibrium distribution of trace elements among the minerals of cumulate rocks, and the concentration of trace elements in the coexisting liquids. Chem. Geol. 118 (1–4), 143–153.

Begg, G.C., Hronsky, J.M.A., Arndt, N.T., Griffin, W.L., O'Reilly, S.Y., Hayward, N., 2010. Lithospheric, Cratonic, and Geodynamic Setting of Ni-Cu-PGE Sulfide Deposits. Econ. Geol. 105 (6), 1057–1070.

Berg, J.H., 1980. Snowflake troctolite in the Hettasch intrusion, Labrador: evidence for magma-mixing and supercooling in a plutonic environment. Contrib. Miner. Petrol. 72 (4), 339–351.

Berg, J.H., Docka, J.A., 1983. Geothermometry in the Kiglapait contact aureole. Labrador. *American Journal of Science* 283 (5), 414–434.

Berg, J.H., Emslie, R.F., Hamilton, M.A., Morse, S.A., Ryan, A.B., Wiebe, R.A., 1994. Anorthositic, granitoid and related rocks of the Nain Plutonic Suite. International Geological Correlation Programme, IGCP Projects, p. 290.

Blanchard, J.A., Ernst, R.E., Samson, C., 2017. Gravity and magnetic modelling of layered mafic–ultramafic intrusions in large igneous province plume center regions: case studies from the 1.27 Ga Mackenzie, 1.38 Ga Kunene-Kibaran, 0.06 Ga Deccan, and 0.13–0.08 Ga High Arctic events. Canadian Journal of Earth Sciences 54 (3), 290–310.

Blanks, D., Holwell, D.A., Fiorentini, M.L., Moroni, M., Giuliani, A., Tassara, S., González-Jiménez, J.M., Boyce, A.J., Ferrari, E., 2020. Fluxing of mantle carbon as a physical agent for metallogenic fertilization of the crust. Nat. Commun. 11 (1), 1–11.

Blundy, J., Wood, B., 2003. Partitioning of trace elements between crystals and melts. Earth Planet. Sci. Lett. 210 (3–4), 383–397.

Bohrson, W. A., Spera, F. J., Heinonen, J. S., Brown, G. A., Scruggs, M. A., Adams, J. v, Takach, M. K., Zeff, G., & Suikkanen, E. (2020). Diagnosing open-system magmatic processes using the Magma Chamber Simulator (MCS): part I—major elements and phase equilibria. *Contributions to Mineralogy and Petrology, 175*, 1–29.

Bolle, O., Trindade, R.I.F., Luc Bouchez, J., Duchesne, J., 2002. Imaging downward granitic magma transport in the Rogaland Igneous Complex. SW Norway. *Terra Nova* 14 (2), 87–92.

Bottinga, Y., & Weill, D. F. (1970). *Densities of liquid silicate systems calculated from partial molar volumes of oxide components*.

Boudreau, A.E., 1995. Crystal aging and the formation of fine-scale igneous layering. Mineralogy and Petrology 54 (1–2), 55–69.

Boudreau, A.E., 2019. Hydromagmatic processes and platinum-group element deposits in layered intrusions. Cambridge University Press.

Boudreau, A.E., Mathez, E.A., McCallum, I.S., 1986. Halogen geochemistry of the Stillwater and Bushveld Complexes: evidence for transport of the platinum-group elements by Cl-rich fluids. J. Petrol. 27 (4), 967–986.

Boudreau, A.E., Love, C., Prendergast, M.D., 1995. Halogen geochemistry of the Great Dyke, Zimbabwe. Contrib. Miner. Petrol. 122 (3), 289–300.

Boudreau, A.E., McBirney, A.R., 1997. The Skaergaard layered series. Part III. Non-dynamic layering. J. Petrol. 38 (8), 1003–1020.

Boudreau, A.E., McCallum, I.S., 1989. Investigations of the Stillwater Complex: Part V. Apatites as indicators of evolving fluid composition. Contrib. Miner. Petrol. 102 (2), 138–153.

Boudreau, A.E., McCallum, I.S., 1992. Concentration of platinum-group elements by magmatic fluids in layered intrusions. Econ. Geol. 87 (7), 1830–1848.

Boudreau, A.E., Love, C., Hoatson, D.M., 1993. Variation in the composition of apatite in the Munni Munni Complex and associated intrusions of the West Pilbara Block. Western Australia. *Geochimica et Cosmochimica Acta* 57 (18), 4467–4477.

Bowen, N.L., 1915. Crystallization-differentiation in silicate liquids. Am. J. Sci. 230, 175–191.

Bowen, N.L., 1922. The reaction principle in petrogenesis. J. Geol. 30 (3), 177–198.

Bradley, D.C., 2008. Passive margins through earth history. Earth Sci. Rev. 91 (1–4), 1–26.

Bradley, D.C., 2011. Secular trends in the geologic record and the supercontinent cycle. Earth Sci. Rev. 108 (1–2), 16–33.

Brown, E.L., Rooney, T.O., Moucha, R., Stein, S., Stein, C.A., 2022. Temporal evolution of mantle temperature and lithospheric thickness beneath the~ 1.1 Ga Midcontinent Rift, North America: Implications for rapid motion of Laurentia. Earth Planet. Sci. Lett. 598, 117848.

Bulle, F., & Layne, G. D. (2016). Multi-element variations in olivine as geochemical signatures of Ni-Cu sulfide mineralization in mafic magma systems—examples from Voisey's Bay and Pants Lake intrusions, Labrador, Canada. *Mineralium Deposita, 51,* 49–69. from Voisey's Bay and Pants Lake intrusions, Labrador, Canada. *Mineralium Deposita, 51,* 49–69.

Burgisser, A., Degruyter, W., 2015. Magma ascent and degassing at shallow levels. The Encyclopedia of Volcanoes 225–236.

Cameron, E.N., 1977. Chromite in the central sector of the eastern Bushveld Complex. South Africa. *American Mineralogist* 62 (11–12), 1082–1096.

Cameron, E.N., 1978. The Lower Zone of the Eastern Bushveld Complex in the Olifants River Trough. J. Petrol. 19 (3), 437–462.

Campbell, I.H., 1968. The origin of heteradcumulate and adcumulate textures in the Jimberlana Norite. Geol. Mag. 105 (4), 378–383.

Campbell, I.H., 1978. Some problems with the cumulus theory. Lithos 11 (4), 311–323.

Campbell, I.H., 2001. Identification of ancient mantle plumes. Special Papers-Geological Society of America 5–22.

Campbell, I., Murck, B., 1993. Petrology of the G and H chromitite zones in the Mountain View area of the Stillwater Complex. Montana. *Journal of Petrology* 34 (2), 291–316.

Campbell, I.H., Naldrett, A.J., 1979. The influence of silicate:sulfide ratios on the geochemistry of magmatic sulfides. Econ. Geol. 74 (6), 1503–1506.

Canil, D., 1997. Vanadium partitioning and the oxidation state of Archaean komatiite magmas. Nature 389 (6653), 842–845.

Cao, Y., Good, D., Linnen, R., Samson, I., Ruthart, R., 2021. Genesis of the low sulfide-high-grade PGE mineralization in the W Horizon, Coldwell Complex, Canada: quantitative modeling for PGE reef-style mineralization in syn-magmatic sills. Miner. Deposita 56, 1151–1176.

Carlson, R.R., Zientek, M.L., 1985. Guide to the Picket Pin Mountain Area. The Stillwater Complex, Montana: Geology and Guide, Montana Bureau of Mines Special Publication 92, 262–276.

Cashman, K.V., Sparks, R.S.J., Blundy, J.D., 2017. Vertically extensive and unstable magmatic systems: a unified view of igneous processes. Science 355 (6331).

Cawthorn, R.G., 1994. Growth nodes at the base of magnetitite layers in the Upper Zone of the Bushveld Complex. S. Afr. J. Geol. 97 (4), 455–461.

Cawthorn, R.G., 2005. Pressure fluctuations and the formation of the PGE-rich Merensky and chromitite reefs. Bushveld Complex. *Mineralium Deposita* 40 (2), 231–235.

Cawthorn, R.G., 2015. The Bushveld Complex, South Africa. In *Layered intrusions*. Springer, pp. 517–587.

Cawthorn, R.G., McCarthy, T.S., 1980. Variations in Cr content of magnetite from the upper zone of the Bushveld Complex — evidence for heterogeneity and convection currents in magma chambers. Earth Planet. Sci. Lett. 46 (3), 335–343.

Cawthorn, R.G., Walraven, F., 1998. Emplacement and crystallization time for the Bushveld Complex. J. Petrol. 39 (9), 1669–1687.

Chai, G., Naldrett, A.J., 1992. The Jinchuan ultramafic intrusion: cumulate of a high-Mg basaltic magma. J. Petrol. 33 (2), 277–303.

Charlier, B., Sakoma, E., Sauvé, M., Stanaway, K., vander Auwera, J., & Duchesne, J.-C. (2008). The Grader layered intrusion (Havre-Saint-Pierre Anorthosite, Quebec) and genesis of nelsonite and other Fe–Ti–P ores. *Lithos*, 101(3–4), 359–378.

Charlier, B., Namur, O., Toplis, M. J., Schiano, P., Cluzel, N., Higgins, M. D., & Auwera, J. vander. (2011). Large-scale silicate liquid immiscibility during differentiation of tholeiitic basalt to granite and the origin of the Daly gap. *Geology*, 39(10), 907–910.

Charlier, B., Grove, T.L., 2012. Experiments on liquid immiscibility along tholeiitic liquid lines of descent. Contrib. Miner. Petrol. 164 (1), 27–44.

Charlier, B., Namur, O., Grove, T.L., 2013. Compositional and kinetic controls on liquid immiscibility in ferrobasalt–rhyolite volcanic and plutonic series. Geochim. Cosmochim. Acta 113, 79–93.

Chen, X., Godel, B., Verrall, M., 2023. Comparison of Laboratory Diffraction Contrast Tomography and Electron Backscatter Diffraction Results: Application to Naturally Occurring Chromites. Microsc. Microanal. 29 (6), 1901–1920.

Cherdantseva, M., Vishnevskiy, A., Jugo, P.J., Martin, L.A.J., Aleshin, M., Roberts, M.P., Shaparenko, E., Langendam, A., Howard, D.L., Fiorentini, M.L., 2024. Caught in the moment: interaction of immiscible carbonate and sulfide liquids in mafic silicate magma—insights from the Rudniy intrusion (NW Mongolia). Miner. Deposita 59 (4), 733–755.

Cherniak, D.J., Dimanov, A., 2010. Diffusion in pyroxene, mica and amphibole. Rev. Mineral. Geochem. 72 (1), 641–690.

Chong, J., Tucker, N., Martin, L., Polito, P., Fiorentini, M., 2024. New metamorphic constraints on the Nova-Bollinger Ni–Cu deposit, Fraser Zone, Western Australia. Aust. J. Earth Sci. 1–26.

Cnudde, V., Boone, M.N., 2013. High-resolution X-ray computed tomography in geosciences: A review of the current technology and applications. Earth-Science Reviews 123, 1–17.

Cole, J., Finn, C.A., Webb, S.J., 2024. Deep magmatic staging chambers for crustal layered mafic intrusions: An example from the Bushveld Complex of southern Africa. Precambr. Res. 403, 107306.

Condie, K.C., 2021. Earth as an evolving planetary system. Academic Press.

Condie, K.C., Aster, R.C., van Hunen, J., 2016. A great thermal divergence in the mantle beginning 2.5 Ga: Geochemical constraints from greenstone basalts and komatiites. Geosci. Front. 7 (4), 543–553.

Condie, K.C., Pisarevsky, S.A., Puetz, S.J., Spencer, C.J., Teixeira, W., Faleiros, F.M., 2022a. A reappraisal of the global tectono-magmatic lull at~ 2.3 Ga. Precambr. Res. 376, 106690.

Condie, K.C., Puetz, S.J., Spencer, C.J., Roberts, N.M.W., 2022b. Secular compositional changes in hydrated mantle: The record of arc-type basalts. Chem. Geol. 607, 121010.

Cong, Y., Dong, Q., Bagas, L., Xiao, K., Wang, K., 2017. Integrated GIS-based modelling for the quantitative prediction of magmatic Ti-V-Fe deposits: A case study in the Panzhihua-Xichang area of southwest China. Ore Geol. Rev. 91, 1102–1118.

Cruden, A., 2006. In: Emplacement and Growth of Plutons: Implications for Rates of Melting and Mass Transfer in Continental Crust. Cambridge University Press, pp. 455–519.

Cruden, A.R., McCaffrey, K.J.W., Bunger, A.P., 2018. Geometric scaling of tabular igneous intrusions: implications for emplacement and growth. In: Breitkreuz, C., Rocchu, S. (Eds.), Physical Geology of Shallow Magmatic Systems: Dykes, Sills, and Laccoliths. Springer.

Dare, S.A.S., Barnes, S.-J., Beaudoin, G., 2012. Variation in trace element content of magnetite crystallized from a fractionating sulfide liquid, Sudbury, Canada: Implications for provenance discrimination. Geochim. Cosmochim. Acta 88, 27–50.

Dare, S.A.S., Barnes, S.-J., Beaudoin, G., Méric, J., Boutroy, E., Potvin-Doucet, C., 2014. Trace elements in magnetite as petrogenetic indicators. Miner. Deposita 49 (7), 785–796.

Darwin, C., 1844. Geological observations on the volcanic islands visited during the voyage of H.M.S. Beagle, together with some brief notices of the geology of Australia and the Cape of Good Hope. Being the second part of the geology of the voyage of the Beagle, under the command of Capt. Fitzroy, R.N. *During the Years 1832 to 1836.* Smith Elder and Co.

Day, J.M.D., Pearson, D.G., Hulbert, L.J., 2008. Rhenium–osmium isotope and platinum-group element constraints on the origin and evolution of the 1· 27 Ga Muskox layered intrusion. J. Petrol. 49 (7), 1255–1295.

de Waard, D., 1976. Anorthosite-adamellite-troctolite layering in the Barth Island structure of the Nain complex. Labrador. *Lithos* 9 (4), 293–308.

Deegan, F.M., Bédard, J.H., Grasby, S.E., Dewing, K., Geiger, H., Misiti, V., Capriolo, M., Callegaro, S., Svensen, H.H., Yakymchuk, C., 2022. Magma–shale interaction in large igneous provinces: implications for climate warming and sulfide genesis. J. Petrol. 63 (9), egac094.

Dhuime, B., Hawkesworth, C.J., Cawood, P.A., Storey, C.D., 2012. A change in the geodynamics of continental growth 3 billion years ago. Science 335 (6074), 1334–1336.

Dhuime, B., Wuestefeld, A., Hawkesworth, C.J., 2015. Emergence of modern continental crust about 3 billion years ago. Nat. Geosci. 8 (7), 552–555.

Dia, A., van Schmus, W.R., Kröner, A., 1997. Isotopic constraints on the age and formation of a Palaeoproterozoic volcanic arc complex in the Kedougou Inlier, eastern Senegal, West Africa. J. Afr. Earth Sc. 24 (3), 197–213.

Ding, S., Plank, T., Wallace, P. J., & Rasmussen, D. J. (2023). Sulfur_X: A model of sulfur degassing during magma ascent. *Geochemistry, Geophysics, Geosystems*, *24*(4), e2022GC010552.

Dong, H., Xing, C., Wang, C.Y., 2013. Textures and mineral compositions of the Xinjie layered intrusion, SW China: Implications for the origin of magnetite and fractionation process of Fe-Ti-rich basaltic magmas. Geosci. Front. 4 (5), 503–515.

Drage, N., Brenan, J., 2023. An experimental study of the effect of pressure on the formation of chromite deposits. J. Petrol. 64 (5), egad031.

Duchesne, J.-C., Liégeois, J.P., Deblond, A., Tack, L., 2004. Petrogenesis of the Kabanga-Musongati layered mafic-ultramafic intrusions in Burundi (Kibaran Belt): Geochemical, Sr-Nd isotopic constraints and Cr-Ni behaviour. Journalof African Earth Sciences 39 (3–5), 133–145. https://doi.org/10.1016/j.jafrearsci.2004.07.055.

Dupuis, C., Beaudoin, G., 2011. Discriminant diagrams for iron oxide trace element fingerprinting of mineral deposit types. Miner. Deposita 46 (4), 319–335.

Eales, H. v, & Costin, G. (2012). Crustally contaminated komatiite: primary source of the chromitites and Marginal, Lower, and Critical Zone magmas in a staging chamber beneath the Bushveld Complex. *Economic Geology*, *107*(4), 645–665.

Eales, H. v. (2000). Implications of the chromium budget of the Western Limb of the Bushveld Complex. *South African Journal of Geology*, *103*(2), 141–150.

Emeleus, C.H., Cheadle, M.J., Hunter, R.H., Upton, B.G.J., Wadsworth, W.J., 1996. The Rum Layered Suite. in *Developments in Petrology* Vol. 15, 403–439.

Ernst, R.E., Bond, D.P.G., Zhang, S., Buchan, K.L., Grasby, S.E., Youbi, N., el Bilali, H., Bekker, A., Doucet, L.S., 2021. Large igneous province record through time and implications for secular environmental changes and geological time-scale boundaries. A Driver of Global Environmental and Biotic Changes, Large Igneous Provinces, pp. 1–26.

Ezad, I.S., Blanks, D.E., Foley, S.F., Holwell, D.A., Bennett, J., Fiorentini, M.L., 2024. Lithospheric hydrous pyroxenites control localisation and Ni endowment of magmatic sulfide deposits. Miner. Deposita 59 (2), 227–236.

Farahbakhsh, E., Maughan, J., Müller, R.D., 2023. Prospectivity modelling of critical mineral deposits using a generative adversarial network with oversampling and positive-unlabelled bagging. Ore Geol. Rev. 105665.

Farquhar, J., Wing, B.A., 2003. Multiple sulfur isotopes and the evolution of the atmosphere. Earth Planet. Sci. Lett. 213 (1–2), 1–13.

Faure, F., Schiano, P., 2005. Experimental investigation of equilibration conditions during forsterite growth and melt inclusion formation. Earth Planet. Sci. Lett. 236 (3–4), 882–898.

Fellows, S.A., Canil, D., 2012. Experimental study of the partitioning of Cu during partial melting of Earth's mantle. Earth Planet. Sci. Lett. 337, 133–143.

Ferré, E.C., Maes, S.M., Butak, K.C., 2009. The magnetic stratification of layered mafic intrusions: Natural examples and numerical models. Lithos 111 (1–2), 83–94.

Ferreira Filho, C.F., Araujo, S.M., 2009. Review of Brazilian chromite deposits associated with layered intrusions: Geological and petrological constraints for the origin of stratiform chromitites. Appl. Earth Sci. 118 (3–4), 86–100.

Finn, C.A., Bedrosian, P.A., Cole, J.C., Khoza, T.D., Webb, S.J., 2015. Mapping the 3D extent of the Northern Lobe of the Bushveld layered mafic intrusion from geophysical data. Precambr. Res. 268, 279–294.

Finn, C.A., Zientek, M., Bloss, B.R., Parks, H., Modroo, J., 2023. Electromagnetic and magnetic imaging of the Stillwater Complex, Montana, USA. Explor. Geophys 54 (6), 553–570.

Finnigan, C.S., Brenan, J.M., Mungall, J.E., McDonough, W.F., 2008. Experiments and models bearing on the role of chromite as a collector of platinum group minerals by local reduction. J. Petrol. 49 (9), 1647–1665.

Fischer, L. A., Wang, M., Charlier, B., Namur, O., Roberts, R. J., Veksler, I. v, Cawthorn, R. G., & Holtz, F. (2016). Immiscible iron-and silica-rich liquids in the Upper Zone of the Bushveld Complex. *Earth and Planetary Science Letters, 443*, 108–117.

Fitzpayne, A., Giuliani, A., Hergt, J., Phillips, D., Janney, P., 2018. New geochemical constraints on the origins of MARID and PIC rocks: Implications for mantle metasomatism and mantle-derived potassic magmatism. Lithos 318, 478–493.

Foley, S.F., Ezad, I.S., van der Laan, S.R., Pertermann, M., 2022. Melting of hydrous pyroxenites with alkali amphiboles in the continental mantle: 1. Melting relations and major element compositions of melts. Geosci. Front. 13 (4), 101380.

Fonseca, R.O.C., Laurenz, V., Mallmann, G., Luguet, A., Hoehne, N., Jochum, K.P., 2012. New constraints on the genesis and long-term stability of Os-rich alloys in the Earth's mantle. Geochim. Cosmochim. Acta 87, 227–242.

Forien, M., Tremblay, J., Barnes, S.-J., Burgisser, A., Pagé, P., 2015. The Role of Viscous Particle Segregation in Forming Chromite Layers from Slumped Crystal Slurries: Insights from Analogue Experiments. J. Petrol. 56 (12), 2425–2444. https://doi.org/10.1093/petrology/egv060.

Fourny, A., Weis, D., Scoates, J.S., 2019. Isotopic and Trace Element Geochemistry of the Kiglapait Intrusion, Labrador: Deciphering the Mantle Source, Crustal Contributions and Processes Preserved in Mafic Layered Intrusions. J. Petrol. 60 (3), 553–590.

Fowler, A.C., Holness, M.B., 2022. The formation of three-grain junctions during solidification. Part II: theory. Contrib. Miner. Petrol. 177 (6), 58.

Gál, B., Molnár, F., Guzmics, T., Mogessie, A., Szabó, C., Peterson, D.M., 2013. Segregation of magmatic fluids and their potential in the mobilization of platinum-group elements in the South Kawishiwi intrusion, Duluth Complex, Minnesota—evidence from petrography, apatite geochemistry and coexisting fluid and melt inclusions. Ore Geology Reviews 54, 59–80.

Ghiorso, M.S., Sack, R.O., 1995. Chemical mass transfer in magmatic processes IV. A revised and internally consistent thermodynamic model for the interpolation and extrapolation of liquid-solid equilibria in magmatic systems at elevated temperatures and pressures. Contributions to Mineralogy and Petrology 119 (2), 197–212.

Glazner, A.F., Bartley, J.M., Coleman, D.S., Gray, W., Taylolr, R.Z., 2004. Are plutons assembled over millions of years by amalgamation from small magma chambers? GSA Today 14, 4–11. https://doi.org/10.1130/1052-5173(2004)014<0004.

Godel, B.M., 2013. High-resolution X-ray computed tomography and its application to ore deposits: From data acquisition to quantitative three-dimensional measurements with case studies from Ni-Cu-PGE deposits. Econ. Geol. 108 (8), 2005–2019.

Godel, B.M., Barnes, S.-J., Maier, W.D., 2006. 3-D distribution of sulfide minerals in the Merensky Reef (Bushveld Complex, South Africa) and the JM Reef (Stillwater Complex, USA) and their relationship to microstructures using X-ray computed tomography. J. Petrol. 47 (9), 1853–1872.

Godel, B.M., Barnes, S.-J., Maier, W.D., 2011a. Parental magma composition inferred from trace element in cumulus and intercumulus silicate minerals: An example from the Lower and Lower Critical Zones of the Bushveld Complex. South-Africa. *Lithos* 125 (1–2), 537–552.

Godel, B., Barnes, S.J., Gürer, D., Austin, P., Fiorentini, M.L., 2013. Chromite in komatiites: 3D morphologies with implications for crystallization mechanisms. Contrib. Miner. Petrol. 165, 173–189.

Godel, B.M., Seat, Z., Maier, W.D., Barnes, S.-J., 2011b. The Nebo-Babel Ni-Cu-PGE sulfide deposit (West Musgrave Block, Australia): Pt. 2. Constraints on parental magma and processes, with implications for mineral exploration. Econ. Geol. 106 (4), 557–584.

Godel, B.M., Rudashevsky, N.S., Nielsen, T.F.D., Barnes, S.J., Rudashevsky, V.N., 2014. New constraints on the origin of the Skaergaard intrusion Cu–Pd–Au mineralization: Insights from high-resolution X-ray computed tomography. Lithos 190, 27–36.

Griffin, W.L., O'Reilly, S.Y., Afonso, J.C., Begg, G.C., 2009. The composition and evolution of lithospheric mantle: a re-evaluation and its tectonic implications. Journal of Petrology 50 (7), 1185–1204.

Griffin, W.L., Begg, G.C., O'Reilly, S.Y., 2013. Continental-root control on the genesis of magmatic ore deposits. Nat. Geosci. 6 (11), 905–910.

Groshev, N.Y., Karykowski, B.T., 2019. The main anorthosite layer of the West-Pana intrusion, Kola Region: Geology and U-Pb age dating. Minerals 9 (2), 71.

Guice, G.L., Törmänen, T., Karykowski, B.T., Johanson, B., Lahaye, Y., 2017. Precious metal mineralization in the Sotkavaara Intrusion, northern Finland: Peak Pt, Pd, Au and Cu offsets in a small intrusion with poorly-developed magmatic layering. Ore Geol. Rev. 89, 701–718.

Günther, T., Haase, K.M., Klemd, R., Teschner, C., 2018. Mantle sources and magma evolution of the Rooiberg lavas, Bushveld large igneous Province, South Africa. Contrib. Miner. Petrol. 173, 1–27.

Guo, F.-F., Maier, W.D., Heinonen, J.S., Hanski, E., Vuollo, J., Barnes, S.-J., Lahaye, Y., Huhma, H., Yang, S., 2023. Geochemistry of 2.45 Ga mafic dykes in northern Finland: Constraints on the petrogenesis and PGE prospectivity of coeval layered intrusions. Lithos 452, 107206.

Hamlyn, P.R., Keays, R.R., 1986. Sulfur saturation and second-stage melts; application to the Bushveld platinum metal deposits. Econ. Geol. 81 (6), 1431–1445.

Hanley, J.J., Mungall, J.E., Pettke, T., Spooner, E.T.C., Bray, C.J., 2008. Fluid and halide melt inclusions of magmatic origin in the Ultramafic and Lower Banded Series, Stillwater Complex, Montana, USA. J. Petrol. 49 (6), 1133–1160.

Harker, A., 1909. The Natural History of Igneous Rocks. Cambridge University Press. https://doi.org/10.1017/CBO9780511920424.

Hart, S.R., Kinloch, E.D., 1989. Osmium isotope systematics in Witwatersrand and Bushveld ore deposits. Econ. Geol. 84 (6), 1651–1655.

Hasterok, D., Chapman, D.S., 2011. Heat production and geotherms for the continental lithosphere. Earth Planet. Sci. Lett. 307 (1–2), 59–70.

Hastie, A.R., Fitton, J.G., Kerr, A.C., McDonald, I., Schwindrofska, A., Hoernle, K., 2016. The composition of mantle plumes and the deep Earth. Earth Planet. Sci. Lett. 444, 13–25.

Hawkesworth, C.J., Dhuime, B., Pietranik, A.B., Cawood, P.A., Kemp, A.I.S., Storey, C.D., 2010. The generation and evolution of the continental crust. J. Geol. Soc. London 167 (2), 229–248.

Hazen, R.M., Papineau, D., Bleeker, W., Downs, R.T., Ferry, J.M., McCoy, T.J., Sverjensky, D.A., Yang, H., 2008. Mineral evolution. Am. Mineral. 93 (11–12), 1693–1720.

Hepworth, L.N., O'Driscoll, B., Gertisser, R., Daly, J.S., Emeleus, C.H., 2018. Linking in situ crystallization and magma replenishment via sill intrusion in the Rum Western Layered Intrusion, NW Scotland. J. Petrol. 59 (8), 1605–1642.

Hepworth, L.N., Kaufmann, F.E.D., Hecht, L., Gertisser, R., O'Driscoll, B., 2020. Braided peridotite sills and metasomatism in the Rum Layered Suite, Scotland. *Contributions to Mineralogy and Petrology* 175 (2), 17.

Hess, H. H. (1960). *Stillwater igneous complex, Montana: a quantitative mineralogical study*.

Higgins, M.D., 1991. The origin of laminated and massive anorthosite, Sept Iles layered intrusion, Quebec, Canada. Contributions to Mineralogy and Petrology 106 (3), 340–354.

Higgins, M.D., 2002. A crystal size-distribution study of the Kiglapait layered mafic intrusion, Labrador, Canada: evidence for textural coarsening. Contrib. Miner. Petrol. 144 (3), 314–330.

Higgins, O., Sheldrake, T., Caricchi, L., 2022. Machine learning thermobarometry and chemometry using amphibole and clinopyroxene: a window into the roots of an arc volcano (Mount Liamuiga, Saint Kitts). Contrib. Miner. Petrol. 177 (1), 10.

Hill, E.J., Pearce, M.A., Stromberg, J.M., 2021. Improving automated geological logging of drill holes by incorporating multiscale spatial methods. Math. Geosci. 53 (1), 21–53.

Hirose, K., Kushiro, I., 1993. Partial melting of dry peridotites at high pressures: determination of compositions of melts segregated from peridotite using aggregates of diamond. Earth Planet. Sci. Lett. 114 (4), 477–489.

Hirschmann, M.M., Kogiso, T., Baker, M.B., Stolper, E.M., 2003. Alkalic magmas generated by partial melting of garnet pyroxenite. Geology 31 (6), 481–484.

Hoatson, D.M., Keays, R.R., 1989. Formation of platiniferous sulfide horizons by crystal fractionation and magma mixing in the Munni Munni layered intrusion, west Pilbara Block. Western Australia. *Economic Geology* 84 (7), 1775–1804. https://doi.org/10.2113/gsecongeo.84.7.1775.

Hoatson, D.M., Sun, S.S., 2002. Archean layered mafic-ultramafic intrusions in the West Pilbara Craton, Western Australia: A synthesis of some of the oldest orthomagmatic mineralizing systems in the world. Econ. Geol. 97 (4), 847–872. https://doi.org/10.2113/gsecongeo.97.4.847.

Holness, M.B., 2024. Self-Organisation in Gabbroic Cumulates: a New Patterning Mechanism Driven by Differential Migration of Immiscible Liquids in a Crystal Mush? J. Petrol. 65 (4). https://doi.org/10.1093/petrology/egae034.

Holness, M. B., Stripp, G., Humphreys, M. C. S., Veksler, I. v, Nielsen, T. F. D., & Tegner, C. (2011). Silicate liquid immiscibility within the crystal mush: late-stage magmatic microstructures in the Skaergaard intrusion, East Greenland. *Journal of Petrology, 52* (1), 175–222.

Holness, M.B., Fowler, A.C., 2022. The formation of three-grain junctions during solidification. Part I: observations. Contrib. Miner. Petrol. 177 (5), 55.

Holness, M.B., Cawthorn, R.G., Roberts, J., 2017a. The thickness of the crystal mush on the floor of the Bushveld magma chamber. Contrib. Miner. Petrol. 172 (11–12), 102.

Holness, M., Nielsen, T., Namur, O., 2024. Differential migration of immiscible liquids in gabbroic crystal mush: the Skaergaard Intrusion. East Greenland, Copernicus Meetings.

Holness, M.B., Vukmanovic, Z., Mariani, E., 2017b. Assessing the role of compaction in the formation of adcumulates: a microstructural perspective. J. Petrol. 58 (4), 643–673.

Holness, M.B., Vukmanovic, Z., O'Driscoll, B., 2023. The formation of chromite chains and clusters in igneous rocks. J. Petrol. 64 (1), egac124.

Holwell, D.A., Barnes, S.J., Le Vaillant, M., Keays, R.R., Fisher, L.A., Prasser, R., 2016. 3D textural evidence for the formation of ultra-high tenor precious metal bearing sulfide microdroplets in offset reefs: an extreme example from the Platinova Reef, Skaergaard Intrusion, Greenland. Lithos 256, 55–74.

Holzheid, A., Sylvester, P., O'Neill, H.S.C., Rubie, D.C., Palme, H., 2000. Evidence for a late chondritic veneer in the Earth's mantle from high-pressure partitioning of palladium and platinum. Nature 406 (6794), 396–399.

Honour, V.C., Holness, M.B., Partridge, J.L., Charlier, B., 2019. Microstructural evolution of silicate immiscible liquids in ferrobasalts. Contrib. Miner. Petrol. 174, 1–24.

Horrocks, T., Holden, E.-J., Wedge, D., Wijns, C., Fiorentini, M., 2019. Geochemical characterisation of rock hydration processes using t-SNE. Comput. Geosci. 124, 46–57.

Hou, T., & Veksler, I. v. (2015). Experimental confirmation of high-temperature silicate liquid immiscibility in multicomponent ferrobasaltic systems. *American Mineralogist*, *100*(5–6), 1304–1307.

Howarth, G.H., Barry, P.H., Pernet-Fisher, J.F., Baziotis, I.P., Pokhilenko, N.P., Pokhilenko, L.N., Bodnar, R.J., Taylor, L.A., Agashev, A.M., 2014. Superplume metasomatism: Evidence from Siberian mantle xenoliths. Lithos 184, 209–224.

Huang, G., Mitchell, R.N., Palin, R.M., Spencer, C.J., Guo, J., 2022. Barium content of Archean continental crust reveals the onset of subduction was not global. Nat. Commun. 13 (1), 6553.

Huppert, H.E., Sparks, R.S.J., 1989. Chilled margins in igneous rocks. Earth Planet. Sci. Lett. 92 (3–4), 397–405.

Hutton, D.H.W., 2009. Insights into magmatism in volcanic margins: bridge structures and a new mechanism of basic sill emplacement–Theron Mountains. Antarctica. *Petroleum Geoscience* 15 (3), 269–278.

Iacono-Marziano, G., Ferraina, C., Gaillard, F., di Carlo, I., Arndt, N.T., 2017. Assimilation of sulfate and carbonaceous rocks: experimental study, thermodynamic modeling and application to the Noril'sk-Talnakh region (Russia). Ore Geol. Rev. 90, 399–413.

Iacono-Marziano, G., Le Vaillant, M., Godel, B.M., Barnes, S.J., Arbaret, L., 2022. The critical role of magma degassing in sulfide melt mobility and metal enrichment. Nat. Commun. 13 (1), 1–10.

Irvine, T.N., 1976. In: Crystallization Sequences in the Muskox Intrusion and Other Layered Intrusions—II. Origin of Chromitite Layers and Similar Deposits of Other Magmatic Ores. Elsevier, pp. 991–1020.

Irvine, T.N., 1977. Origin of chromitite layers in the Muskox intrusion and other stratiform intrusions: A new interpretation. Geology 5 (5), 273–277.

Irvine, T.N., 1980a. Magmatic infiltration metasomatism, double diffusive fractional crystallization, and adcumulus growth in the Muskox intrusion and other layered intrusions. Physics of Magmatic Processes.

Irvine, T.N., 1980b. Chapter 8. Magmatic Infiltration Metasomatism, Double-Diffusive Fractional Crystallization, and Adcumulus Growth in the Muskox Intrusion and other Layered Intrusions. In: Physics of Magmatic Processes. Princeton University Press, pp. 325–384.

Irvine, T.N., 1982. Terminology for layered intrusions. J. Petrol. 23 (2), 127–162.

Irvine, T.N., Andersen, J.C.Ø., Brooks, C.K., 1998. Included blocks (and blocks within blocks) in the Skaergaard intrusion: Geologic relations and the origins of rhythmic modally graded layers. Geol. Soc. Am. Bull. 110 (11), 1398–1447.

Irvine, T.N., Sharpe, M.R., 1982. Source-rock compositions and depths of origin of Bushveld and Stillwater magmas. Carnegie Inst Washington Yearb 81, 294–303.

Irvine, T. N. (1974). *Petrology of the Duke Island Ultramafic Complex Southeastern Alaska* (pp. 1–244). https://doi.org/10.1130/MEM138-p1.

Ivanic, T.J., Nebel, O., Brett, J., Murdie, R.E., 2018. The Windimurra Igneous Complex: an Archean Bushveld? Geol. Soc. Lond. Spec. Publ. 453 (1), 313–348.

Jackson, E.D., 1961. Primary textures and mineral associations in the Ultramafic zone of the Stillwater Complex, Montana.U.S. Geological Survey Professional Paper 358, 103–p.

Jackson, E.D., 1970. The cyclic unit in layered intrusions, a comparison of repetitive stratigraphy in the ultramafic parts of the Stillwater, Muskox, Great Dyke and Bushveld Complex (with discussion). Symposium on the Bushveld Igneous Complex and Other Layered Intrusions 391–424.

Jakobsen, J. K., Veksler, I. v, Tegner, C., & Brooks, C. K. (2011). Crystallization of the Skaergaard intrusion from an emulsion of immiscible iron-and silica-rich liquids: evidence from melt inclusions in plagioclase. *Journal of Petrology*, *52*(2), 345–373.

Järvinen, V., Halkoaho, T.A.A., Konnunaho, J., Heinonen, J.S., Rämö, O.T., 2020. Parental magma, magmatic stratigraphy, and reef-type PGE enrichment of the 2.44-Ga mafic-ultramafic Näränkävaara layered intrusion, Northern Finland. Miner. Deposita 55 (8), 1535–1560.

Järvinen, V., Halkoaho, T., Konnunaho, J., Heinonen, J.S., Kamo, S., Davey, S., Bleeker, W., Karinen, T., Rämö, O.T., 2022. Petrogenesis of the Paleoproterozoic Näränkävaara layered intrusion, northern Finland, Part II: U-Pb ID-TIMS age and Sm-Nd isotope systematics. Bull. Geol. Soc. Finl. 94 (1).

Jenkins, M. C., Mungall, J. E., Zientek, M. L., Butak, K., Corson, S., Holick, P., McKinley, R., & Lowers, H. (2022). The geochemical and textural transition between the Reef Package and its hanging wall, Stillwater Complex, Montana, USA. *Journal of Petrology*, *63*(7), egac053.

Jenkins, M.C., Mungall, J.E., 2018. Genesis of the Peridotite Zone, Stillwater Complex, Montana, USA. J. Petrol. 59 (11), 2157–2190.

Jenkins, M.C., Mungall, J.E., Zientek, M.L., Holick, P., Butak, K., 2020. The nature and composition of the JM reef, Stillwater Complex, Montana, USA. Econ. Geol. 115 (8), 1799–1826.

Jenkins, M.C., Mungall, J.E., Zientek, M.L., Costin, G., Yao, Z., 2021. Origin of the J-M Reef and lower banded series, stillwater complex, Montana, USA. Precambr. Res. 367 (November), 106457. https://doi.org/10.1016/j.precamres.2021.106457.

Jennings, S.S., Hasterok, D., Lucazeau, F., 2021. ThermoGlobe: extending the global heat flow database. Journal TBD.

Jones, P.M., Martin, J., 2021. Increasing the reproducibility of research will reduce the problem of apophenia (and more). Canadian Journal of Anesthesia/journal Canadien D'anesthésie 68 (8), 1120–1134.

Jowitt, S.M., Mudd, G.M., Thompson, J.F.H., 2020. Future availability of non-renewable metal resources and the influence of environmental, social, and governance conflicts on metal production. Commun. Earth Environ. 1 (1), 13.

Jugo, P.J., Lesher, C.M., 2005. Redox changes caused by evaporate and carbon assimilation at Noril'sk and their role in sulfide precipitation [abs.]. Geol. Soc. Am. Abstr. Programs 39 (6), 360.

Kaavera, J., Imai, A., Yonezu, K., Tindell, T., Sanematsu, K., Watanabe, K., 2020. Controls on the disseminated Ni-Cu-PGE sulfide mineralization at the Tubane section, northern Molopo Farms Complex, Botswana: Implications for the formation of conduit style magmatic sulfide ores. Ore Geol. Rev. 126, 103731.

Karinen, T., Moilanen, M., Kuva, J., Lahaye, Y., Datar, B., & Yang, S.-H. (2022). Mustavaara revisited: A revised genetic model for orthomagmatic Fe–Ti–V mineralization in the Koillismaa intrusion. In *Geological Survey of Finland. Bulletin 414 - Monograph*.

Karykowski, B. T., Maier, W. D., Groshev, N. Y., Barnes, S.-J., Pripachkin, P. v, & McDonald, I. (2018). Origin of reef-style PGE mineralization in the paleoproterozoic Monchegorsk Complex, Kola Region, Russia. *Economic Geology*, *113*(6), 1333–1358.

Karykowski, B.T., Polito, P.A., Maier, W.D., Gutzmer, J., Krause, J., 2017. New insights into the petrogenesis of the Jameson Range layered intrusion and associated Fe-Ti-PV-PGE-Au mineralization, West Musgrave Province. Western Australia. *Mineralium Deposita* 52 (2), 233–255.

Kaufmann, F.E.D., Vukmanovic, Z., Holness, M.B., Hecht, L., 2018. Orthopyroxene oikocrysts in the MG1 chromitite layer of the Bushveld Complex: implications for cumulate formation and recrystallization. Contrib. Miner. Petrol. 173, 1–20.

Keays, R.R., 1995. The role of komatiitic and picritic magmatism and S-saturation in the formation of ore deposits. Lithos 34 (1–3), 1–18.

Keays, R.R., Lightfoot, P.C., Hamlyn, P.R., 2012. Sulfide saturation history of the Stillwater Complex, Montana: chemostratigraphic variation in platinum group elements. Miner. Deposita 47, 151–173.

Keevil, H. A., Namur, O., & Holness, M. B. (2020). Microstructures and late-stage magmatic processes in layered mafic intrusions: symplectites from the Sept Îles intrusion, Quebec, Canada. *Journal of Petrology*, *61*(7), egaa071.

Kerr, A., Leitch, A.M., 2005. Self-destructive sulfide segregation systems and the formation of high-grade magmatic ore deposits. Econ. Geol. 100 (2), 311–332.

Kerr, R.C., Tait, S.R., 1985. Convective exchange between pore fluid and an overlying reservoir of denser fluid: a post-cumulus process in layered intrusions. Earth Planet. Sci. Lett. 75 (2–3), 147–156. https://doi.org/10.1016/0012-821X(85)90097-4.

Kgaswane, E.M., Nyblade, A.A., Durrheim, R.J., Julià, J., Dirks, P.H.G.M., Webb, S.J., 2012. Shear wave velocity structure of the Bushveld Complex, South Africa. Tectonophysics 554, 83–104.

Kharbish, S., Eldosouky, A.M., Amer, O., 2022. Integrating mineralogy, geochemistry and aeromagnetic data for detecting Fe–Ti ore deposits bearing layered mafic intrusion, Akab El-Negum, Eastern Desert. Egypt. *Scientific Reports* 12 (1), 15474.

Kieffer, M.A., Dare, S.A.S., Namur, O., 2023. The use of trace elements in apatite to trace differentiation of a ferrobasaltic melt in the Sept- Îles Intrusive Suite, Quebec, Canada: Implications for provenance discrimination. Geochim. Cosmochim. Acta 342, 169–197.

Kieffer, M.A., Dare, S.A.S., Namur, O., Mansur, E.T., 2024. Apatite chemistry as a petrogenetic indicator for mafic layered intrusions. J. Petrol. 65 (4), egae022.

Klayman, J., 1995. Varieties of confirmation bias. Psychol. Learn. Motiv. 32, 385–418.

Knight, R.D., Prichard, H.M., Ferreira Filho, C.F., 2017. Evidence for As contamination and the partitioning of Pd into pentlandite and Co+ platinum group elements into pyrite in the Fazenda Mirabela Intrusion. Brazil. *Economic Geology* 112 (8), 1889–1912.

Koivisto, E., Malehmir, A., Heikkinen, P., Heinonen, S., & Kukkonen, I. (2012). 2D reflection seismic investigations at the Kevitsa Ni-Cu-PGE deposit, northern Finland. *Geophysics*, *77*(5), WC149–WC162.

Konnikov, E. G., Nekrasov, A. N., Kovyazin, S. v, & Simakin, S. G. (2005). Interaction of magmatic fluids and mantle magmas with lower crustal rocks: evidence from inclusions in the minerals of intrusions. *Geochemistry International*, *43*(10), 939–958.

Koppers, A.A.P., Becker, T.W., Jackson, M.G., Konrad, K., Müller, R.D., Romanowicz, B., Steinberger, B., Whittaker, J.M., 2021. Mantle plumes and their role in Earth processes. Nat. Rev. Earth Environ. 2 (6), 382–401.

Kruger, F.J., 1994. The Sr-isotopic stratigraphy of the western Bushveld Complex. S. Afr. J. Geol. 97 (4), 393–398.

Kruger, F.J., Cawthorn, R.G., Walsh, K.L., 1987. Strontium isotopic evidence against magma addition in the Upper Zone of the Bushveld Complex. Earth Planet. Sci. Lett. 84 (1), 51–58.

Kruger, W., Latypov, R., 2020. Fossilized solidification fronts in the Bushveld Complex argue for liquid-dominated magmatic systems. NatureCommunications 11 (1), 1–11.

Labotka, T.C., Kath, R.L., 2001. Petrogenesis of the contact-metamorphic rocks beneath the Stillwater Complex. Montana. *Geological Society of America Bulletin* 113 (10), 1312–1323.

Lambart, S., Laporte, D., Schiano, P., 2013. Markers of the pyroxenite contribution in the major-element compositions of oceanic basalts: Review of the experimental constraints. Lithos 160, 14–36.

Larsen, L.M., Sørensen, H., 1987. The Ilímaussaq intrusion—progressive crystallization and formation of layering in an agpaitic magma. Geol. Soc. Lond. Spec. Publ. 30 (1), 473–488.

Latypov, R., & Chistyakova, S. (2022). Misinterpretation of zircon ages in layered intrusions. *South African Journal of Geology 2022*, *125*(1), 13–26.

Latypov, R.M., Chistyakova, S., Alapieti, T.T., 2008a. Revisiting problem of chilled margins associated with marginal reversals in mafic–ultramafic intrusive bodies. Lithos 99 (3), 178–206.

Latypov, R.M., Chistyakova, S.Y., Alapieti, T.T., 2008b. Infiltration metasomatism in layered intrusions revisited: a reinterpretation of compositional reversals at the base of cyclic units. Mineral. Petrol. 92 (1–2), 243–258.

Latypov, R., Chistyakova, S., Page, A., Hornsey, R., 2015. Field evidence for the in situ crystallization of the Merensky Reef. J. Petrol. 56 (12), 2341–2372.

Latypov, R., Chistyakova, S., Barnes, S.J., Hunt, E.J., 2017. Origin of Platinum Deposits in Layered Intrusions by In Situ Crystallization: Evidence from Undercutting Merensky Reef of the Bushveld Complex. J. Petrol. 58 (4), 715–761.

Latypov, R., Costin, G., Chistyakova, S., Hunt, E.J., Mukherjee, R., Naldrett, T., 2018. Platinum-bearing chromite layers are caused by pressure reduction during magma ascent. Nat. Commun. 9 (1), 462.

Latypov, R., Chistyakova, S., Barnes, S.J., Godel, B., Delaney, G.W., Cleary, P.W., Radermacher, V.J., Campbell, I., Jakata, K., 2022a. Chromitite layers indicate the existence of large, long-lived, and entirely molten magma chambers. Sci. Rep. 12 (1), 4092.

Latypov, R., Chistyakova, S., Hornsey, R.A., Costin, G., van der Merwe, M., 2022b. A 5-km-thick reservoir with> 380,000 km3 of magma within the ancient Earth's crust. Sci. Rep. 12 (1), 1–12.

Latypov, R.M., Namur, O., Bai, Y., Barnes, S.J., Chistyakova, S.y., Holness, M.B., Iacono-Marziano, G., Kruger, W.A.J., O'Driscoll, B., Smith, W.D., Virtanen, V.J., Wang, C.Y., Xing, C.-M., Charlier, B., 2024a. Layered intrusions: Fundamentals, novel observations and concepts, and controversial issues. Earth Sci. Rev. 249, 104653.

Latypov, R.M., Chistyakova, S.Y., Letsoele, C., 2024b. Massive chromitites of the Bushveld Complex, South Africa: A critical review of existing hypotheses. Earth Sci. Rev. 256, 104858.

Latypov, R., Chistyakova, S., Barnes, S., Letsoele, C., Kruger, W., 2024c. Mostly solidified hardground at the top of the crystal pile in the Bushveld magma chamber. Lithos 478, 107621.

Le Vaillant, M., Barnes, S.J., Mole, D.R., Fiorentini, M.L., Laflamme, C., Denyszyn, S.W., Austin, J., Patterson, B., Godel, B.M., Hicks, J., 2020. Multidisciplinary study of a complex magmatic system: The Savannah Ni-Cu-Co Camp, Western Australia. Ore Geology Reviews 117, 103292.

Lesher, C.M., 2017. Roles of xenomelts, xenoliths, xenocrysts, xenovolatiles, residues, and skarns in the genesis, transport, and localization of magmatic Fe-Ni-Cu-PGE sulfides and chromite. Ore Geol. Rev. 90, 465–484.

Lesher, C. M., & Groves, D. I. (1986). Controls on the formation of komatiite-associated nickel-copper sulfide deposits. *Geology and Metallogeny of Copper Deposits: Proceedings of the Copper Symposium 27th International Geological Congress Moscow, 1984*, 43–62.

Lesher, C.M., Burnham, O., 2001. Multicomponent elemental and isotopic mixing in Ni–Cu–(PGE) ores at Kambalda, Western Australia. *the Canadian Mineralogist* 39 (2), 421–446.

Leuthold, J., Blundy, J.D., Brooker, R.A., 2015. Experimental petrology constraints on the recycling of mafic cumulate: a focus on Cr-spinel from the Rum Eastern Layered Intrusion, Scotland. Contrib. Miner. Petrol. 170, 1–27.

Li, C., Lightfoot, P.C., Amelin, Y., Naldrett, A.J., 2000. Contrasting petrological and geochemical relationships in the Voisey's Bay and Mushuau intrusions, Labrador, Canada: implications for ore genesis. Econ. Geol. 95 (4), 771–799.

Li, C., Naldrett, A.J., 1999. Geology and petrology of the Voisey's Bay intrusion: reaction of olivine with sulfide and silicate liquids. Lithos 47, 1–31. https://doi.org/10.1016/s0024-4937(99)00005-5.

Lima, H.A.F., Ferreira Filho, C.F., Pimentel, M.M., Dantas, E.L., de Araújo, S.M., 2008. Geology, petrology and geochronology of the layered mafic-ultramafic intrusions in the Porto Nacional area, central Brazil. J. S. Am. Earth Sci. 26 (3), 300–317.

Lindsley, D.H., Andersen, D.J., 1983. A two-pyroxene thermometer. Journal of Geophysical Research: Solid Earth 88 (S02), A887–A906.

Lino, L.M., Carvalho, P.R., Vlach, S.R.F., Quiroz-Valle, F.R., 2023. Evidence for silicate liquid immiscibility in recharging, alkali-rich tholeiitic systems: the role of unmixing in the petrogenesis of intermediate, layered plutonic bodies and bimodal volcanic suites. Lithos 450, 107193.

Lipin, B.R., 1993. Pressure increases, the formation of chromite seams, and the development of the ultramafic series in the Stillwater Complex. Montana. *Journal of Petrology* 34 (5), 955–976.

Liu, M., Mao, J., Zhang, Z., Li, L., Long, T., Chao, W., 2024. Current supply status, demand trends and security measures of chromium resources in China. Green and Smart Mining Engineering 1 (1), 53–57.

Liu, Y., Samaha, N.-T., Baker, D.R., 2007. Sulfur concentration at sulfide saturation (SCSS) in magmatic silicate melts. Geochim. Cosmochim. Acta 71 (7), 1783–1799.

Liu, H., Sun, W., Zartman, R., Tang, M., 2019. Continuous plate subduction marked by the rise of alkali magmatism 2.1 billion years ago. *Nature*. Communications 10 (1), 3408.

Liu, M.-Y., Zhou, M.-F., Su, S.-G., Chen, X.-G., 2021. Contrasting Geochemistry of Apatite from Peridotites and Sulfide Ores of the Jinchuan Ni-Cu Sulfide Deposit. NW China. *Economic Geology* 116 (5), 1073–1092.

Maier, W.D., 2005. Platinum-group element (PGE) deposits and occurrences: Mineralization styles, genetic concepts, and exploration criteria. J. Afr. Earth Sc. 41 (3), 165–191.

Maier, W. D., & Barnes, S.-J. (2005). *Application of lithogeochemistry to exploration for PGE deposits.*

Maier, W.D., Groves, D.I., 2011. Temporal and spatial controls on the formation of magmatic PGE and Ni–Cu deposits. Miner. Deposita 46 (8), 841–857.

Maier, W.D., Barnes, S.J., Gartz, V., Andrews, G., 2003. Pt-Pd reefs in magnetitites of the Stella layered intrusion, South Africa: A world of new exploration opportunities for platinum group elements. Geology 31 (10), 885–888.

Maier, W.D., Barnes, S.-J., 2004. Pt/Pd and Pd/Ir ratios in mantle-derived magmas: a possible role for mantle metasomatism. S. Afr. J. Geol. 107 (3), 333–340.

Maier, W.D., Barnes, S.-J., Groves, D.I., 2013. The Bushveld Complex, South Africa: formation of platinum–palladium, chrome- and vanadium-rich layers via hydrodynamic sorting of a mobilized cumulate slurry in a large, relatively slowly cooling, subsiding magma chamber. Miner. Deposita 48 (1), 1–56.

Maier, W.D., Rasmussen, B., Fletcher, I.R., Godel, B.M., Barnes, S.-J., Fischer, L.A., Yang, S.-H., Huhma, H., Lahaye, Y., 2014. Petrogenesis of the ~ 2.77 Ga Monts de Cristal complex, Gabon: Evidence for direct precipitation of Pt-arsenides from basaltic magma. J. Petrol. 56 (7), 285–1308.

Maier, W.D., Howard, H.M., Smithies, R.H., Yang, S.-H., Barnes, S.J., O'Brien, H., Huhma, H., Gardoll, S.J., 2015a. Magmatic ore deposits in mafic-ultramafic intrusions of the Giles Event, Western Australia. Ore Geol. Rev. 71, 405–436.

Maier, W.D., Määttä, S., Yang, S.-H., Oberthür, T., Lahaye, Y., Huhma, H., Barnes, S.-J., 2015b. Composition of the ultramafic–mafic contact interval of the Great Dyke of Zimbabwe at Ngezi mine: Comparisons to the Bushveld Complex and implications for the origin of the PGE reefs. Lithos 238, 207–222.

Maier, W.D., Barnes, S.-J., Karykowski, B.T., 2016. A chilled margin of komatiite and Mg-rich basaltic andesite in the western Bushveld Complex, South Africa. Contrib. Miner. Petrol. 171 (6), 1–22.

Maier, W.D., Halkoaho, T.A.A., Huhma, H., Hanski, E.J., Barnes, S.-J., 2018. The Penikat intrusion, Finland: geochemistry, geochronology, and origin of platinum–palladium reefs. J. Petrol. 59 (5), 967–1006.

Maier, W.D., Barnes, S.-J., Muir, D., Savard, D., Lahaye, Y., Smith, W.D., 2021. Formation of Bushveld anorthosite by reactive porous flow. Contrib. Miner. Petrol. 176, 1–12.

Maier, W.D., Barnes, S.-J., Smith, W.D., 2023. Petrogenesis of the Mesoarchean Stella layered intrusion, South Africa: implications for the origin of PGE reefs in the upper portion of layered intrusions. Miner. Deposita 58 (8), 1477–1497.

Maier, R. P., Dare, S. A., & Smith, W. D. (2024). Petrogenesis of the 1149 Ma Etoile Suite Mafic Intrusion, Quebec: implications for vanadium mineralisation in Proterozoic anorthosite-bearing terranes. Mineralium Deposita, 1-27.Mallmann, G., & O'Neill, H. S. C. (2009). The crystal/melt partitioning of V during mantle melting as a function of oxygen fugacity compared with some other elements (Al, P, Ca, Sc, Ti, Cr, Fe, Ga, Y, Zr and Nb). *Journal of Petrology*, 50(9), 1765–1794.

Mallmann, G., O'Neill, H.S.C., 2009. The crystal/melt partitioning of V during mantle melting as a function of oxygen fugacity compared with some other elements (Al, P, Ca, Sc, Ti, Cr, Fe, Ga, Y, Zr and Nb). J. Petrol. 50 (9), 1765–1794.

Mansur, E.T., Barnes, S.-J., 2020. The role of Te, As, Bi, Sn and Sb during the formation of platinum-group-element reef deposits: Examples from the Bushveld and Stillwater Complexes. Geochimica et Cosmochimica Acta 272, 235–258.

Mansur, E.T., Barnes, S.-J., Duran, C.J., 2020a. An overview of chalcophile element contents of pyrrhotite, pentlandite, chalcopyrite, and pyrite from magmatic Ni-Cu-PGE sulfide deposits. Miner. Deposita 1–26.

Mansur, E.T., Ferreira Filho, C.F., Oliveira, D.P.L., 2020b. The Luanga deposit, Carajás Mineral Province, Brazil: Different styles of PGE mineralization hosted in a medium-size layered intrusion. Ore Geol. Rev. 118, 103340.

Mansur, E.T., Dare, S.A.S., Slagstad, T., Sandstad, J.S., 2024. Distribution of chalcophile elements during crystallization and alteration of magmatic Ni-Cu-Co sulfide deposits in the anorthositic Espedalen Complex, Norway: pentlandite as an indicator for tracking metal tenors. Miner. Deposita 1–25.

Markl, G., Marks, M., Schwinn, G., Sommer, H., 2001. Phase equilibrium constraints on intensive crystallization parameters of the Ilímaussaq Complex, South Greenland. J. Petrol. 42 (12), 2231–2257.

Marks, M., Markl, G., 2015. The ilímaussaq alkaline complex, South Greenland. In *Layered Intrusions*. Springer, pp. 649–691.

Marsh, J.S., Allen, P., Fenner, N., 2003. The geochemical structure of the Insizwa lobe of the Mount Ayliff Complex with implications for the emplacement and evolution of the complex and its Ni-sulfide potential. South African Journal of Geology 106 (4), 409–428.

Marsh, J.S., Pasecznyk, M.J., Boudreau, A.E., 2021. Formation of chromitite seams and associated anorthosites in layered intrusion by reactive volatile-rich fluid infiltration. J. Petrol. 62 (2), egaa109.

Mathez, E.A., Kinzler, R.J., 2017. Metasomatic chromitite seams in the Bushveld and Rum layered intrusions. Elements 13 (6), 397–402.

Mathison, C.I., 1987. Pyroxene oikocrysts in troctolitic cumulates—evidence for supercooled crystallization and postcumulus modification. Contrib. Miner. Petrol. 97 (2), 228–236.

Matzen, A.K., Baker, M.B., Beckett, J.R., Wood, B.J., Stolper, E.M., 2017. The effect of liquid composition on the partitioning of Ni between olivine and silicate melt. Contrib. Miner. Petrol. 172 (1), 1–18.

Mavrogenes, J.A., O'Neill, H.S.C., 1999. The relative effects of pressure, temperature and oxygen fugacity on the solubility of sulfide in mafic magmas. Geochim. Cosmochim. Acta 63 (7–8), 1173–1180.

Mayo, C.W., Crockett, W.H., 1964. Cognitive complexity and primacy-recency effects in impression formation. J. Abnorm. Soc. Psychol. 68 (3), 335.

McBirney, A.R., 1987. Constitutional zone refining of layered intrusions. In *Origins of igneous layering*. Springer, pp. 437–452.

McBirney, A.R., 1995. Mechanisms of differentiation in the Skaergaard Intrusion. J. Geol. Soc. London 152 (3), 421–435.

McBirney, A.R., Noyes, R.M., 1979. Crystallization and Layering of the Skaergaard Intrusion. J. Petrol. 20 (3), 487–554.

McBirney, A.R., Sonnenthal, E.L., 1990. Metasomatic replacement in the Skærgaard Intrusion, East Greenland: Preliminary observations. Chem. Geol. 88 (3–4), 245–260.

McCallum, I.S., 1987. Petrology of the igneous rocks. Rev. Geophys. 25 (5), 1021–1042.

McCallum, I.S., 1996. The Stillwater Complex. Layered Intrusions 441–484.

McCallum, I.S., Meurer, W.P., 2002. A Traverse Through the Banded Series in the Picket Pin Area of the Stillwater Comple. In: 9th International Platinum Symposium, pp. 1–7.

McCuaig, T.C., Beresford, S.W., Hronsky, J.M.A., 2010. Translating the mineral systems approach into an effective exploration targeting system. Ore Geol. Rev. 38 (3), 128–138.

McDonald, I., Holwell, D.A., 2011. Geology of the northern Bushveld Complex and the setting and genesis of the Platreef Ni-Cu-PGE deposit. Rev. Econ. Geol. 17, 297–327.

McDonough, W.F., Sun, S.S., 1995. The composition of the Earth. Chem. Geol 120, 223–253.

Menand, T., 2011. Physical controls and depth of emplacement of igneous bodies: A review. Tectonophysics 500 (1–4), 11–19.

Menand, T., de Saint-Blanquat, M., & Annen, C. (2011). Emplacement of magma pulses and growth of magma bodies. In *Tectonophysics* (Vol. 500, Issues 1–4, pp. 1–2). Elsevier.

Meurer, W.P., Boudreau, A.E., 1998. Compaction of igneous cumulates part II: compaction and the development of igneous foliations. J. Geol. 106 (3), 293–304.

Miller, J. D., & Severson, M. J. (2009). Field Guide to the Geology and Mineralization of Mafic Layered Intrusions of the Duluth and Beaver Bay Complexes, Northeastern Minnesota.

Miller Jr, J.D., Ripley, E.M., 1996. Layered intrusions of the Duluth complex, Minnesota, USA. Layered Intrusions 257–301.

Miller Jr, J.D., Weiblen, P.W., 1990. Anorthositic rocks of the Duluth Complex: Examples of rocks formed from plagioclase crystal mush. J. Petrol. 31 (2), 295–339.

Miller Jr, J. D. (1999). Information Circular 44. Geochemical Evaluation of Platinum Group Element (PGE) Mineralization in the Sonju Lake Intrusion, Finland, Minnesota.

Mitchell, A.A., Scoon, R.N., 2012. The Platreef of the Bushveld Complex, South Africa: a new hypothesis of multiple, non-sequential magma replenishment based on observations at the Akanani Project, north-west of Mokopane. S. Afr. J. Geol. 115 (4), 535–550.

Mokchah, N., Mathieu, L., 2022. Origin and Evolution of the Iron-Rich Upper Unit and Fe–Ti–V Mineralization of the Neoarchean Lac Doré Layered Intrusion, Chibougamau, Québec. J. Petrol. 63 (3), egac006.

Molina, J.F., Cambeses, A., Moreno, J.A., Morales, I., Montero, P., Bea, F., 2021. A reassessment of the amphibole-plagioclase NaSi-CaAl exchange thermometer with applications to igneous and high-grade metamorphic rocks. Am. Mineral. 106 (5), 782–800.

Mondal, S.K., Mathez, E.A., 2007. Origin of the UG2 chromitite layer, Bushveld Complex. J. Petrol. 48 (3), 495–510.

Morse, S.A., 1969. The Kiglapait Layered Intrusion, Labrador, Vol. 112. Geological Society of America.

Morse, S.A., 1981. Kiglapait geochemistry IV: the major elements. Geochim. Cosmochim. Acta 45 (3), 461–479.

Morse, S.A., Nolan, K.M., 1985. Kiglapait geochemistry VII: Yttrium and the rare earth elements. Geochim. Cosmochim. Acta 49 (7), 1621–1644.

Morse, S. A. (2015). Kiglapait Intrusion, Labrador. In *Layered Intrusions* (pp. 589–648). Springer.

Mudd, G.M., Jowitt, S.M., Werner, T.T., 2018. Global platinum group element resources, reserves and mining–a critical assessment. Sci. Total Environ. 622, 614–625.

Mukherjee, R., Latypov, R., Balakrishna, A., 2017. An intrusive origin for some UG-1 chromitite layers in the Bushveld Igneous Complex, South Africa: Insights from field relationships. Ore Geol. Rev. 90, 94–109.

Mungall, J.E., 2002. Kinetic controls on the partitioning of trace elements between silicate and sulfide liquids. J. Petrol. 43 (5), 749–768.

Mungall, J.E., 2005. Exploration for Platinum Group Element Deposits Mineralogical Association of Canada Short Course Series Volume 35. Short Course Series Volume 35.

Mungall, J.E., 2013. Geochemistry of Magmatic Ore Deposits. Second Edition, In Treatise on Geochemistry.

Mungall, J.E., 2015. Physical controls of nucleation, growth and migration of vapor bubbles in partially molten cumulates. Layered Intrusions 331–377.

Mungall, J. E., & Brenan, J. M. (2003). *Experimental evidence for the chalcophile behavior of the halogens.*

Mungall, J.E., Brenan, J.M., 2014. Partitioning of platinum-group elements and Au between sulfide liquid and basalt and the origins of mantle-crust fractionation of the chalcophile elements. Geochim. Cosmochim. Acta 125, 265–289.

Mungall, J.E., Harvey, J.D., Balch, S.J., Azar, B., Atkinson, J., Hamilton, M.A., 2010. Eagle's Nest: A Magmatic Ni-Sulfide Deposit in the James Bay Lowlands, Ontario. Canada. Economic Geology, Special Pu, pp. 539–557.

Mungall, J.E., Brenan, J.M., Godel, B.M., Barnes, S.J., Gaillard, F., 2015. Transport of metals and sulfur in magmas by flotation of sulfide melt on vapour bubbles. Nat. Geosci. 8 (3), 216–219.

Mungall, J.E., Kamo, S.L., McQuade, S., 2016. U-Pb geochronology documents out-of-sequence emplacement of ultramafic layers in the Bushveld Igneous Complex of South Africa. Nat. Commun. 7 (1), 1–13.

Mungall, J.E., Jenkins, C.M., Robb, S.J., Yao, Z., Brenan, J.M., 2020. Upgrading of magmatic sulfides, revisited. Econ. Geol. 115 (8), 1827–1833.

Naldrett, A.J., 2004. Magmatic Sulfide Deposits: Geology. Springer Science & Business Media, Geochemistry and Exploration.

Naldrett, A. J., & Lehmann, J. (1988). Spinel non-stoichiometry as the explanation for Ni-, Cu-and PGE-enriched sulfides in chromitites. In *Geo-platinum 87* (pp. 93–109). Springer.

Naldrett, A.J., Wilson, A., Kinnaird, J., Yudovskaya, M., Chunnett, G., 2012. The origin of chromitites and related PGE mineralization in the Bushveld Complex: new mineralogical and petrological constraints. Miner. Deposita 47 (3), 209–232.

Namur, O., Charlier, B., Holness, M.B., 2012. Dual origin of Fe–Ti–P gabbros by immiscibility and fractional crystallization of evolved tholeiitic basalts in the Sept Îles layered intrusion. Lithos 154, 100–114.

Namur, O., Abily, B., Boudreau, A.E., Blanchette, F., Bush, J.W.M., Ceuleneer, G., Charlier, B., Donaldson, C.H., Duchesne, J.-C., Higgins, M.D., 2015. Igneous layering in basaltic magma chambers. In *Layered intrusions*. Springer, pp. 75–152.

Namur, O., Charlier, B., Toplis, M. J., Higgins, M. D., Liwanag, J., & vander Auwera, J. (2010). Crystallization sequence and magma chamber processes in the ferrobasaltic Sept Îles layered intrusion, Canada. *Journal of Petrology*, *51*(6), 1203–1236. https://doi.org/10.1093/petrology/egq016.

Namur, O., Charlier, B., Toplis, M. J., Higgins, M. D., Hounsell, V., Liégeois, J.-P., & vander Auwera, J. (2011). Differentiation of tholeiitic basalt to A-type granite in the Sept Îles layered intrusion, Canada. *Journal of Petrology*, *52*(3), 487–539.

Nance, R.D., Murphy, J.B., Santosh, M., 2014. The supercontinent cycle: a retrospective essay. Gondw. Res. 25 (1), 4–29.

Naslund, H.R., 1989. Petrology of the Basistoppen Sill, East Greenland: a calculated magma differentiation trend. J. Petrol. 30 (2), 299–319.

Nebel, O., Arculus, R.J., Ivanic, T.J., Rapp, R., Wills, K.J.A., 2013. Upper Zone of the Archean Windimurra layered mafic intrusion, Western Australia: insights into fractional crystallization in a large magma chamber. Journal of Mineralogy and Geochemistry 191 (1), 83–107.

Nicholson, D.M., Mathez, E.A., 1991. Petrogenesis of the Merensky Reef in the Rustenburg section of the Bushveld Complex. Contrib. Miner. Petrol. 107 (3), 293–309.

Nicklas, R.W., Puchtel, I.S., Baxter, E.F., 2024. Concordance of V-in-olivine and Fe-XANES oxybarometry methods in mid-ocean ridge basalts. Earth Planet. Sci. Lett. 625, 118492.

Nielsen, T.F.D., Andersen, J.C.Ø., Holness, M.B., Keiding, J.K., Rudashevsky, N.S., Rudashevsky, V.N., Salmonsen, L.P., Tegner, C., Veksler, I.V., 2015. The Skaergaard PGE and gold deposit: the result of in situ fractionation, sulfide saturation, and magma chamber-scale precious metal redistribution by immiscible Fe-rich melt. J. Petrol. 56 (8), 1643–1676.

Nielsen, T.F.D., Brooks, C.K., Keiding, J.K., 2019. Bulk liquid for the Skaergaard intrusion and its PGE-Au mineralization: composition, correlation, liquid line of descent, and timing of sulfide saturation and silicate–silicate immiscibility. J. Petrol. 60 (10), 1853–1880.

Nolan, K.M., Morse, S.A., 1986. Marginal rocks resembling the estimated bulk composition of the Kiglapait intrusion. Geochim. Cosmochim. Acta 50 (10), 2381–2386.

O'Driscoll, B., Stevenson, C.T.E., Troll, V.R., 2008. Mineral lamination development in layered gabbros of the British Palaeogene Igneous Province: a combined anisotropy of magnetic susceptibility, quantitative textural and mineral chemistry study. J. Petrol. 49 (6), 1187–1221.

O'Driscoll, B., Donaldson, C.H., Daly, J.S., Emeleus, C.H., 2009. The roles of melt infiltration and cumulate assimilation in the formation of anorthosite and a Cr-spinel seam in the Rum Eastern Layered Intrusion. NW Scotland. *Lithos* 111 (1–2), 6–20.

O'Driscoll, B., VanTongeren, J.A., 2017. Layered intrusions: from petrological paradigms to precious metal repositories. Elements: an International Magazine of Mineralogy, Geochemistry, and Petrology 13 (6), 383–389.

O'Neill, H.S.C., 2021. The thermodynamic controls on sulfide saturation in silicate melts with application to ocean floor basalts. Magma Redox Geochemistry 177–213.

Palin, R.M., Santosh, M., Cao, W., Li, S.-S., Hernández-Uribe, D., Parsons, A., 2020. Secular change and the onset of plate tectonics on Earth. Earth Sci. Rev. 207, 103172.

Parker, A.P., Clay, P.L., Boudreau, A.E., Burgess, R., O'Driscoll, B., 2022. Magmatic volatiles and platinum-group element mineralization in the Stillwater layered intrusion, USA. Am. Mineral. 107 (5), 797–814.

Parks, J., Hill, R.E.T., 1986. Phase compositions and cryptic variation in a 2.2-km section of the Windimurra layered gabbroic intrusion, Yilgarn Block, Western Australia; a comparison with the Stillwater Complex. Econ. Geol. 81 (5), 1196–1202.

Pearson, D.G., Irvine, G.J., Ionov, D.A., Boyd, F.R., Dreibus, G.E., 2004. Re–Os isotope systematics and platinum group element fractionation during mantle melt extraction: a study of massif and xenolith peridotite suites. Chem. Geol. 208 (1–4), 29–59.

Peck, D.C., Keays, R.R., Ford, R.J., 1992. Direct crystallization of refractory platinum-group element alloys from boninitic magmas: Evidence from western Tasmania. Aust. J. Earth Sci. 39 (3), 373–387.

Pedersen, J.M., Ulrich, T., Whitehouse, M.J., Kent, A.J.R., Tegner, C., 2021. The volatile and trace element composition of apatite in the Skaergaard intrusion, East Greenland. Contrib. Miner. Petrol. 176 (12), 102.

Pehrsson, S.J., Eglington, B.M., Evans, D.A.D., Huston, D., Reddy, S.M., 2016. Metallogeny and its link to orogenic style during the Nuna supercontinent cycle. Geol. Soc. Lond. Spec. Publ. 424 (1), 83–94.

Pierru, R., Andrault, D., Manthilake, G., Monteux, J., Devidal, J.L., Guignot, N., King, A., Henry, L., 2022. Deep mantle origin of large igneous provinces and komatiites. *Science.* Advances 8 (44), eabo1036.

Polat, A., Fryer, B.J., Samson, I.M., Weisener, C., Appel, P.W.U., Frei, R., Windley, B.F., 2012. Geochemistry of ultramafic rocks and hornblendite veins in the Fiskenæsset layered anorthosite complex, SW Greenland: Evidence for hydrous upper mantle in the Archean. Precambr. Res. 214–215, 124–153.

Polito, P.A., Karykowski, B.T., Best, F.C., Crawford, A.J., 2017. Magnetite-hosted Cu-PGE and Fe-sulfide mineralization in 1078 Ma layered mafic intrusions in the west Musgraves region of Western Australia. Ore Geol. Rev. 90, 510–531.

Porwal, A., González-Álvarez, I., Markwitz, V., McCuaig, T.C., Mamuse, A., 2010. Weights-of-evidence and logistic regression modeling of magmatic nickel sulfide prospectivity in the Yilgarn Craton. Western Australia. *Ore Geology Reviews* 38 (3), 184–196.

Prendergast, M. D. (2021). Variant Offset-Type Platinum Group Element Reef Mineralization in Basal Olivine Cumulates of the Kapalagulu Intrusion, Western Tanzania. *Economic Geology.*

Prevec, S.A., 2018. Igneous rock associations 23. The Bushveld Complex, South Africa: new insights and paradigms. Geosci. Can. 45 (3), 117–135.

Prichard, H.M., Barnes, S.-J., Godel, B.M., Reddy, S.M., Vukmanovic, Z., Halfpenny, A., Neary, C.R., Fisher, P.C., 2015. The structure of and origin of nodular chromite from the Troodos ophiolite, Cyprus, revealed using high-resolution X-ray computed tomography and electron backscatter diffraction. Lithos 218, 87–98.

Prichard, H.M., Mondal, S.K., Mukherjee, R., Fisher, P.C., Giles, N., 2018. Geochemistry and mineralogy of Pd in the magnetitite layer within the upper gabbro of the Mesoarchean Nuasahi Massif (Orissa, India). Miner. Deposita 53 (4), 547–564.

Puetz, S.J., Condie, K.C., 2019. Time series analysis of mantle cycles Part I: Periodicities and correlations among seven global isotopic databases. Geosci. Front. 10 (4), 1305–1326.

Queffurus, M., Barnes, S.-J., 2015. A review of sulfur to selenium ratios in magmatic nickel-copper and platinum-group element deposits. Ore Geol. Rev. 69, 301–324.

Reynolds, I.M., 1985. The nature and origin of titaniferous magnetite-rich layers in the upper zone of the Bushveld Complex; a review and synthesis. Econ. Geol. 80 (4), 1089–1108.

Ripley, E.M., 2005. Re/Os isotopic and fluid inclusion studies of fluid-rock interaction in the contact aureole of the Duluth Complex. Minnesota. *Geochimica et Cosmochimica Acta Supplement* 69 (10), A332.

Ripley, E.M., Li, C., 2003. Sulfur isotope exchange and metal enrichment in the formation of magmatic Cu-Ni-(PGE) deposits. Econ. Geol. 98 (3), 635–641.

Ripley, E.M., Li, C., 2013. Sulfide Saturation in Mafic Magmas: Is External Sulfur Required for Magmatic Ni-Cu-(PGE) Ore Genesis? Econ. Geol. 108, 45–58.

Ripley, E.M., Severson, M.J., Hauck, S.A., 1998. Evidence for sulfide and Fe-Ti-P-rich liquid immiscibility in the Duluth Complex. Minnesota. *Economic Geology* 93 (7), 1052–1062.

Robins, B., 1972. Crescumulate layering in a gabbroic body on Seiland, northern Norway. Geol. Mag. 109 (6), 533–542.

Roman, A., Jaupart, C., 2016. The fate of mafic and ultramafic intrusions in the continental crust. Earth Planet. Sci. Lett. 453, 131–140.

Rose, L.A., Brenan, J.M., 2001. Wetting properties of Fe-Ni-Co-Cu-OS melts against olivine: Implications for sulfide melt mobility. Econ. Geol. 96 (1), 145–157.

Ruiz, F. V., della Giustina, M. E. S., de Oliveira, C. G., Dantas, E. L., & Hollanda, M. H. B. (2019). The 3.5 Ga São Tomé layered mafic-ultramafic intrusion, NE Brazil: Insights into a Paleoarchean Fe-Ti-V oxide mineralization and its reworking during West Gondwana assembly. *Precambrian Research, 326*, 462–478.

Ryan, C.G., Kirkham, R., Moorhead, G.F., Parry, D., Jensen, M., Faulks, A., Hogan, S., Dunn, P.A., Dodanwela, R., Fisher, L.A., Pearce, M., Siddons, D.P., Kuczewski, A., Lundström, U., et al., 2018. Maia Mapper: High definition XRF imaging in the lab. Journal of Instrumentation 13, 8 p.

Samalens, N., Barnes, S.-J., Sawyer, E.W., 2017. The role of black shales as a source of sulfur and semimetals in magmatic nickel-copper deposits: Example from the Partridge River Intrusion, Duluth Complex, Minnesota, USA. Ore Geol. Rev. 81, 173–187.

Santosh, M., Groves, D.I., 2023. The Not-So-Boring Billion: A metallogenic conundrum during the evolution from Columbia to Rodinia supercontinents. Earth Sci. Rev. 236, 104287.

Sato, E., Sato, H., 2009. Study of effect of magma pocket on mixing of two magmas with different viscosities and densities by analogue experiments. J. Volcanol. Geoth. Res. 181 (1–2), 115–123.

Sawyer, E.W., 2014. The inception and growth of leucosomes: microstructure at the start of melt segregation in migmatites. J. Metam. Geol. 32 (7), 695–712.

Schoenberg, R., Kruger, F.J., Nägler, T.F., Meisel, T., Kramers, J.D., 1999. PGE enrichment in chromite layers and the Merensky Reef of the western Bushveld Complex; a Re–Os and Rb–Sr isotope study. Earth Planet. Sci. Lett. 172 (1–2), 49–64.

Schofield, N., Alsop, I., Warren, J., Underhill, J.R., Lehné, R., Beer, W., Lukas, V., 2014. Mobilizing salt: Magma-salt interactions. Geology 42 (7), 599–602.

Schoneveld, L., Barnes, S.J., Luolavirta, K., Hu, S., Verrall, M., Le Vaillant, M., 2024. Extent and survival of zoned pyroxene within intrusions hosting magmatic sulfides: Implications for zoned pyroxene as a prospectivity indicator. Miner. Deposita 1–17.

Schoneveld, L., Barnes, S. J., Makkonen, H. v, Le Vaillant, M., Paterson, D. J., Taranovic, V., Wang, K.-Y., & Mao, Y.-J. (2020). Zoned pyroxenes as prospectivity indicators for magmatic Ni-Cu sulfide mineralization. *Frontiers in Earth Science, 8*, 256.

Scoates, J.S., Scoates, R.F.J., 2024. The Muskox intrusion: Overview of a major open-system layered intrusion and its role as a sub-volcanic magma reservoir in the Mackenzie large igneous province. Lithos 107560.

Scoates, J.S., Wall, C.J., Friedman, R.M., Weis, D., Mathez, E.A., VanTongeren, J.A., 2021. Dating the Bushveld Complex: Timing of Crystallization, Duration of Magmatism, and Cooling of the World's Largest Layered Intrusion and Related Rocks. Journal of Petrology.

Scoon, R.N., Costin, G., 2018. Chemistry, morphology and origin of magmatic-reaction chromite stringers associated with anorthosite in the Upper Critical Zone at Winnaarshoek, Eastern Limb of the Bushveld Complex. J. Petrol. 59 (8), 1551–1578.

Scoon, R.N., Mitchell, A.A., 2023. Petrogenesis of the Marginal Sill Phase and Lower Zone in the Eastern Limb of the Bushveld Complex: Incremental development of igneous layering and syn-magmatic emplacement of peridotite intrusions and sills. S. Afr. J. Geol. 126 (4), 425–450.

Sharpe, M.R., 1981. The chronology of magma influxes to the eastern compartment of the Bushveld Complex as exemplified by its marginal border groups. J. Geol. Soc. London 138 (3), 307–326.

She, Y.-W., Song, X.-Y., Yu, S.-Y., He, H., 2015. Variations of trace element concentration of magnetite and ilmenite from the Taihe layered intrusion, Emeishan large igneous province, SW China: Implications for magmatic fractionation and origin of Fe-Ti-V oxide ore deposits. J. Asian Earth Sci. 113, 1117–1131.

Shepherd, K., Namur, O., Toplis, M.J., Devidal, J.-L., Charlier, B., 2022. Trace element partitioning between clinopyroxene, magnetite, ilmenite and ferrobasaltic to dacitic magmas: an experimental study on the role of oxygen fugacity and melt composition. Contrib. Miner. Petrol. 177 (9), 90.

Simakin, A., Salova, T., Borisova, A.Y., Pokrovski, G.S., Shaposhnikova, O., Tyutyunnik, O., Bondarenko, G., Nekrasov, A., Isaenko, S.I., 2021. Experimental Study of Pt Solubility in the CO-CO2 Fluid at Low f O2 and Subsolidus Conditions of the Ultramafic-Mafic Intrusions. Minerals 11 (2), 225.

Simandl, G.J., Paradis, S., 2022. Vanadium as a critical material: economic geology with emphasis on market and the main deposit types. Appl. Earth Sci. 131 (4), 218–236.

Simundic, A.-M., 2013. Bias in research. Biochemia Medica 23 (1), 12–15.

Smith, W.D., Fay, L., Mungall, J.E., Far, M.S., Djon, L., 2024. Olivine compositions reveal an andesitic parent magma for the Archean palladium-mineralized Lac des Iles Complex of Ontario. Canada. *Minerarlium Deposita* 1–25.

Smith, W.D., Albrechtsen, B., Maier, W.D., Mungall, J.E., 2025. Petrogenesis and Ni-Cu-(PGE) prospectivity of the Mount Ayliff Complex in the Karoo Igneous Province: new insights from the Ingeli and Horseshoe lobes. Geol. Soc. Lond. Spec. Publ. 552 (1), SP552-2023.

Smith, C.H., Kapp, H.E., 1963. The Muskox intrusion, a recently discovered layered intrusion in the Coppermine River area, Northwest Territories, Canada. Mineralogical Society of America 1, 30–35.

Smith, W.D., Maier, W.D., 2021. The geotectonic setting, age and mineral deposit inventory of global layered intrusions. Earth Sci. Rev. 103736.

Smith, W.D., Maier, W.D., Barnes, S.J., Moorhead, G., Reid, D., Karykowski, B.T., 2021a. Element mapping the Merensky Reef of the Bushveld Complex. Geosci. Front. 12 (3), 101101.

Smith, W.D., Maier, W.D., Bliss, I., 2021b. The geology, geochemistry, and petrogenesis of the Huckleberry Cu-Ni-PGE prospect in the Labrador Trough, Canada: Perspectives for regional prospectivity. Ore Geol. Rev. 128, 103905.

Smith, W.D., Maier, W.D., Muir, D.D., Andersen, J.C.Ø., Williams, B.J., Henry, H., 2023. New perspectives on the formation of the Boulder Bed of the western Bushveld Complex. South Africa. *Mineralium Deposita* 58 (3), 617–638.

Smythe, D.J., Wood, B.J., Kiseeva, E.S., 2017. The S content of silicate melts at sulfide saturation: new experiments and a model incorporating the effects of sulfide composition. Am. Mineral. 102 (4), 795–803.

Solovova, I.P., Yudovskaya, M.A., Kinnaird, J.A., Wilson, A.H., Zinovieva, N.G., 2021. A siliceous komatiitic source of Bushveld magmas revealed by primary melt inclusions in olivine. Lithos 388–389, 106094. https://doi.org/10.1016/j.lithos.2021.106094.

Song, X.-Y., Qi, H.-W., Hu, R.-Z., Chen, L.-M., Yu, S.-Y., Zhang, J.-F., 2013. Formation of thick stratiform Fe-Ti oxide layers in layered intrusion and frequent replenishment of fractionated mafic magma: evidence from the Panzhihua intrusion, SW China. Geochem. Geophys. Geosyst. 14 (3), 712–732.

Spandler, C.J., Eggins, S.M., Arculus, R.J., Mavrogenes, J.A., 2000. Using melt inclusions to determine parent-magma compositions of layered intrusions: Application to the Greenhills Complex (New Zealand), a platinum group minerals–bearing, island-arc intrusion. Geology 28 (11), 991–994.

Spandler, C.J., Mavrogenes, J., Arculus, R.J., 2005. Origin of chromitites in layered intrusions: Evidence from chromite-hosted melt inclusions from the Stillwater Complex. Geology 33 (11), 893–896. https://doi.org/10.1130/G21912.1.

Sparks, R. S. J., Annen, C., Blundy, J. D., Cashman, K. v, Rust, A. C., & Jackson, M. D. (2019). Formation and dynamics of magma reservoirs. *Philosophical Transactions of the Royal Society A, 377*(2139), 20180019.

Spencer, C.J., Murphy, J.B., Kirkland, C.L., Liu, Y., Mitchell, R.N., 2018. A Palaeoproterozoic tectono-magmatic lull as a potential trigger for the supercontinent cycle. Nat. Geosci. 11 (2), 97–101.

Spier, C.A., Daczko, N.R., Zhou, R., 2024. Zircon coupled dissolution-precipitation textures distinguish xenocrystic cargo from rare magmatic zircon in the Paleoarchean Bacuri Mafic-Ultramafic layered Complex. Brazil. *Precambrian Research* 404, 107342.

Straub, S.M., Gomez-Tuena, A., Stuart, F.M., Zellmer, G.F., Espinasa-Perena, R., Cai, Y., Iizuka, Y., 2011. Formation of hybrid arc andesites beneath thick continental crust. Earth Planet. Sci. Lett. 303 (3–4), 337–347.

Sullivan, N.A., Zajacz, Z., Brenan, J.M., Hinde, J.C., Tsay, A., Yin, Y., 2022a. The solubility of gold and palladium in magmatic brines: Implications for PGE enrichment in mafic-ultramafic and porphyry environments. Geochimica et Cosmochimica Acta 316, 230–252.

Sullivan, N.A., Zajacz, Z., Brenan, J.M., Tsay, A., 2022b. The solubility of platinum in magmatic brines: Insights into the mobility of PGE in ore-forming environments. Geochim. Cosmochim. Acta 316, 253–272.

Sun, J., Melo, A. T., Kim, J. D., & Wei, X. (2020). Unveiling the 3D undercover structure of a Precambrian intrusive complex by integrating airborne magnetic and gravity gradient data into 3D quasi-geology model building. *Interpretation, 8*(4), SS15–SS29.

Sushchenko, A., Groshev, N., Rundkvist, T., Kompanchenko, A., Savchenko, Y., 2023. Apatite as an Indicator for the Formation of PGE Mineralization as Exemplified by Anorthosites of the Kievey Deposit, Fedorova-Pana Layered Complex, Kola Peninsula. Russia. Minerals 13 (12), 1473.

Swanson-Hysell, N.L., Hoaglund, S.A., Crowley, J.L., Schmitz, M.D., Zhang, Y., Miller Jr, J.D., 2021. Rapid emplacement of massive Duluth Complex intrusions within the North American Midcontinent rift. Geology 49 (2), 185–189.

Tang, Q., Li, C., Ripley, E.M., Bao, J., Su, T., Xu, S., 2021. Sr-Nd-Hf-O isotope constraints on crustal contamination and mantle source variation of three Fe-Ti-V oxide ore deposits in the Emeishan large igneous province. Geochim. Cosmochim. Acta 292, 364–381.

Tang, D., Qin, K., Evans, N.J., Fang, L., 2023. Silicate mineral inclusions in chromite from the Eastern Bushveld complex: Implications for the origin and evolution of hydrous melt during chromite mineralization in the Critical Zone. Lithos 438, 106997.

Tanner, D., McDonald, I., Harmer, R.E.J., Muir, D.D., Hughes, H.S.R., 2019. A record of assimilation preserved by exotic minerals in the lowermost platinum-group element deposit of the Bushveld Complex: The Volspruit Sulfide Zone. Lithos 324, 584–608.

Taranovic, V., Barnes, S.J., Beresford, S., Williams, M., MacRae, C., Schoneveld, L.E., 2022. Nova-Bollinger Ni-Cu sulfide ore deposits, Fraser zone, Western Australia: Petrogenesis of the host intrusions. Econ. Geol. 117 (2), 455–484.

Tegner, C., Robins, B., Reginiussen, H., Grundvig, S., 1999. Assimilation of crustal xenoliths in a basaltic magma chamber: Sr and Nd isotopic constraints from the Hasvik layered intrusion. Norway. *Journal of Petrology* 40 (3), 363–380.

Tegner, C., Thy, P., Holness, M.B., Jakobsen, J.K., Lesher, C.E., 2009. Differentiation and compaction in the Skaergaard intrusion. J. Petrol. 50 (5), 813–840.

Tollari, N., Barnes, S.-J., Cox, R.A., Nabil, H., 2008. Trace element concentrations in apatites from the Sept-Îles Intrusive Suite, Canada—implications for the genesis of nelsonites. Chem. Geol. 252 (3–4), 180–190.

Toplis, M.J., Carroll, M.R., 1995. An experimental study of the influence of oxygen fugacity on Fe-Ti oxide stability, phase relations, and mineral—melt equilibria in ferro-basaltic systems. J. Petrol. 36 (5), 1137–1170.

Toplis, M.J., Corgne, A., 2002. An experimental study of element partitioning between magnetite, clinopyroxene and iron-bearing silicate liquids with particular emphasis on vanadium. Contributions to Mineralogy and Petrology 144 (1), 22–37.

Ulmer, G., 1969. Experimental investigations of chromite spinels. Magmatic Ore Deposits 114–131.

Upton, B.G.J., Parsons, I., Emeleus, C.H., Hodson, M.E., 1996. Layered Alkaline Igneous Rocks of the Gardar Province, South Greenland. in *Developments in Petrology* Vol. 15, 331–363.

VanTongeren, J.A., Mathez, E.A., 2012. Large-scale liquid immiscibility at the top of the Bushveld Complex. South Africa. *Geology* 40 (6), 491–494.

Veksler, I. V. (2006). Crystallized melt inclusions in gabbroic rocks. In: Webster, J. D. (ed.) Melt Inclusions in Plutonic Rocks. Mineralogical Association of Canada Short Courses 36, 100ˆ122. Veksler, I. v, & Charlier, B. (2015). Silicate liquid immiscibility in layered intrusions. In *Layered intrusions* (pp. 229–258). Springer.

Virtanen, V.J., Heinonen, J.S., Barber, N., Molnár, F., 2021. The effects of assimilation on sulfide saturation and the formation of norite-hosted Cu-Ni deposits in the Duluth Complex, Minnesota. In: Lithosphere 2021: Eleventh Symposium on Structure, Composition and Evolution of the Lithosphere, p. 147.

Virtanen, V.J., Heinonen, J.S., Barber, N.D., Molnár, F., 2022. Complex effects of assimilation on sulfide saturation revealed by modeling with the Magma Chamber Simulator: A case study on the Duluth Complex, Minnesota, USA. Econ. Geol. 117 (8), 1881–1899.

Virtanen, V.J., Höytiä, H.M.A., Iacono-Marziano, G., Yang, S., Moilanen, M., Törmänen, T., 2024a. From the mantle source to the crustal sink: magmatic differentiation and sulfide saturation of the Paleoproterozoic komatiites of the Central Lapland Greenstone Belt, Finland. *Contributions to Mineralogy and Petrology* 179 (7), 73.

Virtanen, V.J., Heinonen, J.S., Märki, L., Galvez, M.E., Molnár, F., 2024b. Sedimentary and metamorphic processes priming black shale for magmatic assimilation of sulfur: an example from the Virginia Formation, Minnesota, United States. Mineralium Deposita 1–17.

Vogel, D.C., Keays, R.R., James, R.S., Reeves, S.J., 1999. The geochemistry and petrogenesis of the Agnew Intrusion, Canada: A product of S-undersaturated, high-Al and low-Ti tholeiitic magmas. J. Petrol. 40 (3), 423–450.

von Gruenewaldt, G., 1993. Ilmenite-apatite enrichments in the Upper Zone of the Bushveld Complex: a major titanium-rock phosphate resource. Int. Geol. Rev. 35 (11), 987–1000.

Voordouw, R., Gutzmer, J., Beukes, N.J., 2009. Intrusive origin for upper group (UG1, UG2) stratiform chromitite seams in the Dwars River area, Bushveld Complex, South Africa. *Mineralogy and Petrology* 97 (1–2), 75.

Vukmanovic, Z., Holness, M.B., Monks, K., Andersen, J.C., 2018. The Skaergaard trough layering: sedimentation in a convecting magma chamber. Contrib. Miner. Petrol. 173 (5), 1–18.

Vukmanovic, Z., Holness, M.B., Stock, M.J., Roberts, R.J., 2019. The creation and evolution of crystal mush in the Upper Zone of the Rustenburg Layered Suite, Bushveld Complex, South Africa. J. Petrol. 60 (8), 1523–1542.

Wager, L.R., Brown, G.M., 1968. Layered igneous intrusions. Oliver and Boyd, Edinburgh and London, pp. 1–588.

Wager, L.R., Deer, W.A., 1939. Geological Investigations in East Greenland. Part III. The Petrology of the Skaergaard Intrusion, Kangerdlugssuaq, East Greenland. Geogr. J. 95 (5), 394.

Wager, L.R., Brown, G.M., Wadsworth, W.J., 1960. Types of igneous cumulates. Journal of Petrology 1 (1), 73–85.

Wall, C.J., Scoates, J.S., Weis, D., Friedman, R.M., Amini, M., Meurer, W.P., 2018. The stillwater complex: Integrating zircon geochronological and geochemical constraints on the age, emplacement history and crystallization of a large, open-system layered intrusion. J. Petrol. 59 (1), 153–190.

Walter, M.J., 1998. Melting of garnet peridotite and the origin of komatiite and depleted lithosphere. J. Petrol. 39 (1), 29–60.

Wang, K., Wang, C.Y., Ren, Z.-Y., 2018. Apatite-hosted melt inclusions from the Panzhihua gabbroic-layered intrusion associated with a giant Fe–Ti oxide deposit in SW China: insights for magma unmixing within a crystal mush. Contrib. Miner. Petrol. 173, 1–14.

Waters, D.J., Lovegrove, D.P., 2002. Assessing the extent of disequilibrium and overstepping of prograde metamorphic reactions in metapelites from the Bushveld Complex aureole, South Africa. J. Metam. Geol. 20 (1), 135–149.

Waterton, P., Mungall, J., Pearson, D.G., 2021. The komatiite-mantle platinum-group element paradox. Geochim. Cosmochim. Acta 313, 214–242.

Wieser, P., & Gleeson, M. (2022). *PySulfSat: an open-source Python3 tool for modelling sulfide and sulfate saturation.*

Wieser, P.E., Vukmanovic, Z., Kilian, R., Ringe, E., Holness, M.B., Maclennan, J., Edmonds, M., 2019. To sink, swim, twin, or nucleate: A critical appraisal of crystal aggregation processes. Geology 47 (10), 948–952.

Wilson, A.H., 2012. A chill sequence to the Bushveld Complex: insight into the first stage of emplacement and implications for the parental magmas. J. Petrol. 53 (6), 1123–1168.

Wilson, J. R., Robins, B., Nielsen, F. M., Duchesne, J.-C., & vander Auwera, J. (1996). The Bjerkreim-Sokndal Layered Intrusion, Southwest Norway. *Developments in Petrology*, *15*(C), 231–255.

Wilson, P.I.R., McCaffrey, K.J.W., Wilson, R.W., Jarvis, I., Holdsworth, R.E., 2016. Deformation structures associated with the Trachyte Mesa intrusion, Henry Mountains, Utah: Implications for sill and laccolith emplacement mechanisms. J. Struct. Geol. 87, 30–46.

Wilson, A.H., Tredoux, M., 1990. Lateral and vertical distribution of platinum-group elements and petrogenetic controls on the sulfide mineralization in the P1 pyroxenite layer of the Darwendale subchamber of the Great Dyke, Zimbabwe. Econ. Geol. 85 (3), 556–584.

Xing, C.-M., Wang, C.Y., Charlier, B., Namur, O., 2022. Ubiquitous dendritic olivine constructs initial crystal framework of mafic magma chamber. Earth Planet. Sci. Lett. 594, 117710.

Yang, S.-H., Hanski, E., Li, C., Maier, W. D., Huhma, H., Mokrushin, A. v, Latypov, R., Lahaye, Y., O'Brien, H., & Qu, W.-J. (2016). Mantle source of the 2.44–2.50-Ga mantle plume-related magmatism in the Fennoscandian Shield: evidence from Os, Nd, and Sr isotope compositions of the Monchepluton and Kemi intrusions. *Mineralium Deposita*, *51*, 1055–1073.

Yang, S.-H., Maier, W.D., Godel, B.M., Barnes, S.-J., Hanski, E.J., O'Brien, H., 2019. Parental magma composition of the Main Zone of the Bushveld Complex: evidence from in situ LA-ICP-MS trace element analysis of silicate minerals in the cumulate rocks. J. Petrol. 60 (2), 359–392.

Yao, Z., Mungall, J.E., 2020. Flotation mechanism of sulfide melt on vapour bubbles in partially molten magmatic systems. Earth Planet. Sci. Lett. 542, 116294.

Yao, Z., Mungall, J.E., 2022. Magnetite layer formation in the Bushveld complex of South Africa. Nat. Commun. 13 (1), 1–11.

Yao, Z., Qin, K., Mungall, J.E., 2018. Tectonic controls on Ni and Cu contents of primary mantle-derived magmas for the formation of magmatic sulfide deposits. Am. Mineral. 103 (10), 1545–1567.

Yao, Z., Mungall, J.E., Jenkins, M.C., 2021. The Rustenburg Layered Suite formed as a stack of mush with transient magma chambers. Nat. Commun. 12 (1), 505.

Yasseri, T., Reher, J., 2022. Fooled by facts: quantifying anchoring bias through a large-scale experiment. J. Comput. Soc. Sci. 5 (1), 1001–1021.

Yudovskaya, M., Belousova, E., Kinnaird, J., Dubinina, E., Grobler, D.F., Pearson, N., 2017. Re-Os and S isotope evidence for the origin of Platreef mineralization (Bushveld Complex). Geoch. Cosmo. Acta. 214, 282–307.

Zhang, X., Song, X.-Y., Chen, L.-M., Xie, W., Yu, S.-Y., Zheng, W.-Q., Deng, Y.-F., Zhang, J.-F., Gui, S.-G., 2012. Fractional crystallization and the formation of thick Fe–Ti–V oxide layers in the Baima layered intrusion, SW China. Ore Geol. Rev. 49, 96–108.

Zientek, M. L., Causey, J. D., Parks, H. L., & Miller, R. J. (2014). *Platinum-group elements in southern Africa: mineral inventory and an assessment of undiscovered mineral resources.* US Geological Survey.